Theses and Dissertations   1. Thesis and Dissertation Collection, all items

1982

Ocean floor geomagnetic data collection system

Gritzke, Arnold Richard; Johnson, Robert Henry, II

Monterey, California. Naval Postgraduate School

http://hdl.handle.net/10945/20281

NAVAL POSTGRADUATE SCHOOL
Monterey, California

THESIS

OCEAN FLOOR GEOMAGNETIC DATA
COLLECTION SYSTEM

by

Arnold Richard Gritzke

and

Robert Henry Johnson II

December 1982

Thesis Advisor: J. Powers

Unclassified

REPORT DOCUMENTATION PAGE		READ INSTRUCTIONS BEFORE COMPLETING FORM
1. REPORT NUMBER	2. GOVT ACCESSION NO.	3. RECIPIENT'S CATALOG NUMBER
4. TITLE (and Subtitle) Ocean Floor Geomagnetic Data Collection System		5. TYPE OF REPORT & PERIOD COVERED Master's Thesis December 1982
		6. PERFORMING ORG. REPORT NUMBER
7. AUTHOR(s) Arnold Richard Gritzke Robert Henry Johnson II		8. CONTRACT OR GRANT NUMBER(s)
9. PERFORMING ORGANIZATION NAME AND ADDRESS Naval Postgraduate School Monterey, California 93940		10. PROGRAM ELEMENT, PROJECT, TASK AREA & WORK UNIT NUMBERS
11. CONTROLLING OFFICE NAME AND ADDRESS Naval Postgraduate School Monterey, CA 93940		12. REPORT DATE December 1982
		13. NUMBER OF PAGES 179
14. MONITORING AGENCY NAME & ADDRESS(if different from Controlling Office)		15. SECURITY CLASS. (of this report) Unclassified
		15a. DECLASSIFICATION/DOWNGRADING SCHEDULE

16. DISTRIBUTION STATEMENT (of this Report)

Approved for public release; distribution unlimited

17. DISTRIBUTION STATEMENT (of the abstract entered in Block 20, if different from Report)

.

18. SUPPLEMENTARY NOTES

19. KEY WORDS (Continue on reverse side if necessary and identify by block number)

Geomagnetic Noise;   Telemetry Spar Buoy;

Fiber Optic Data Link; Pulse Code Modulation

20. ABSTRACT (Continue on reverse side if necessary and identify by block number)

The second generation design of the Naval Postgraduate School's ocean-floor geomagnetic data collection system is described with emphasis on modifications for improvement over its predecessor. These improvements include 15 channel parallel analog-to-serial pulse code modulation conversion, fiber optic data link, and radio telemetry to shore recording equipment. The system has flexibility in operating depth, an increase in data   (continued)

DD _{1 JAN 73} FORM 1473   EDITION OF 1 NOV 68 IS OBSOLETE
 S/N 0102-014-6601 |

1

Item 20. (continued)

acquisition time, synchronization with land site data, and a
data format that is readily converted to digital for computer
assisted analysis.

Ocean Floor Geomagnetic Data Collection System

by

Arnold Richard Gritzke
Lieutenant Commander, United States Navy
B. S., University of Utah, 1972
and
Robert Henry Johnson II
Lieutenant, United States Navy
B. S., University of Washington, 1976

Submitted in partial fulfillment of the
requirements for the degree of

MASTER OF SCIENCE IN PHYSICS

from the

NAVAL POSTGRADUATE SCHOOL

December 1982

ABSTRACT

The second generation design of the Naval Postgraduate School's ocean floor geomagnetic data collection system is described with emphasis on modifications for improvement over its predecessor. These improvements include 15 channel parallel analog-to-serial pulse code modulation conversion, fiber optic data link, and radio telemetry to shore recording equipment. The system has flexibility in operating depth, an increase in data acquisition time, synchronization with land site data, and a data format that is readily converted to digital for computer assisted analysis.

TABLE OF CONTENTS

LIST OF TABLES

8

LIST OF FIGURES

ACKNOWLEDGEMENTS

I. INTRODUCTION

This thesis research is part of a continuing effort by the Naval Postgraduate School to obtain a long term data base for the improved understanding and interpretation of the ELF electromagnetic environment in the vicinity of the sea floor. The overall project emphasizes the importance of acquiring measurements of geomagnetic fluctuations on the sea floor over a period of several years at various locations and depths while simultaneously obtaining data at a land based site. Primary objectives include the interpretation of signals covering four decades of frequency from 0.01HZ to 100HZ through the use of total field magnetometers, induction coils and ULF/ELF receivers. This phase of data collection covers the 0.01HZ to 20HZ range utilizing induction coils as sensors.

The magnetic noise in the sea is of interest both from a geophysical viewpoint as well as for naval applications. In addition to undersea field magnetometry, some areas of current geophysical interest are the measurement of marine geomagnetic anomalies near centers of sea floor spreading, characterization of magnetic fields induced by ocean waves, geophysical exploration and the utilization of low frequency waveguides present under the sea floor. Applications of interest to the Navy are in the areas of mine-warfare, submarine detection, submarine communication using a superconducting quantum interference device (SQUID) as the sensing element for an extremely low frequency (ELF) receiving antenna system, and possibly as a means of remote verification of underground nuclear detonations.

To achieve an understanding of the nature of the fluctuating undersea geomagnetic spectrum, it is necessary to develop a data base with goals for high quality and great quantity. The collection system utilized by the predecessors [1] of this research team acknowledged a shortfall in both these goals. Their collection system consisted of two channels, each with a coil antenna sensor, preamplifier, variable gain amplifier, voltage controlled oscillator, reference oscillator, and an analog cassette tape recorder configured as depicted in Figure 1.1. The components were encapsulated in Benthos glass spheres with the deployed configuration as shown in figure 1.2. The data collected with this system was limited by virtue of the equipment restrictions and deployment techniques. The analog tape recorder posed the greatest limitation. The data acquisition time was limited by the cassette tape length to a maximum of 45 minutes per channel per system deployment. The accuracy of the data was greatly dependent upon the stability of the oscillators. Additionally the utility for comparison of the data with data taken at a nearby land station is questionable since the synchronization of the data could only be crudely approximated.

The particular objectives of this thesis research was to improve the ocean floor geomagnetic collection system design in an effort to improve data quality and quantity while attaining time synchronization of land-ocean data. A secondary objective was to develop procedures for computer assisted data analysis. Lastly the associated thesis report is to act as a systems manual in an effort to provide continuity for future system users.

In the design of an ocean floor magnetic data collection system, it is necessary to consider the constraints placed upon the system as a result of its function and the environment to which it is subjected.
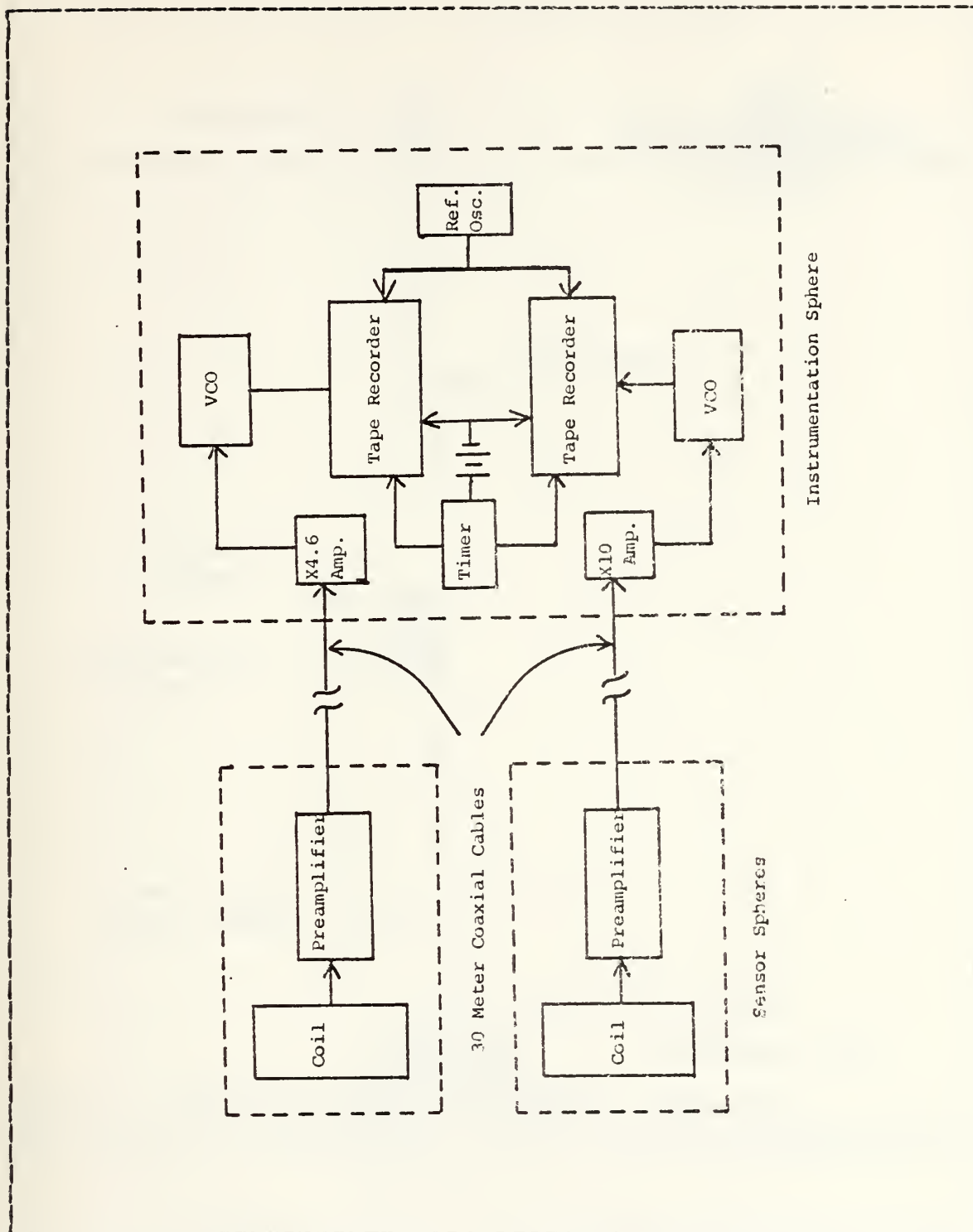
Figure 1.1   Data Acquisition System Schematic
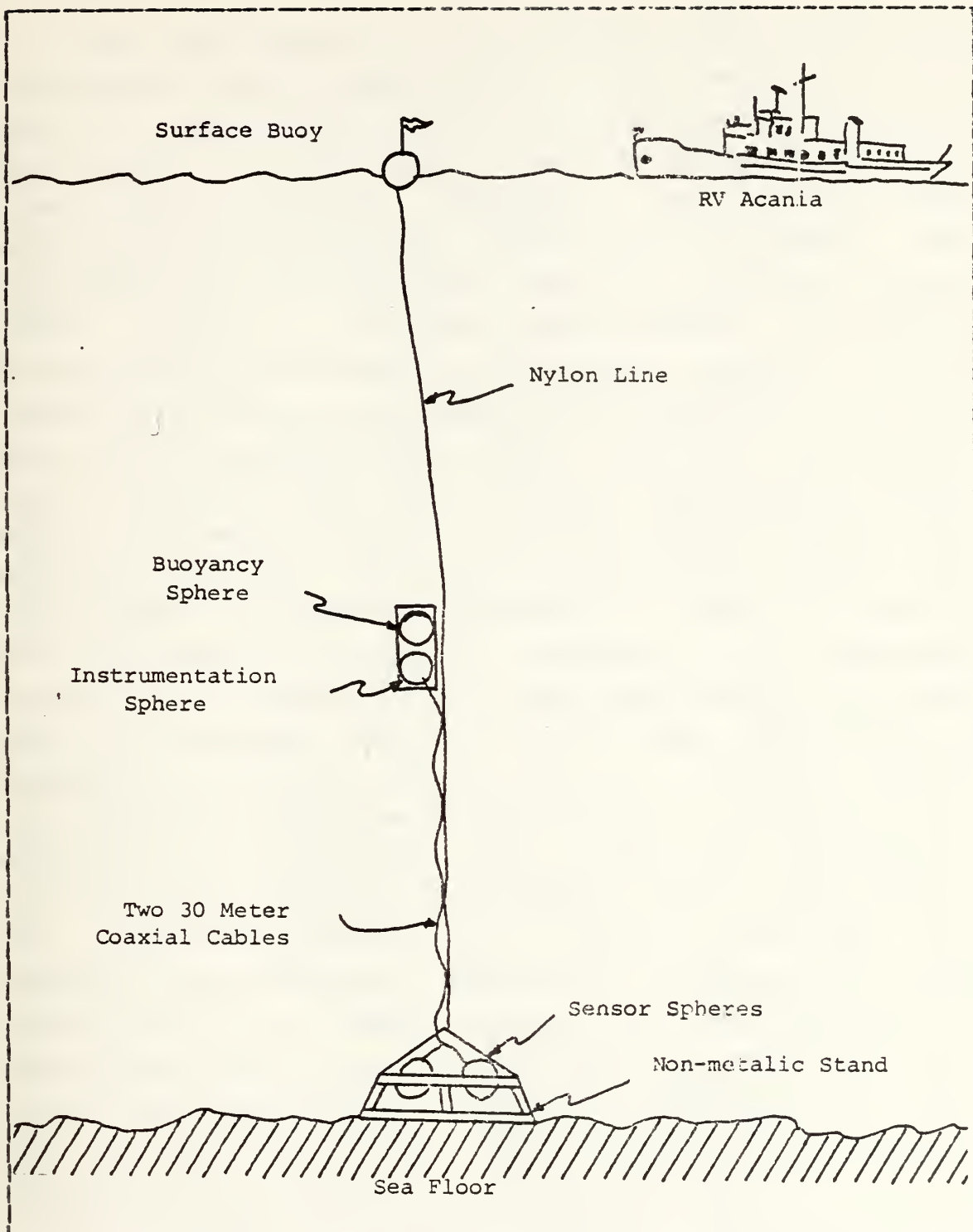
Figure 1.2   Diagram of Deployed System Configuration

It is the function of the system to sense geomagnetic fluctuations near the ocean floor in the frequency range of interest, process and transmit those signals to the surface for telemetry to shore based receiving equipment for dual (ocean-land) recording, decoding, and analysis while maintaining the information content of the signals. One requirement of the integrated system is to ensure signal purity. That is, the system should measure the magnetic signals while minimizing, to the extent possible, system induced variations in the signal being measured. It is well known that a magnetic field can be set up by an electric field (Ampere's Law). This mutual interference between system components must be avoided where possible and minimized otherwise. To achieve maximum signal purity, the sensors must be isolated magnetically as much as possible from the rest of the system. Because of the low signal strength of the collected data, some amplification must take place at the sensor location to allow for transmission by nonferrous metallic cable to a remotely located instrumentation subsystem. Further magnetic isolation may be achieved by utilization of a fiber optic data link from the instrumentation sphere to the telemetry bouy. Additionally, near surface interference is a matter of concern. Low frequency electromagnetic radiation can penetrate the ocean surface for up to several meters with the potential of channelling down the link and providing perturbations to the signal being measured if a metallic conductor cable were used for data transmission. This "antenna effect" can be eliminated by employment of a fiber optic link.

Due to space and power limitations, transmission line signal attenuation may be an important consideration in deep sea locations. Low loss fiber optics can reduce or eliminate this concern.

The advantage of fiber-optic links have been demonstrated world-wide by experimental optical wave guide systems. Among the important features are low transmission loss, wide transmission bandwidth, insensitivity to electromagnetic and radio frequency interference, and suitability for digital communications, and pulse modulation methods (for amplitude modulation techniques, fiber optic cable losses are independent of transmission frequency) [2].

Optical fibers are attractive since a single strand is sufficient to carry the information signal and cannot be short-circuited by exposure to sea water. Also recent trends, through advanced technical expertise in fiber manufacturing have narrowed the economic gap between long haul optical fibers and their foremost competitor, copper wire and cables [3].

Any practical design ultimately rests upon the requirements of the user, his resources and capabilities as well as the technology of the day. The major goals have been stated as that of signal purity and data quantity. It has been shown, although not rigorously, that a fiber optic data link is a viable alternative to the metallic transmission line in the achievement of signal purity. The improvement of data acquisition time is gained through RF transmission of data to shore receiving equipment. Data acquisition time is thereby limited only by power supply capacity and the schedule of the deploying ship.

As indicated earlier, fiber optic systems are suitable for digital and pulse modulation methods of data transmission. In addition, analog transmission may be accomplished. There are several pulse modulation methods available. Among them are pulse position modulation (PPM), pulse width modulation (PWM), pulse amplitude modulation

(PAM), and pulse code modulation (PCM). PCM is the best known, and today the most important pulse modulation system. Three separate operations are involved in providing a PCM signal. The first is to interrogate the message signal at regularly spaced intervals (sampling). The second is to approximate the measured amplitude value to the nearest permitted voltage reference level (quantizing). The third operation is to represent the approximated (quantized) amplitude values as a series of coded pulses.

In PCM, several pulses per sample are used to signify the amplitude value, instead of one pulse per sample as in the cases of PAM, PPM, or PWM. Consequently, PCM systems require an increased bandwidth (within the capability of fiber optic systems) for their transmission. However, any small deformations in the height or width of the pulses are irrelevant since it is only necessary to know whether the pulse is present or absent in order to retrieve the original message. Moreover, in a PCM transmission, noise is nonaccumulative because noisy PCM signals can easily be cleaned up, when it becomes necessary, by the process of regeneration. Thus the quality of a PCM transmission is dependent on the sampling, quantizing, and coding processes, and not the length nor the noise of the transmission media. By contrast, the PAM, PWM, and PPM systems are continuously affected by noise and cannot be cleaned up, or regenerated. The noise is accumulative and the longer the distance of transmission, the greater will be the noise [4].

Additionally, the desired resolution of the measured signals may be achieved in a PCM system by selection of the sampled word length and the sampling rate.

Both the digital and analog transmission methods are inferior to PCM. The loss of a bit of digital data obscures the value of the sampled data. Analog data may be

irretrievably altered by noise. PCM, then, is perhaps the ideal transmission method for our application.

This report delineates an ocean floor geomagnetic data collection system that employs coil antenna sensors, a pulse code modulation system, fiber optic link, RF data link, and recording equipment. It also details procedures for decoding and digitizing the data as well those for computer assisted data processing for eventual analysis.

II. SYSTEM DESIGN

A. EQUIPMENT CONFIGURATION

The general arrangement of the Generation II System components in their deployed mode is shown in Figure 2.1.

1. Data Collection Equipment

A fuctional block diagram of the data aquisition system illustrated in Figure 2.2 reveals the following major components:

1. coil antenna sensors (2)
2. preamplifiers (2)
3. preconditioners (2)
4. pulse code modulation system (1)
5. optical transmitter (1)
6. optical receiver (1)
7. radio frequency transmitter (1)
8. radio frequency receiver (1)
9. instrumentation tape recorder (1)

The system components are discussed in the following subsections:

a. Sensor Subsystem

The sensor subsystem is currently designed with two sensors each consisting of a coil antenna sensor, a preamplifier and a battery power supply housed in a Benthos glass sphere with a 0.404 meter inner diameter. The sensor and the instrumentation subsystems are interconnected by two 30 meter long, coaxial cables terminated at each end with Brantner connectors and Bentos sphere penetrators through the glass walls to the enclosed equipment.
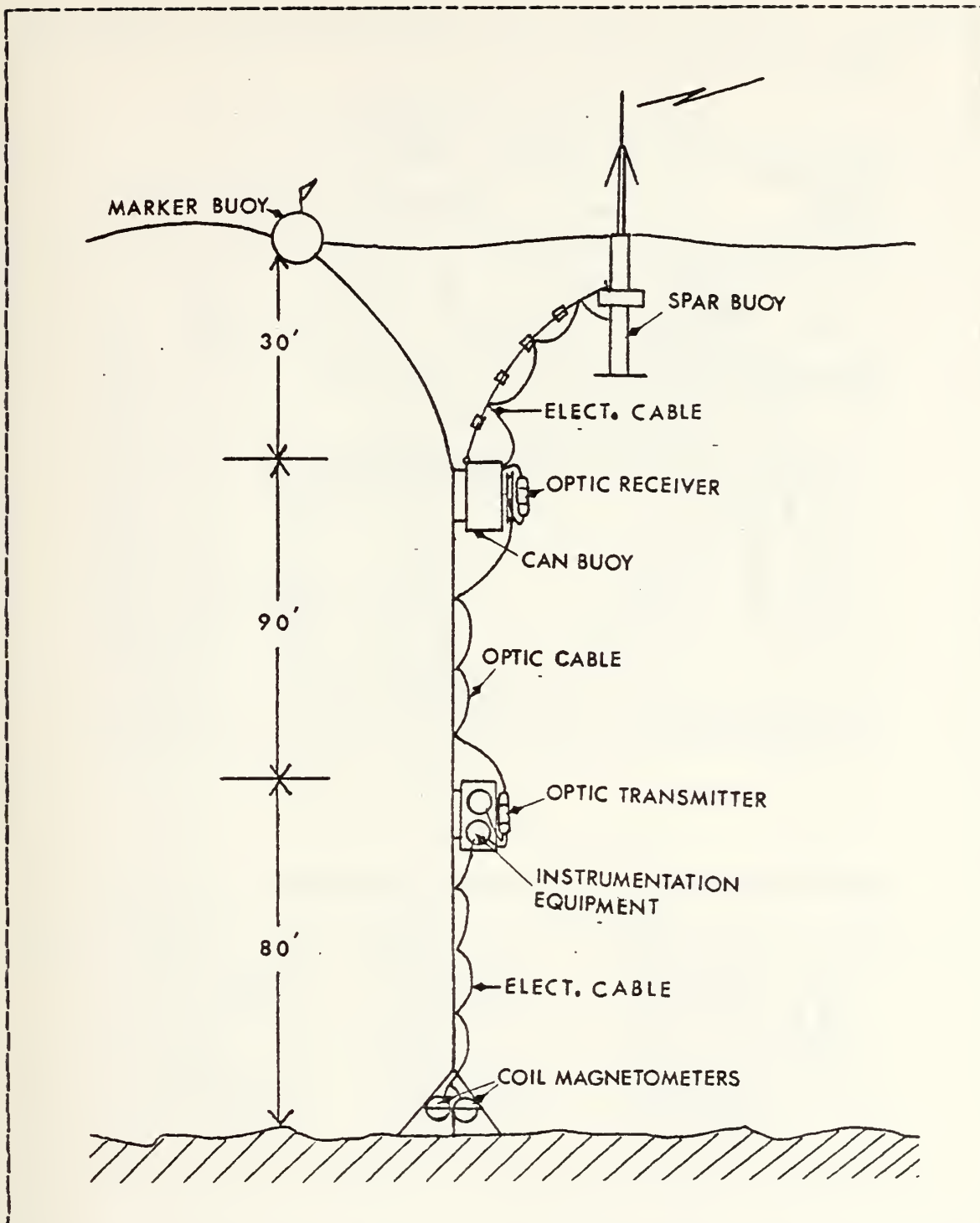
Figure 2.1   Diagram of Deployed Generation II System

21
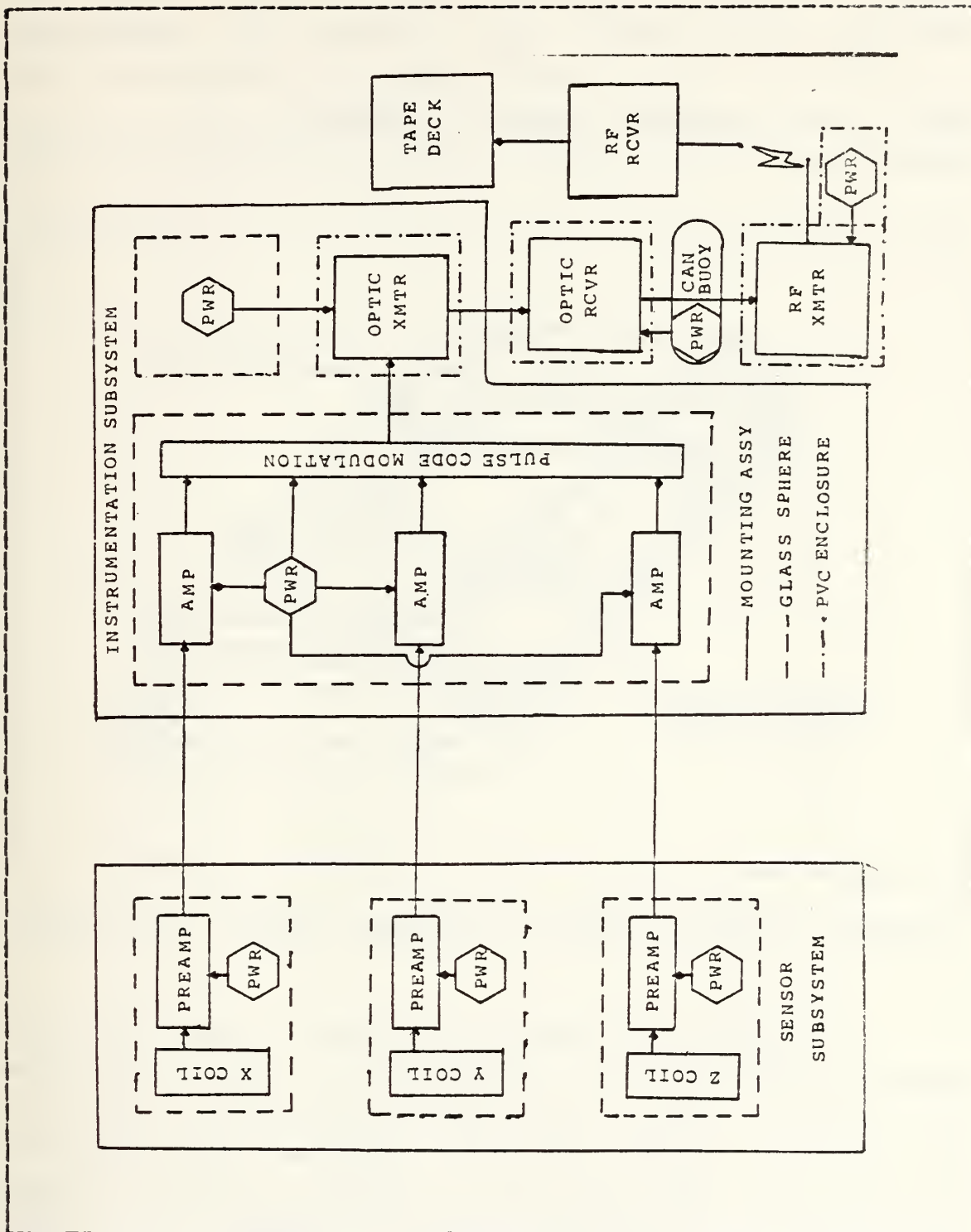
Figure 2.2   Block Diagram of Generation II System
             Configuration

22

The sensor spheres are mounted in Benthos hardhat
enclosures. The hardhats are bolted to the equipment
mounting assembly with nylon bolts.

(1) Equipment Mounting Assembly The equipment
mounting assembly depicted in Figure 2.3 is a non-metallic

3/4" Fiber-Glass
Mounting Plates

Free Flooding
ABS Structure
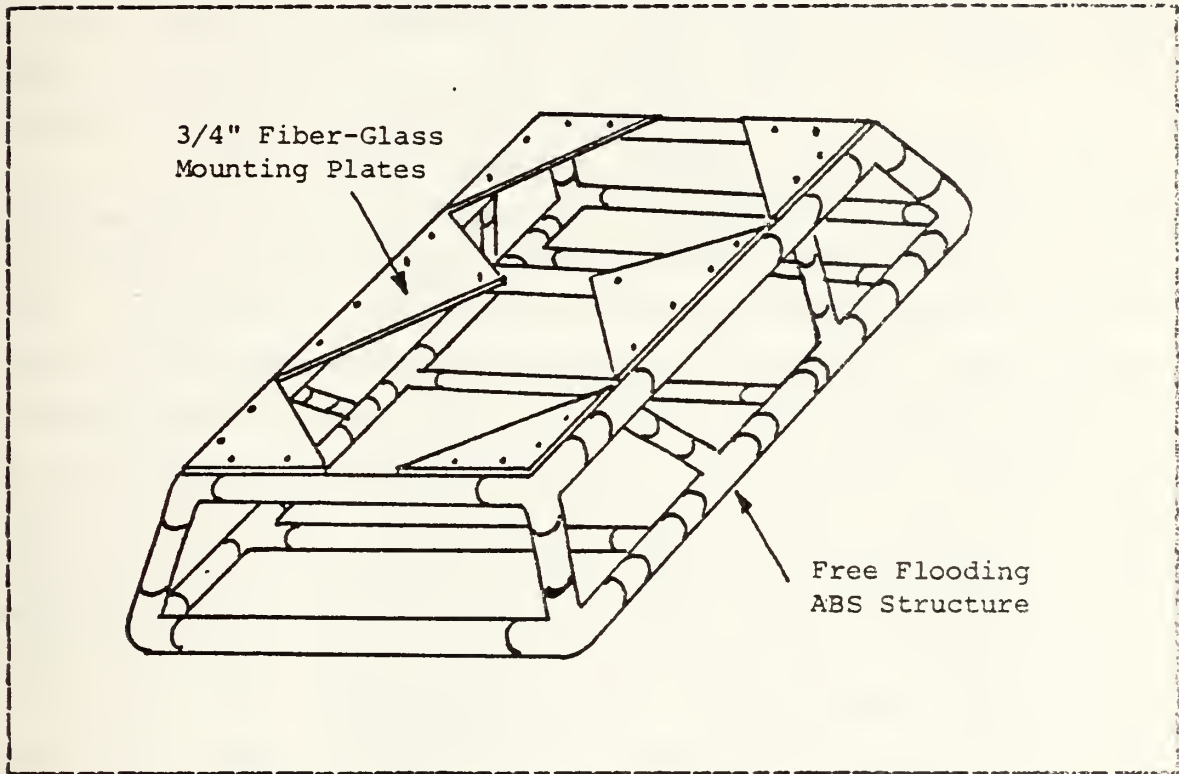
Figure 2.3   Sensor Subsystem Equipment Mounting Assembly

stand that permits ease of deployment and provides
structural support and protection for the sensor spheres.
The sensor stand design calls for a light,   free flooding
structure with removable strap on weights to obtain the
required negative buoyancy, but still allow for portability
and ease of handling in system deployment.   A non-metallic
material is necessary in the stand construction to avoid the
effects of induced currents due to electro-chemical

23

reactions at the interface of a metal surface and the electrically conductive seawater. The stand is constructed of light weight, high strength, Acrylonitrile-Butadiene-Styrene (ABS) piping which is well suited for this application. The weights are fashioned from lengths of ABS piping filled with lead, sand and transformer oil. The pipes are capped off at each end to provide a water tight, non-metallic, and compact means of adding the necessary negative buoyancy to the stand.

(2) Coil Antenna Sensor Each sensor is a continuously wound coil antenna manufactured from 5460 turns of 18 gauge copper magnet wire by Elna Engineering of Palo Alto, California. The coils weigh approximately 100 pounds each with dimensions as depicted in Figure 2.4. The average enclosed area of each coil is 0.0824 square meters which is determined by taking the average of the areas obtained by computing the area for both the inner radius and the outer radius. The dimensions of the sensor are constrained by the geometry of the glass spheres. The coil resistance is 120 ohms with a self-inductance of approximately 9.31 henries.

(3) Preamplifier The preamplifier selected for use in the sensor sphere is the model 13-10A low noise ELF amplifier manufactured by Dr. Alan Phillips of SRI International. The final stage of the amplifier contains an active low-pass filter with a cutoff frequency at 20 Hz. Such filtering is necessary to reject the effects of 60 Hz signals and harmonics due to the presence of power lines for the similar system used for land data acquisition. Stray frequencies above 20 Hz do not penetrate significantly to depths at which the ocean system is operated (50-60 meters). The overall preamplifier gain is approximately 55 dB.

A schematic diagram of the preamplifier circuit is contained in Figure A.1. The gain and filtering characteristics of
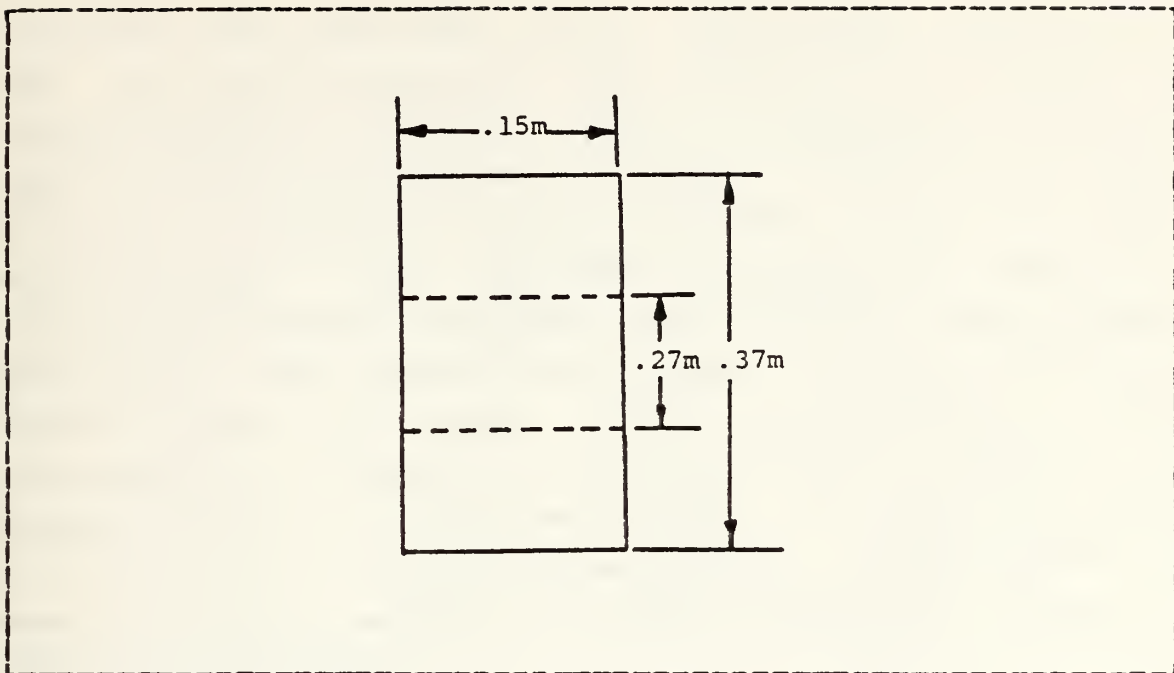
Figure 2.4   Induction Coil Sensor Dimensions

the system are illustrated in Appendix C. and are relevant
to the discussion concerning system transfer functions. The
preamplifier is powered by two .75 AH, 12 volt mercury
batteries mounted in a section of 1 inch PVC. The batteries
are arranged in such a fashion as to give the required plus
or minus 12 volts and ground. The preamplifier is housed in
an aluminum case to shield in fields developed by the
preamplifier circuitry. The preamplifier and battery pack
are attached to either side of the coil antenna sensor with
electrical tape. The interconnections are made by coaxial
connection for both the coil input to the preamplifier and
the preamplifier output to the Bentos sphere penetrators
while the power supply input is made with a keyed
three-prong Jones connector.

Power drain on various components of the system
is a serious consideration when trying to maximize

on-station data collection time. It is also desirable to have the system sealed and made ready for sea prior to transportation to the ship. Thus, an externally actuated magnetic activation circuit is employed. This circuit shown in Figure A.2 employs a normally open reed switch. The reed switch affixed to the top inside of the glass sphere is closed when a magnet is placed in its vicinity from outside the sphere. The closed circuit biases transistor switches closed cutting off power to the preamplifier. This arrangement is advantageous as it allows packaging in advance of the of the deployment date. It should be noted however, that this circuit does deplete a nominal amount of power; so final packaging is usually completed one day in advance of deployment.

b. Instrumentation Subsystem

The function of the instrumentation subsystem is to receive the two analog outputs from the preamplifiers, condition them to the requirements of the follow on circuitry, multiplex the channelized signals, convert them from analog to digital format and pulse code modulate them for input to the fiber optic data link.

(1) Equipment Mounting Assembly The equipment mounting assembly is shown in Figure 2.5. Constructed of aluminum it supports two Benthos glass spheres, housed in Benthos hardhat enclosures. One sphere houses the instrumentation subsystem while the other has a battery pack to power the optical transmitter. In addition, the optical transmitter assembly is attached to the vertical member of the mounting assembly. The design incorporates quick release clamps for rapid engagement or disengagement from the main support line (250 feet of 1 inch polypropylene line).
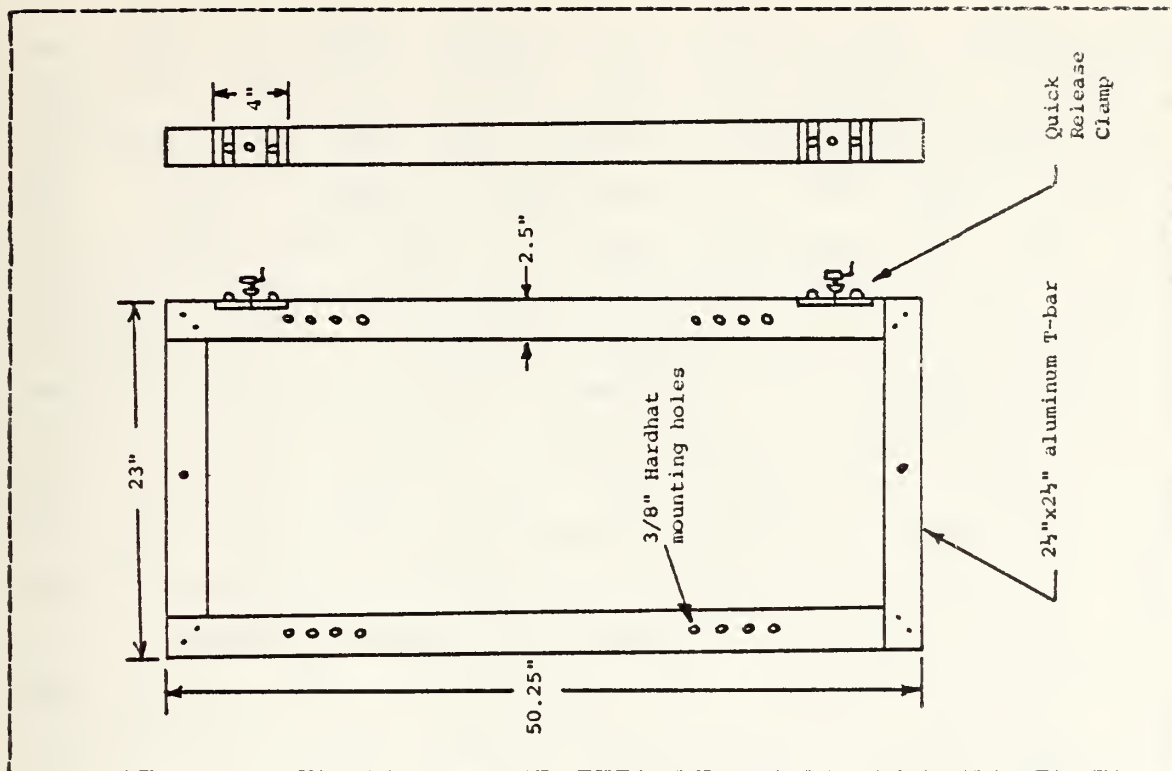
Figure 2.5   Instrumentation Subsystem Equipment Mounting
              Assembly

(2) Signal Conditioner The signal conditioners
receive the analog signals from the coil preamplifiers in
parallel fashion, amplifies them on the order of 30 dB and
limits signals with peak amplitudes greater than 7.5 volts.
The circuit is presented in Figure A.3.

(3) Pulse Code Modulation (PCM) System The pulse
code modulation system chosen for use in the ocean floor
geomagnetic data collection system is one designed and
manufactered by Dr. Robert Lowe, Lowecom Inc., also of
Scripp's Institute of Oceanography, La Jolla, California.
The device, schematically illustrated in Figure A.4 and A.5
features 15 channel analog input capability and offers the
option of selectable rates of 2^n samples per second, where n

27

may take on integer values of 3 to 7. By appropriately jumpering the analog input pins, the sampling rate may be increased five fold. The system is currently deployed with the coil-x output connected to PCM input channels 1,4,7,10,13 and coil y output connected to PCM input channels 2,5,8,11,14 with the remainder of the channels grounded. With a selected sampling rate of 32 samples per second, this configuration results in 160 samples per second of each coil's signal. While channel input capacity and sampling rate capability are much greater than current needs dictate, they provide growth potential. The additional channels could be utilized for a three coil system, input from a pressure sensor for swell wave data, temperature sensor, or real time clock data. The PCM system design includes the option for analog or digital data output from channel 14 with a minor change in the external pin interconnections.

The PCM system incorporates a crystal oscillator and associated CMOS integrated circuitry to develop the clocking pulses, a 16 channel CMOS analog multiplexer, a 16 channel, 12 bit CMOS analog-to-digital converter and associated circuitry to provide the pulse coding. The crystal clock oscillator operating at a frequency of 24.576 KHz produces a square wave output with a loss bit rate of 1 bit in one million. This frequency combined with the inherent delays of the associated clock-logic circuitry provides the 128 samples per second sampling rate. By external pin interconnections, the other sampling rates may be selected. The clock pulses gate the analog multiplexer, digital-to-analog converter and follow on associated circuitry that form the pulse code words. The basic output is a bi-phased pulse coded signal that is adjusted to TTL standards by adjustments to the offset and gain trimmers, P2

and P3 respectively. The data is organized in frames. Each frame is headed by a sync code word which is followed sequentially by the pulse coded samples from PCM channels 1 through 15. The sync code word is a pulse coded digital word with a decimal value between 0 and 4096. This word is preselected and hardwired on the circuit board by connecting a logic high or low, as appropriate, to pins a through i and k through m. The sync code word is essential to the decoding process. Additionally, it provides protection against confusing the land acquired data with that taken from the ocean floor as each system has its own sync code word. Currently sync code words 3538 and 2520 are associated with the land and sea sites respectively. Sync code word 3155 had been used in test and sea floor data collection before the September runs. The 3155 board also had plus or minus 5 volt range on the A/D converter while all other boards where plus or minus 10 volts.

Gould Gelyte rechargable batteries (plus and minus 12 Volt and ground) are utilized for all power requirements within the instrumentation sphere. The current consumption of the preconditioner and the PCM system is approximately 28 ma. at the 32 sample per second rate.

The externally actuated magnetic activation circuit described in section II.A.1.a.(3) is utilized to activate the instrumentation sphere equipment upon deployment.

The equipment interconnections are all coaxial except that the power input is made with a keyed three pronged plug and socket connector. Care must be taken to ensure the x and y coil output leads are connected to their respective PCM inputs.

Appendix D discusses the details of data flow in the PCM system utilized in the generation II geomagnetic data collection system design.

c. Optical Data Link

The optical data link eliminates the concern of antenna effect discussed briefly in section I while introducing a variable length section in the system that gives flexibility for operations at various depths. Fiber optic system design considerations as well as an overview on the theory and state of fiber optic technology are discussed in Appendix E.
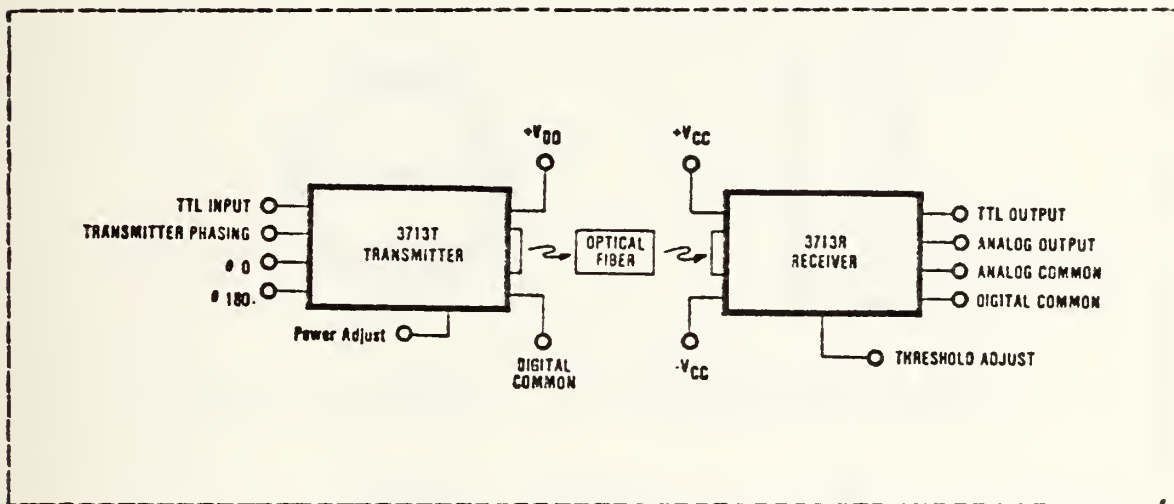
Figure 2.6 Simplified Block Diagram of the Optical Data Link

The fiber optic data link consists of an optical transmitter and receiver each housed in an environmental enclosure and connected by a fiber optic cable (see Figure 2.6). During deployment the cable is stored on and dispensed from a plastic reel fashioned from a 20 inch bicycle rim (see figure 2.7 for details).

30

25.5"

3.5"

16.5"

Optic Receiver
PVC Enclosure

Optical Cable
Storage Reel
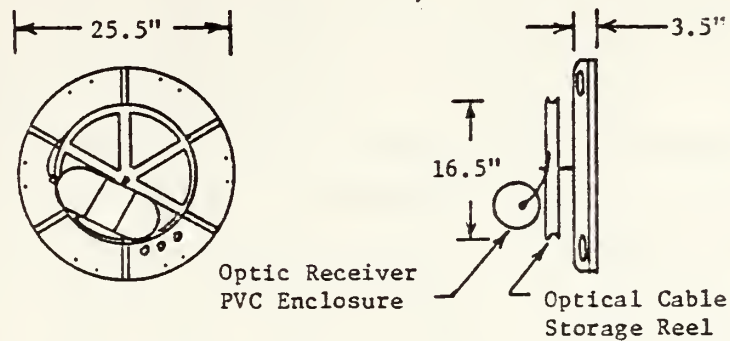
a. Top View Cover (Side 1)   b. Side View Cover (Side 1)

23"

12"
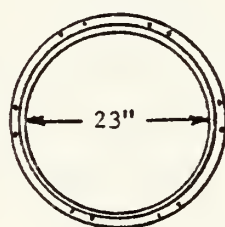
c. Top View Buoy Cylinder   d. Side View Buoy Cylinder

Quick
Release
Clamps
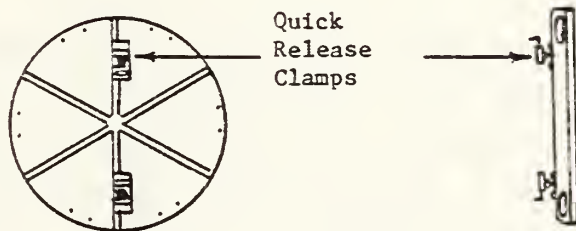
e. Top View Cover (Side 2)   f. Side View Cover (Side 2)

Figure 2.7   Diagram of Can Buoy and Optic Receiver Assembly

31

(1) Optical Transmitter/Receiver Set The optical transmitter and receiver are the Burr-Brown 3713T and 3713R respectively. The 3713T and 3713R when connected by a suitable fiber optic cable form a 250 Kbaud NRZ fiber optic data link capable of operation to 1.7 kilometer. The 3713T fiber optic transmitter is an electrical-to-optical transducer designed for digital transmission over single fiber channels. Transmitter circuitry converts TTL level inputs to optical pulses at data rates from DC to 2 Kbaud NRZ.

The 3713R fiber optic receiver is an optical-to-electrical transducer designed for reception of digital data over single fiber channels. The receiver circuitry converts optical pulses to TTL level outputs with a receiver sensitivity of 15 nW and data rates to 250 Kbaud NRZ.

An integrated optical connector on both the 3713T and 3713R allows easy interfacing between modules and optical fiber without problems of source/fiber/detector alignment. The metal packages of the 3713T and 3713R provide immunity to electromagnetic radiation and direct printed circuit board mounting with no additional heat sink required.

A simplified block diagram of the 3713T transmitter is shown in Figure A.5. The input stage uses a Schimitt Trigger Exclusive OR Gate 3, for noise immunity and its logic is configured so the phasing of the transmitter is pin programmable. When the transmitter phasing terminal is connected to theta-0, the light output is in phase with the digital input signal. The LED is on when the TTL input is high. Connecting the transmitter phasing terminal to theta-180 causes the reverse to happen: the LED is on for a digital low. This option is selectable on the ocean floor geomagnetic data collection system through the installation of a single pole, double throw switch. The system is

32

operated in the in-phase mode. The advantage of the theta-180 mode is it makes it possible to detect a break in the fiber cable when the data link is idle. However, an idle PCM signal does not provide a continuous TTL low and thereby obviates the advantage. Amplifier A1 and the current switch drive a light emitting diode (LED). The optical power output of the 3713T transmitter may be adjusted by controlling the resistance between the power adjust pin and ground. This controls the peak or "on" current in the LED. When the resistor is minimum the LED output is maximum and as the resistance is increased, the LED output asymptotically approaches a minimum value. In the ocean system the resistor is adjusted to provide a 240 millivolt peak-to-peak receiver output signal.

A simplified block diagram of the 3713R receiver is shown in Figure A.7. Input light is converted to a current by the PIN photodiode CR1 which is connected in the photovoltaic mode for maximum sensitivity. A low bias current FET input current-to-voltage converter transforms the diode current into a voltage (Va) which is further amplified by A2 and presented to comparator A3 as Vb where it is compared to the threshold voltage Vt. For maximum noise immunity it is desirable to have the threshold voltage set to a value corresponding to a level half way between the high and low value regardless of the actual light level at the input. In the 3713R, this is accomplished by a peak detector automatic threshold circuit. A pulse of light input causes a voltage pulse at Vb which is stored in the automatic threshold circuit, divided in half, and supplied to the comparator as the threshold input Vt. Thus, Vt is a voltage corresponding to the midpoint of the light and no light conditions of the diode. Since the automatic threshold circuit uses a capacitance hold technique, the threshold

voltage Vt is subject to decay when the light is removed from CR1. A no-light condition of approximately 0.5 second duration (a 1 baud data rate) can be used with no significant effect on noise immunity. The PCM system presents data to the optical data link at about a 5K baud rate and is therefore within the conditions for maximized noise immunity. The analog output terminal of the 3713R is the output of the linear amplifier A1. The voltage at this terminal is proportional to the input power to the receiver. As such, it makes an excellent diagostic point for testing the fiber optic cable. Monitoring the analog output terminal gives a relative measure of cable loss at the transmitted wavelength and a direct measurement of receiver signal-to-noise ratio when the transmitter is off. In the ocean floor geomagnetic data collection system the modulation input is taken from the optical receiver analog output since the output amplitude can be adjusted by varying the optical transmitter power adjust resistor. An output level of 200 to 240 millivolts is utilized to ensure RF transmitter modulation without overdriving its circuits.

(2) <u>Fiber Optic Cable</u> The fiber optic cable is described in detail in appendix E. The fiber is a 63.5 micrometer radius, low noise, graded index, multimode, single strand optical fiber cladded and sheathed with strength members as illustrated in Figure E.2. Approximately 300 feet of type 5058 cable is stored on the storage reel shown in Figure 2.7.a. The fiber optic link gives flexibility in system operating depths as all other system parameters are fixed. The cable is affixed to the polypropylene line with electrical tape at about ten foot intervals with some slack to allow for stretching of the main support line. The electrical tape is fastened in such a way as to provide a tab that aids in quick removal during recovery.

(3) <u>Couplings</u> The coupling system ultilized is
the AMP Optimate Single Position Fiber Optic Cable Connector
System. Since AMP connectors were not available with
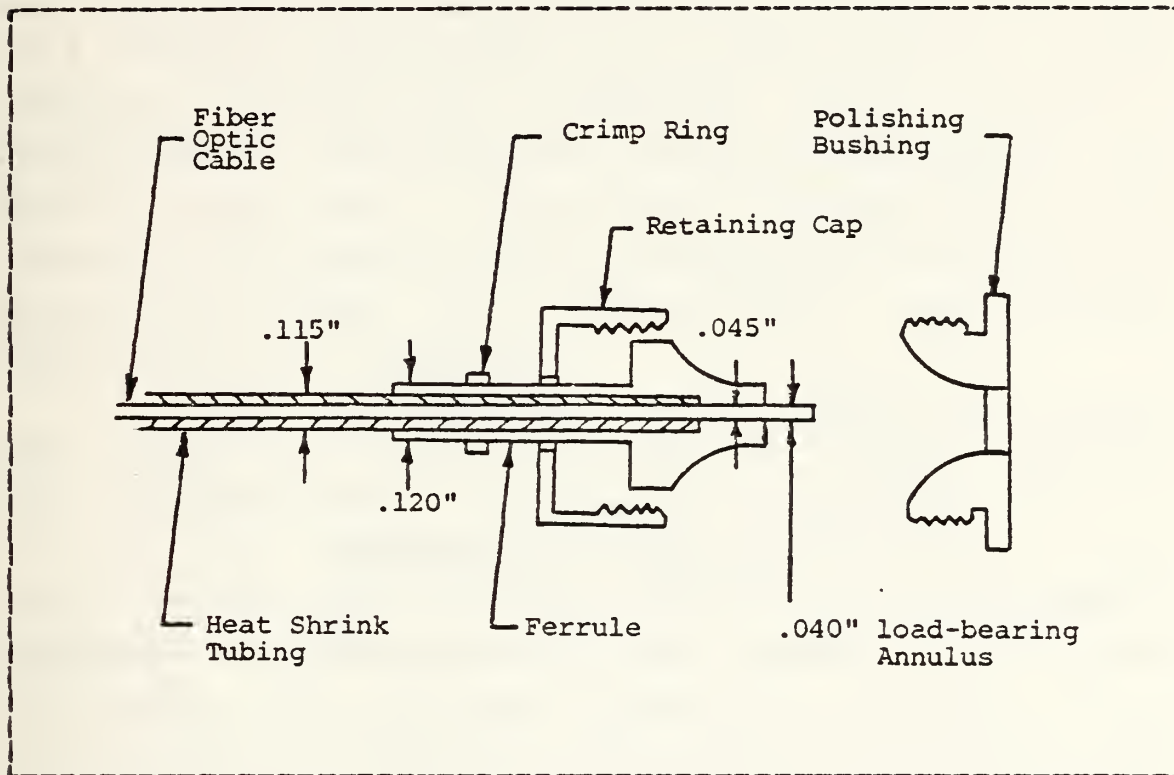
Figure 2.8   Fiber Optic Cable Connector Assembly

parameters compatible with the fiber optic cable intended
for the system's optical data link, the fiber optic cable
was given an additional jacket of heat shrink tubing. The
heat shrink tubing builds up the outside diameter of the
cable to near that of the inside diameter of the connector
as shown in Figure2.8. The optic cable is allowed to extend
about 1/16 inch from the face of the connector. The cable
and the heat shrink tubing is bonded to the connector shaft
by a few drops of cyanoacrylate glue. The retaining cap is

35

secured in a position about the ferrule by the crimp ring
mounted 1/16 inch behind the cap. The polishing bushing is
placed over the connector and securely mated to the
retaining cap. The polishing is accomplished by applying a
figure eight motion to the fiber against various grit abra-
sive paper while it is submerged under a half inch of water.
A 9 X 9 inch aluminum baking pan is very suitable for the
procedure. Polishing is accomplished using 5 grades of
silicon carbide finishing paper; 320,400,600,3 micron, 0.3
micron in that order. The polishing is completed when the
surface of the polishing bushing immediately surrounding the
ferrule is polished to a glossy finish. The polishing
bushing should not be reused.

        The AMP connectors remove concern of optical
power losses due to lateral misalignment, angular misalign-
ment, end separation and end preparation quality.

        (4)   Environmental Enclosure The optic trans-
mitter and receiver are each housed in an environmental
enclosure that maintains water-tight integrity in the ocean
environment. The enclosure illustrated in Figure 2.9 is
manufactured from 6 inch I.D. PVC pipe. One end of the pipe
and its associated end cap are machined to a true round as
near to initial dimensions as possible. Typical finished
dimensions are :

        PVC PIPE   I.D.   6.090 ± 0.003 inches
                     O.D.   6.600 ± 0.003 inches
        PVC END CAP I.D.   6.615 ± 0.015 inches

An "O"-ring groove is machined to 0.093 inches deep by 0.160
inches wide located 0.75 inches from the machined end of the
pipe to conform with a 6.25 X 1/8 inch "O"-ring. The pipe is
reinforced with rings made of 0.75 inch sheet PVC material.
These rings are slotted 0.25 inch below ring center to serve
as a support for the optical transmitter or receiver circuit

boards. The machined end cap is fitted with two Brantner connectors and a vent plug. The opposite end cap is fitted with the fiber optic through-hull penetrator. All these fittings are equipped with an "O"-ring seal. The end cap supporting the fiber optic through-hull penetrator is bonded to the unmachined end of the pipe with PVC cement. The fiber optic cable is passed through the penetrator and initially fastened with cyanoacrylate glue. A final treatment of DEVCON 5-minute epoxy serves to secure the cable/penetrator interface.

The fiber outside the penetrator is protected from bending stresses by application of three layers of heat shrink tubing that extend into the penetrator. Each layer of tubing is longer in length than the preceding one so that the cable flexibility increases as a function of distance from the penetrator. Initial design tests indicated the weakest point in the optical link was the point at which the cable entered the penetrator. Tests subsequent to the application of the tubing indicated this point to be one of the strongest.

(5) Battery Power Supplies The optic transmitter is powered by a 6 volt, 8.5 AH rechargeable sealed lead acid battery configured with a 100 ohm series limiter resistor. This battery is housed in a Benthos glass sphere mounted with the instrumentation sphere in the equipment mounting assembly discussed in II.A.1.b.(1).

The optic receiver power supply is a Gould Gelyte (+ 12, - 12 volt and ground) battery pack mounted in the can buoy. The battery pack is rated for 18 AH.

d. Can Buoy

The can buoy, illustrated, in Figure 2.7, provides 71 pounds of positive buoyancy (this is inclusive

37
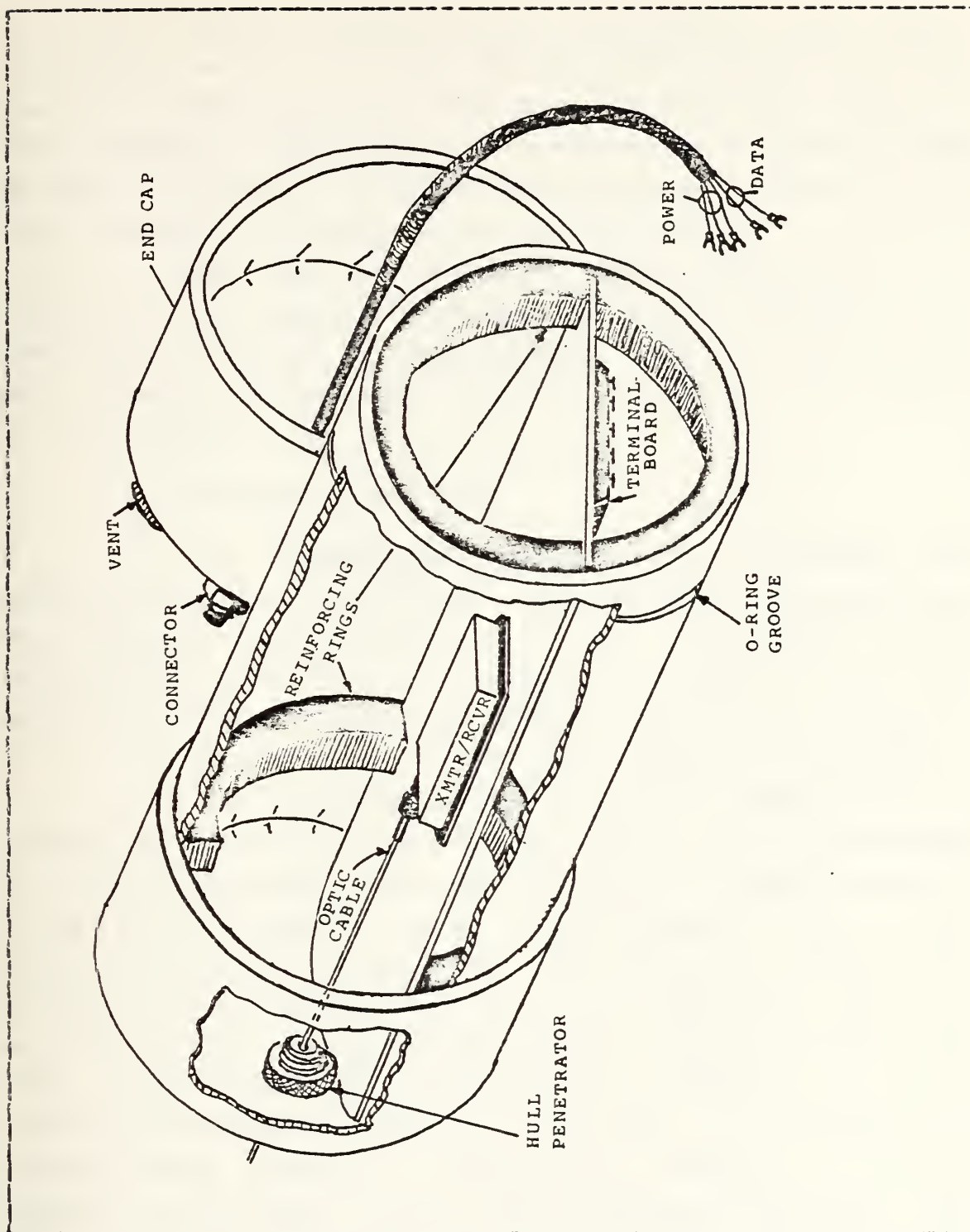
Figure 2.9   Optic Transmitter/Receiver Enclosure

of battery weight) to the system. It contains a Gould Gelyte rechargable (+ 12, - 12 volt and ground) battery pack that powers the optic receiver. The power is delivered through a three conductor cable equipped with Brantner connectors. The can buoy is fitted with additional Brantner connectors for data transmission in and out to the spar buoy.

The axle of the fiber optic storage reel is mounted in the center of the can buoy cover containing the electrical connectors. The opposite cover is fitted with quick release clamps which are used to secure the buoy to the main support line.

e. Telemetry Spar Buoy

(1) Description The spar buoy designed and constructed by Dr. M.E.Thomas, Applied Physics Laboratory, Johns Hopkins University and LT. P.M. Rutherford, Naval Postgraduate School [5], is depicted in Figure 2.10. The spar buoy is partitioned into several·sections as follows:

(a) Transmitter Power Supply/Lead Ballast

Including the dampening plate, this is the bottom two feet of the NPS spar buoy. It is constructed of 5 inch PVC tubing. This section contains three 6 volt/8.5 AH lead acid batteries, which provide power to the transmitter, plus ninety pounds of lead weights. Water tight integrity is maintained by a 3/4 inch thick PVC plug with two "O"-rings to aid in pressure sealing (Figure 2.11). The power leads from the batteries are soldered to a pin assembly permanently housed in the plug. The transmitter receives power through a cable which attaches to the pin assembly in the plug by way of a Brantner connector. The slip coupling adjoining the bottom and free flooding sections is permanently adhered to the bottom section with PVC cement.

(b) Free-Flooding Section

The purpose of the free flooding section is primarily to enhance the separation of the center of buoyancy (cb) and the center of gravity (cg). This section is constructed of a 5 foot length of 6 inch PVC pipe. A series of holes are drilled towards the bottom of the section to act as flood ports. Holes at the top are vents. The power cable from the batteries to the transmitter traverses this section.

(c) Middle Section

This section is composed of three sub-units, the lowest portion housing the transmitter. The transmitter utilized is taken from a P3C Orion sonobuoy system. It has a power output of one watt and operates in channel 29 at a frequency of 171.65 MHz. Its watertight integrity is maintained by a PVC plug identical to that between the lower and free flooding sections. The power cable leading from the bottom plug is attached to this plug with a Brantner connector. Precautionary measures that are to be taken during this portion of the assembly will be discussed in the next section entitled transportation and assembly. Just above the transmitter housing is the buoyancy collar shown in Figure 2.12. The collar provides the spar buoy with an additional eighty pounds of positive buoyancy, again enhancing further separation of the cb and cg. The remaining portion of the middle section is composed of the middle mast which houses the transmitting cable leading to the antenna. This middle mast is reinforced by 1/2 inch and 1 inch PVC tubing. The 1/2 inch sections are each individually sealed. The 1 inch section serves as a channel for the transmitting cable. This section is sealed using a PVC ring and adhesive. The antenna cable protrudes through the center and the hole is made water tight with application of silicon based rubber sealant.
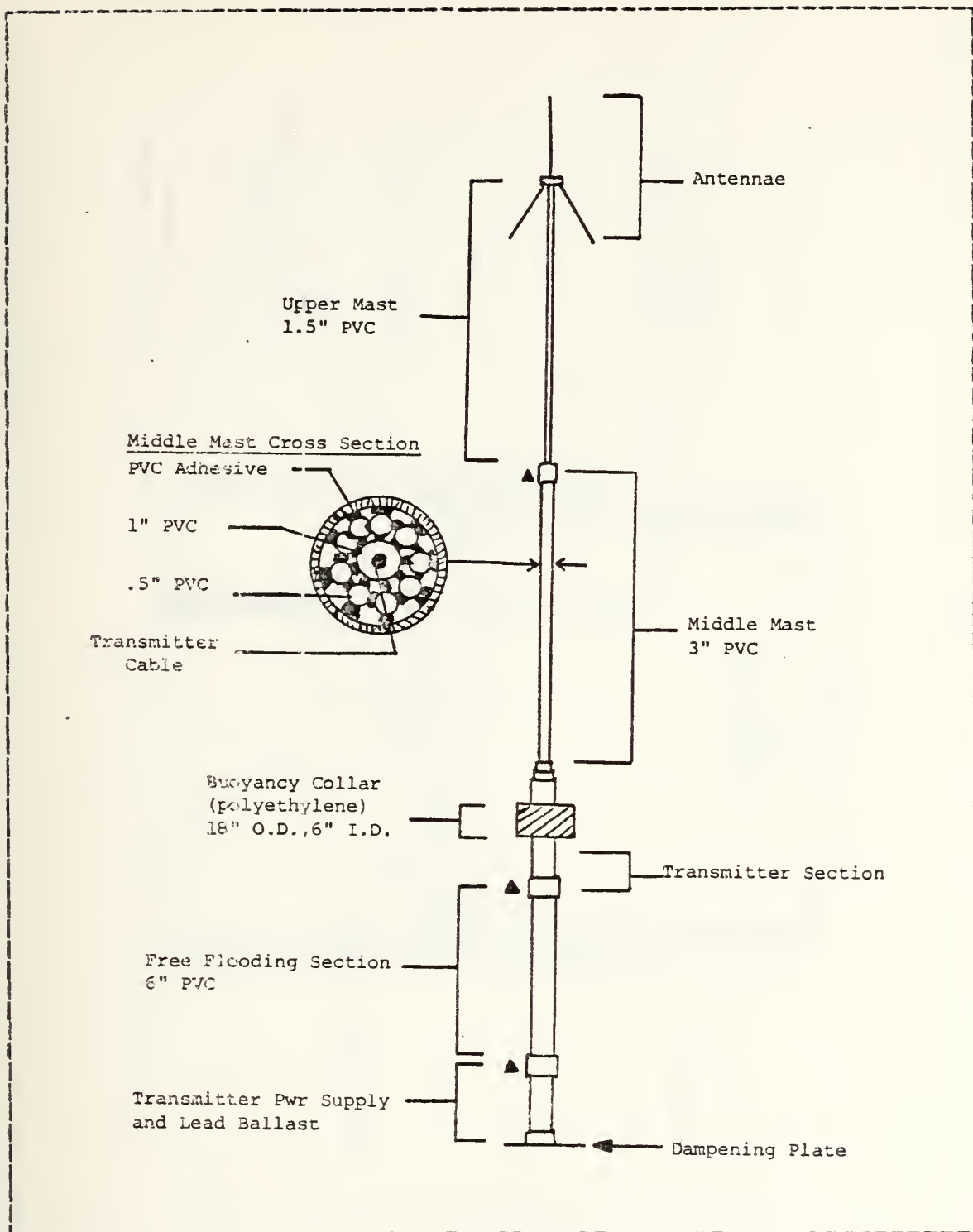
Figure 2.10   Illustration of the Telemetry Spar Buoy

41
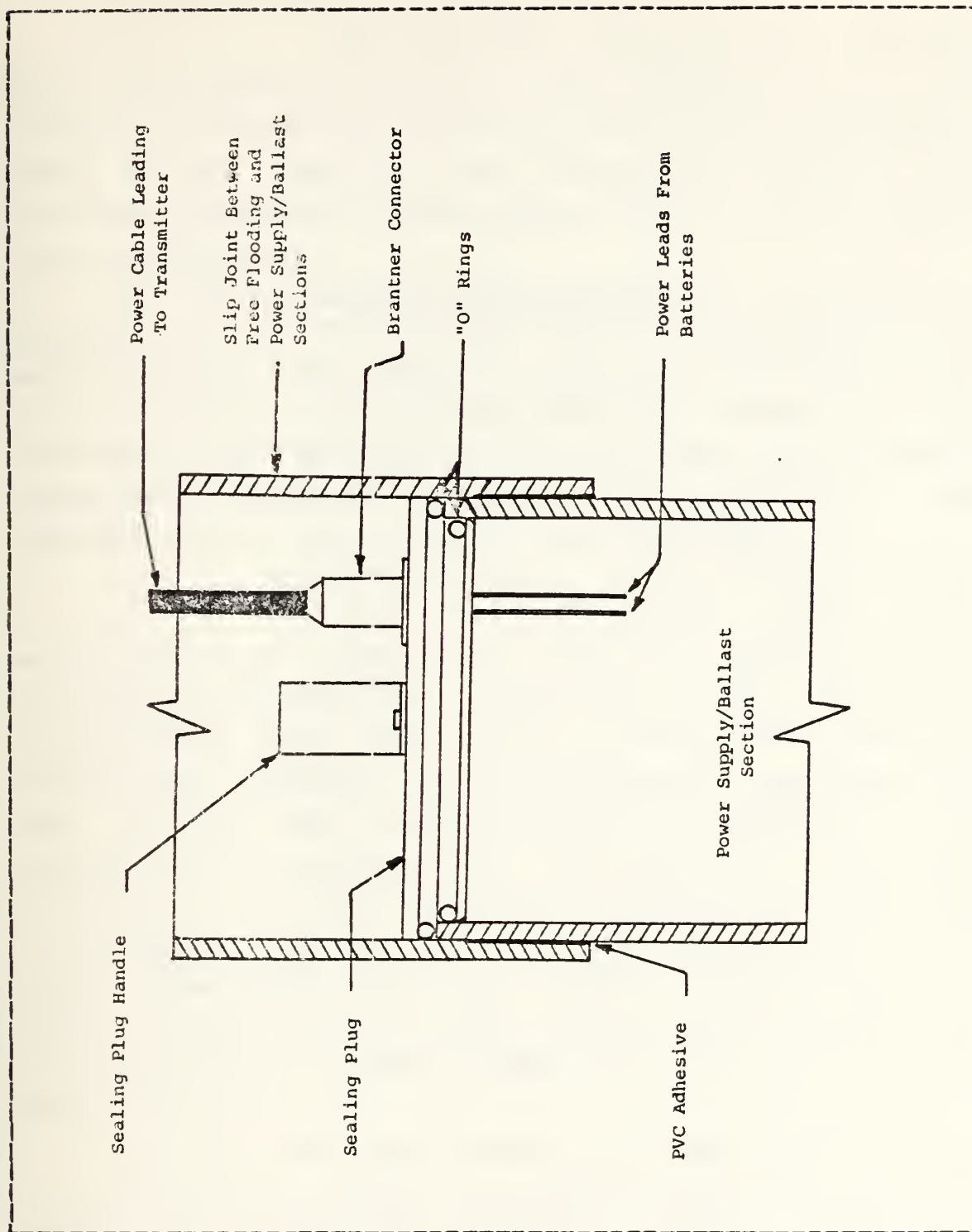
Figure 2.11   Seal Design for Free Flooding and Power
Supply/Ballast Sections

42

(d) Upper Mast/Antenna

The remaining portion of the telemetry spar buoy consists of an eight foot section of 1/2 inch PVC tubing. It houses the remaining length of the transmission cable and is capped by the transmitting antenna which utilizes a reflecting ground plane which is at 150 degrees from the vertical.

(2) Transportation/Assembly The spar buoy is transferred to and from the R/V Acania via a pickup truck in most instances. This method of transportation requires that the spar buoy be easily broken down into lengths that are compatible with the length of the pickup bed. The following subsections discuss the procedures for the assembly of each affected section and the precautions required.

(a) Power/Ballast and Free Flooding Sections

Place the lead ballast in the bottom section prior to inserting the batteries. Ensure that the "O"-rings are sufficiently coated with a thin film of high vacuum grease. Insert plug so that it snuggly fits below the marked level. CAUTION: prior to connecting the power cable jack to the plug, ensure that the indentation in the Brantner plug is lined up with its counterpart on the jack. Failure to do so could damage the transmitter by reversing the polarity. Next slip the free flooding section into the joint. The holes that allow flooding are to be at the bottom. Ensure that the marks on both slip joint and free flood section are aligned. Bolt the free flood section in place.

(b) Free Flooding and Middle Section

Prior to joining these two sections, insert the transmitter assembly. First, connect the transmission cable then slide the transmitter in place again ensuring a snug fit and proper placement of the plug in line
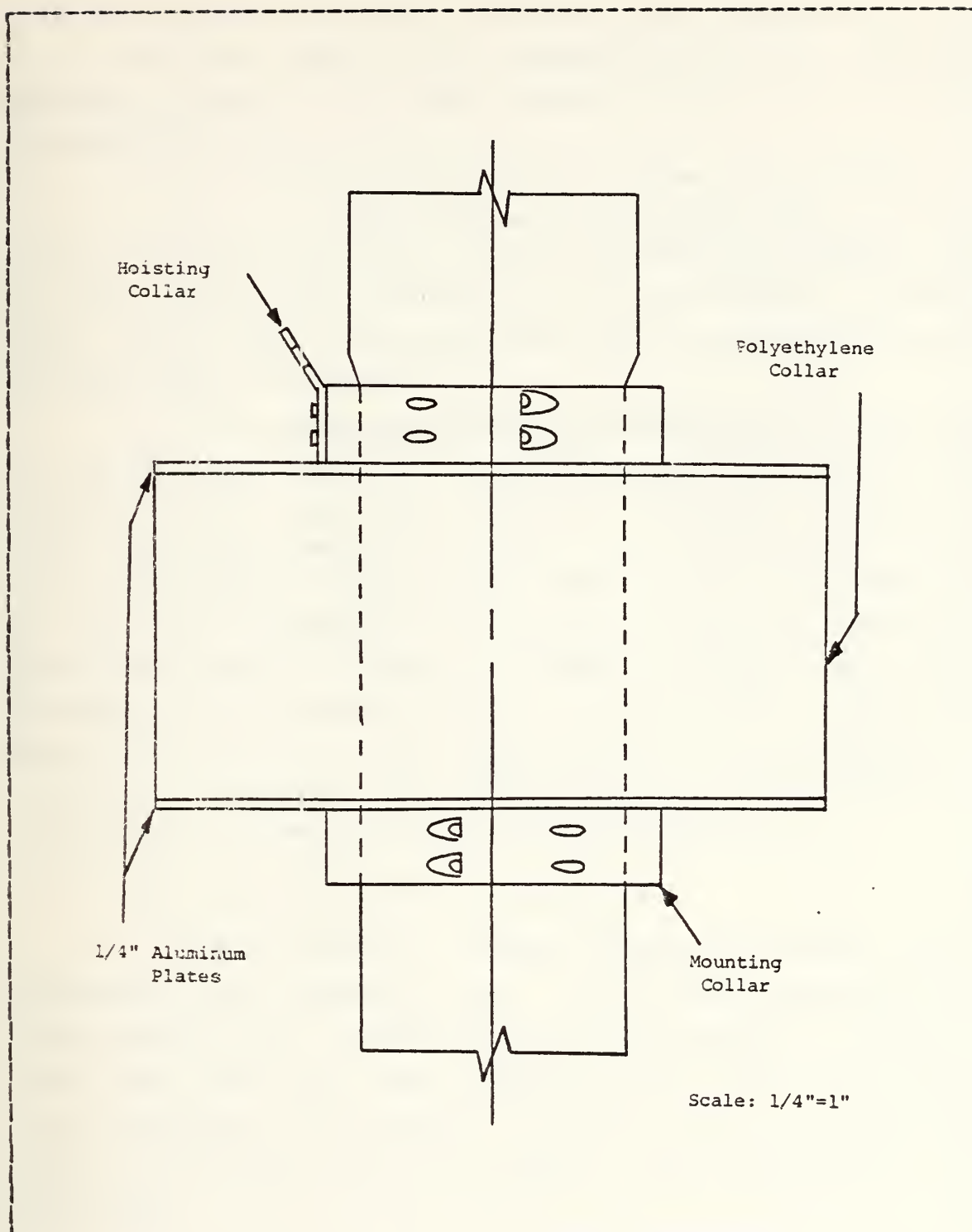
Figure 2.12   Telemetry Spar Buoy Buoyancy Collar
                    Illustration

with the interior markings. CAUTION: it is important to have a 50 ohm dummy load on the transmitter at this point of assembly since it is being powered without the antenna attached.

(c) Middle Section to Upper Mast/Antenna

This portion of the spar buoy is to be bolted in place while the remaining portion is hanging over the side of the ship hoisted up by the Acania's on board crane. Ensure that the transmission cable is connected prior to upper mast attachment.

(3) Deployment/Recovery/Disassembly All sections of the spar buoy shall be assembled onboard the Acania with exception of the upper mast prior to deployment. Attach the crane line approximately five feet up from the tether point on the spar buoy. Once lowered over the side, the buoy can be temporarily secured to the ship's railing and lowered an additional amount to enable attachment of the upper mast. The buoy is next lowered into the water and tended along side until the rest of the system components are deployed.

Recovery and disassembly is accomplished by following the reverse of the above procedure.

f.   Receiving Station Equipment

The receiving station equipment consists of an AN/ARR-52A radio receiving set, an HP 3964A instrumentation tape recorder and two dual trace oscilloscopes. AN/PRC 77 radio sets serve as a voice communications link. The equipment arrangement is as shown in Figure 2.13. The antennas used in conjuction with the telemetry link are double, tuned YAGI type.
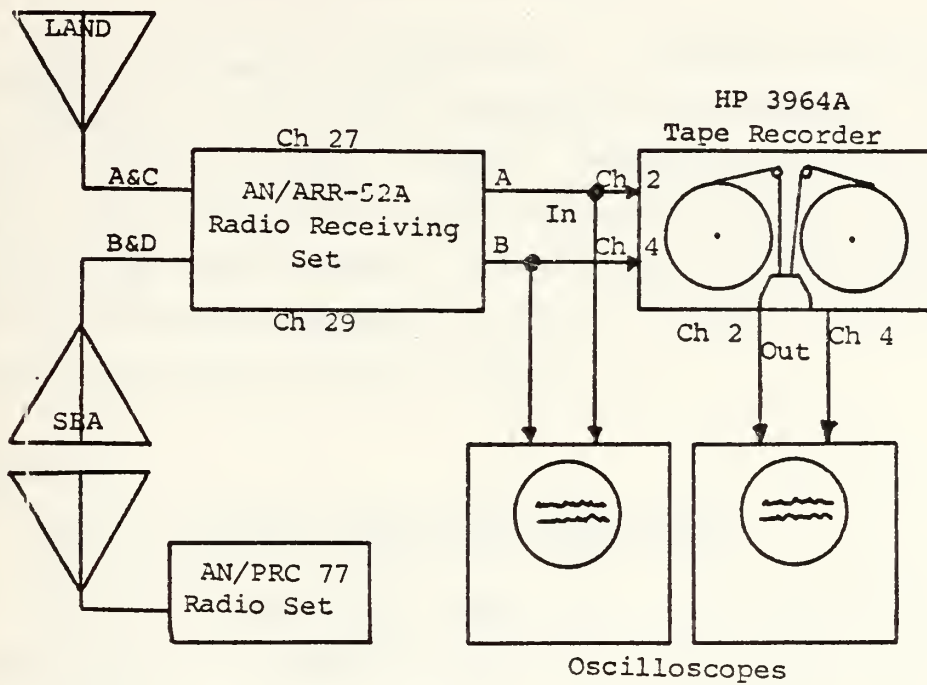
Figure 2.13   Receiving Station Equipment Configuration

III. DATA PROCESSING

Currently the data is processed to develop various data plots generated on the Naval Postgraduate School's IBM 3033 computer. Prior to the actual generation of the plots however, the PCM encoded data which was stored on analog tape utilizing the equipment described in section II.A.1.f. (receiving station equipment) must be decoded, digitalized, and transcribed onto digital tape.

A. HARDWARE

1. PCM to Digital Conversion Equipment

Several electronic components are utilized to decode the PCM data to discrete analog form and then to digital form which is ultimatly stored on 9 track digital tape. This data processing system is shown schematically in Figure 3.1, illustrating data flow and control links. Central control of this process is accomplished with a Hewlett Packard 9845A computer utilizing an operator interactive program titled "PCM PROG". After execution of the program, the computer requests entry of specific function control parameters into the computer and other equipment. These inputs are used to control synchronization of equipment start, digital tape drive speed, decode rate, decode time, and synchronization code word entry into the decoder. The PCM encoded data is fed into the system from the HP 3964A 4 channel tape recorder previously used to store the data. Utilization of a different recorder may introduce noise due to a difference in head alignment and drive speeds. Such noise decreases the signal-to-noise ratio upon which decode synchronization

depends. Should decode synchronization not occur, a lower
analog tape drive speed and sample rate must be selected,
resulting in longer processing time. The decoding of the
PCM encoded data is accomplished with a Marine Profiles,
Inc. Model 319 PCM decoder. Two Monsanto AM-6419/USM-368
oscilloscopes are used to display the PCM encoded data and
the discrete analog data. The discrete analog data is
processed by the computer to develop the digital data which
is recorded on 6250 bpi/1200 ft. 9 track digital storage
tape. A Kennedy Model 9800 digital recorder and computer
interface are employed for that purpose.
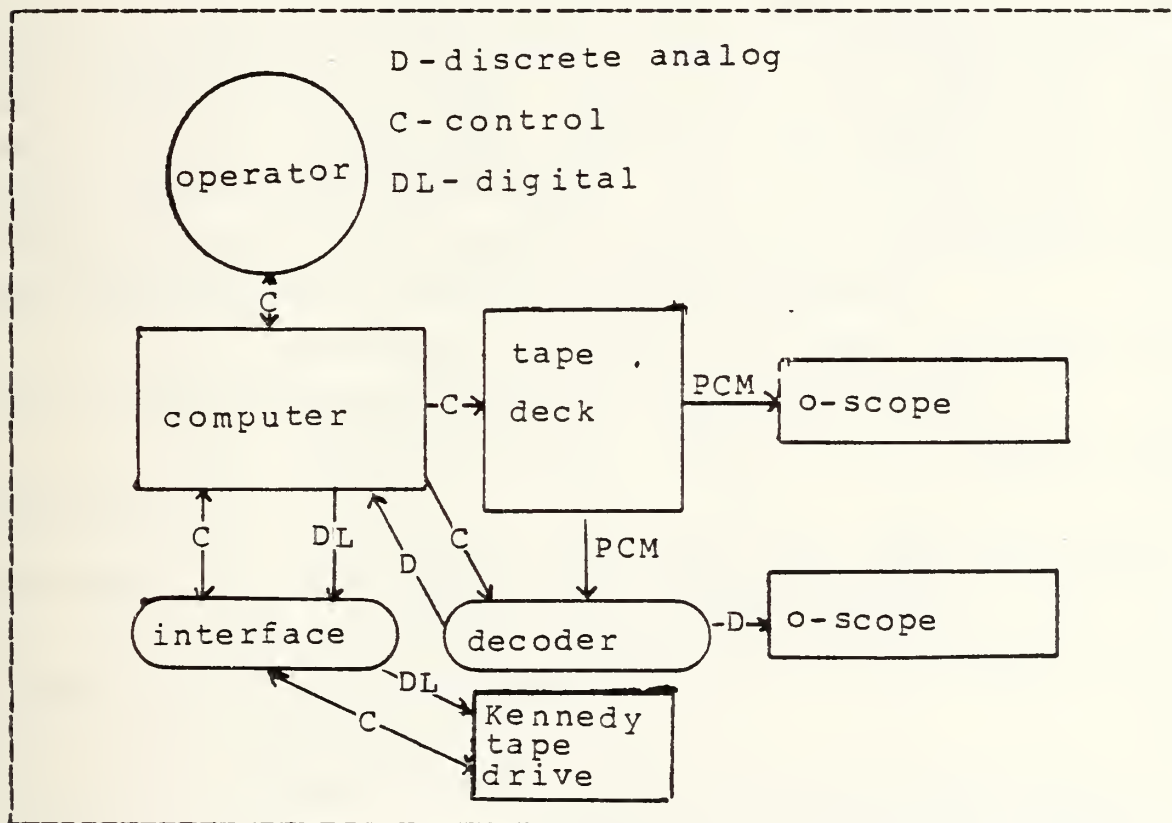
Figure 3.1   Decoding System Data Flow and Control

48

a. Decoding Procedure

The following steps illustrate the procedure for
decoding the PCM encoded raw data into digitalized data and
then placing it onto a 9 track digital tape which can then
be delivered to the IBM 3033 computer for data processing.

1. Disconnect the coaxial cable labled number 7
from the output of the HP 3968A tape recorder located in the
equipment rack adjacent to the HP 9845A computer.

2. Connect cable 7 into the output channel
desired for decoding of the HP 3964A 4 channel tape
recorder.

3. Energize the HP 3964A tape recorder, the two
Monsanto AM-6419/USM-368 oscilloscopes, the Kennedy interface
and AANDERAA tape transfer interface, the model 319 PCM
decoder, and the HP 9845A computer (the ON/OFF switch is
located on the right hand side). Also, on the PCM model 319
decoder place the fan toggle switch in the UP position and
the AC/DC/OFF toggle switch to the AC position.

4. Place into the right hand side tape reader of
the HP 9845A computer the program named "PCM PROG".

5. Mount the analog tape onto the HP 3964A tape
recorder.

6. On the HP 9845A computer, type the command
GET "MT" and press EXECUTE to initiate processing.

7. On the PCM decoder place the following func-
tions to the listed positions:

        SOURCE - 1
        SAMPLE RATE - 64 (for 3 3/4 recorder speed)
                     - 128 (for 7 1/2 recorder speed)
        INVERT/NORMAL - NORMAL
        OUTPUT/SAMPLE RATE - 0
        RECORDS/FILE - INFINITY
        SYNC CODE - 000

8. Press RUN on the computer, ignore "enter y to skip tape init" (displayed on the computer's CRT), and press CONTINUE.

9. The computer now indicates "load tape" into the Kennedy unit and "put on line". To do this energize the Kennedy unit, load the tape according to the diagram located on the inside of the unit's door, press the LOAD button and the ON-LINE button located on the front on the Kennedy unit.

10. The computer now indicates "enter sync code". Type into the computer 3658 or 3155 as appropriate for the sea system or 2620 for the land site system and press CONTINUE.

11. Enter transfer time in minutes and seconds into the computer. Example 20 minutes and 20 seconds would be typed in as 20,20. After this is done press CONTINUE.

12. Push the STOP switch on the PCM unit and push CONTINUE on the computer.

13. Push the START switch on the PCM unit simultaneously with the PLAY button on the Hewlett Packard tape recorder.

14. If data transfer must be ended early, push the KO button on the computer to halt data transfer. If this option is elected then T must be entered on the computer following the KO command to write end of tape to the tape.

15. "End of run" will be indicated on the computer CRT. At this time deenergize all the equipment and disconnect cable 7 from the 4 channel tape recorder and reconnect it to the 8 channel tape recorder located in the equipment rack.

16. Finally, remove the yellow ring from the digital tape to ensure that the tape is not inadvertently over written.

2. Main Computer Hardware

The data is read from the digital tape into the IBM 3033 computer via software developed by Lcdr. J. Fisher of the Naval Postgraduate School. The data is unpacked (placed into a format where it can easily be accessed and manipulated) and converted into a spectrum of frequencies using a Fast Fourier Transform routine. This data is then plotted using a peripheral Versatec plotter for spectral display.

B. SOFTWARE

The programs are written in the FORTRAN IV programming language and are briefly discussed below.

1. Test Program

The test program shown in Appendix F was developed to test the computer manipulation against known data to ensure the resulting plots would meet expectations. With the exception of the internally generated data, the program is essentially the same as the Main Program shown in Appendix H and explained in paragraph 3 below.

2. Mass Storage Program

The digital data tapes are unlabled with data organized in 16 word frames, the first word of which is the sync code followed by 15 data words. The data words are organized x,y,z,x,y,z,.... . Since the sea system has only two sensor coils at this writting, the z data is zero. The land system data has actual values for x,y, and z. The data from both a land and sea data tape is entered into the IBM 3033 computer mass storage system (MSS) utilizing the mass storage program shown in Appendix G. Currently only the x and y coil data is read into MSS where it is available for access by the Main Program.

3. Main Program

The Main Program utilizes the x and y coil inputs from simultaneous land and sea data to develop various plots for comparision and analysis. The Main Program utilizes a large number of arrays with the intention of maintaining each bit of original data or calculation, ready for recall at any time for futher computation. Equivalent arrays are employed because the plotting routine is not able to handle complex arrays. Ocean arrays are indicated with the suffix 'O' and land arrays with the suffix 'L'. By successive calls of "SUBROUTINE RD", an array of the x data and y data called xxx(I) and yyy(I) respectively is established. One such array is called a block of data. The data words in the array are integer values between 2048 and 4096.

After a block of data is entered, the integer values are converted to complex values of voltage as seen at the front of the PCM board between -10.0 and +10.0 volts for systems utilizing PCM boards with sync codes of 2620 and 3653. For systems utilizing sync code 3155 the voltages vary between -5.0 and +5.0 volts. The xxx and yyy arrays represent data taken from the x and the y coils respectively without application of the system transfer functions.

The voltage values (which vary over time) are transformed into the frequency domain by utilizing the subroutine "FOURT" which performs a Fast Fourier Transform (FFT). It utilizes the Cooley-Tukey FFT algorithm.

This section of the program applies the system transfer functions to the data that has been transformed into the frequency domain. The discussion of the origin of the transfer functions is given in Appendix C. The actual transfer functions vary as a function of frequency. They can however, be approximated by straight line segments for different frequency ranges. These line segments are

52

generated by least squares approximation. The data entering this section enters with units of voltage and is converted into units of nano-Teslas by the transfer functions.

The previously mentioned sections of the program are embedded within a do-loop which allows the analysis of a long period of data consisting of a number (NR) of blocks. The Ith element of each block is then multiplied by its complex conjugate, averaged and converted to power (nano-Tesla squared) and stored. Once the program has passed through the averaging loop for the last time it has computed the arithmetic average for each frequency point in the arrays.

The next section of the program calculates the Stokes parameters 0 through 3 of the individual site ortho-ganal components and the coherence of the planar circular polarization parameters between site components. The remainder of the program sets up the parameters and titles for the plots.

A more detailed description of these programs may be found in Reference [6].

IV. EXPERIMENTAL RESULTS

A. DATA QUALITY

Test data points were developed by applying a 5.0 volt peak-to-peak sinusoidal input of 1,5,10, and 15 Hz to the PCM board. The data was sampled, PCM encoded, transmitted, received, taped, decoded, digitalized, and transcribed. A computer assisted voltage vs. time plot of the 1.0 Hz data resulted in a 1.0 Hz sinusoidal signal. A plot of the transform of the 5.0 volt, 5.0 Hz signal resulted in an impulse function at 5.0 Hz. These results illustrate that the system functions as designed from the PCM input through the data processing with the exception of the application of the system transfer functions. The system transfer functions (which take into account the amplification of the preamplifier and signal conditioners as well as the transformation from volts to nano-Teslas) are described in Appendix C.

B. DATA QUANTITY

The following data acquisition period resulted in the indicated simultaneous land/sea data from La Mesa Village and Monterey Bay:

1. 10:32 AM to 2:43 PM, 25 July 1982
2. 11:22 AM, 17 Aug. 1982 to 09:10 AM, 18 Aug. 1982
3. 09:32 AM, 16 Sep. 1982 to 09:58 AM, 17 Sep. 1982

This represents 50 hours and 30 minutes of accumulated data during three collection runs.

Sections A and B above illustrate achievement of the stated goal to develop a data acquisition system with a capability to gather simultaneous land/sea data with high quality in great quantity.

C. PLOTS OF PROCESSED ACTUAL DATA

Appendix I consists of a number of actual data plots. It is not the intent here to analyze these plots but, to merely illustrate the progress of the Naval Postgraduate School's Geomagnetic Research Team effort. On-going work in data analysis includes power spectral density, coherence, correlation and directionality studies.

V. CONCLUSIONS AND RECOMMENDATIONS

A. CONCLUSIONS

The Generation II system designed for this research was successfully employed in the continuing effort of geomagnetic data collection with the specific task of recording quality simultaneous land/sea data with increased quantity over its predecessor systems. The data collected with this system was only limited by power supply capacity and by the schedule of the Research Vessel Acania.

B. RECOMMENDATIONS

A better means of positioning the sensors on the seafloor still remains a problem. The ability to accurately position and detect sensor orientation will become critical in future data acquisition and component field correlation experiments. The exact orientation method to use will be directly related to the acquisition system chosen for future measurements. A flux gate magnetometer may possibly be employed to indicate orientation of the antenna coil sensor assembly to the earth's magnetic field.

Although, the research team and the ship's crew were well versed in the system's configuration and deployment techniques, the deployment time averaged about 45 minutes as a result of the system's size and complexity. Furthermore, deployment could only be accomplished in calm seas at a maximum depth of 200 feet. To alleviate these problems the design of a generation III system is recommended. The design should include size reduction and system simplification. The simplification may be achieved by concentration of several generation III components into a single package.

56

Additional problems to overcome in future systems are the lack of robustness of the spar buoy and fiber optic systems. The antenna ground plane elements where manufactured from aluminum and ocassionally fractured under stress during transportation or deployment. Future systems should utilize stainless steel elements. The spar buoy sank on one occasion due to compression of the buoyancy collar during heavy seas. The buoyancy collar should be replaced by a noncompressable floatation device. During recovery, the fiber optic cable was crushed on one occasion and kinked on another. This problem may be corrected by utilizing a fiber optic cable that is jacketed with a heavy rubber sheath.

A final recommendation is to incorporate a pressure sensor to measure surface and internal wave activity. This additional information will allow the analyst to determine the contribution by waves to the geomagnetic data.

APPENDIX A

A. EQUIPMENT SCHEMATICS

The equipment utilized in this project was locally designed and/or constructed, commercially available or available through military channels and locally modified. The system equipment schematics are presented in the following figures:

1. Preamplifier (Figure A.1)
2. Magnetic Activation Circuit (Figure A.2)
3. Pre-amp and PCM Preconditioner (Figure A.3)
4. Pulse Code Modulation System (Figure A.4, A.5)
5. Optical Transmitter (Figure A.6)
6. Optical Receiver (Figure A.7)
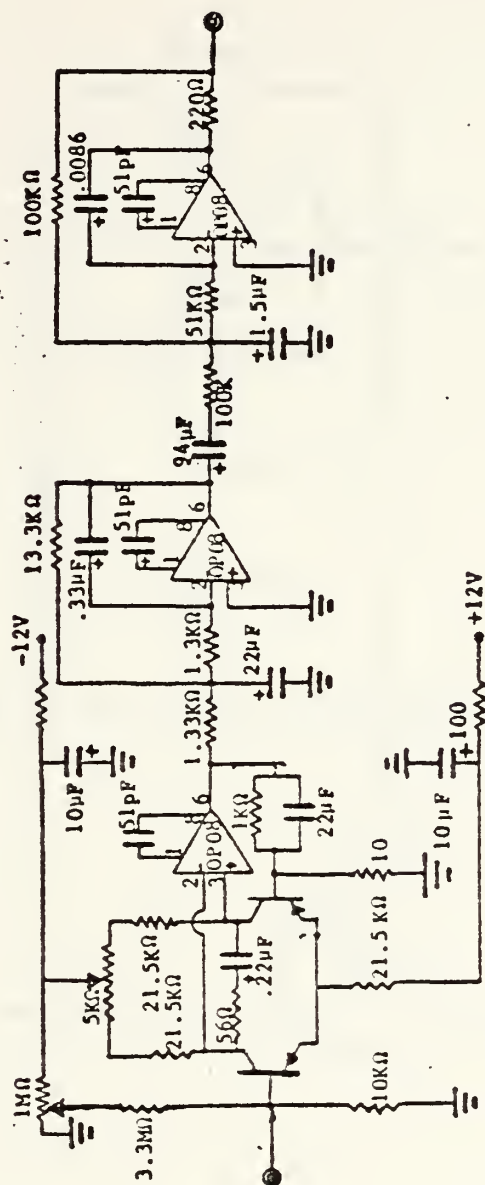
Figure A.1   Preamplifier Schematic

59
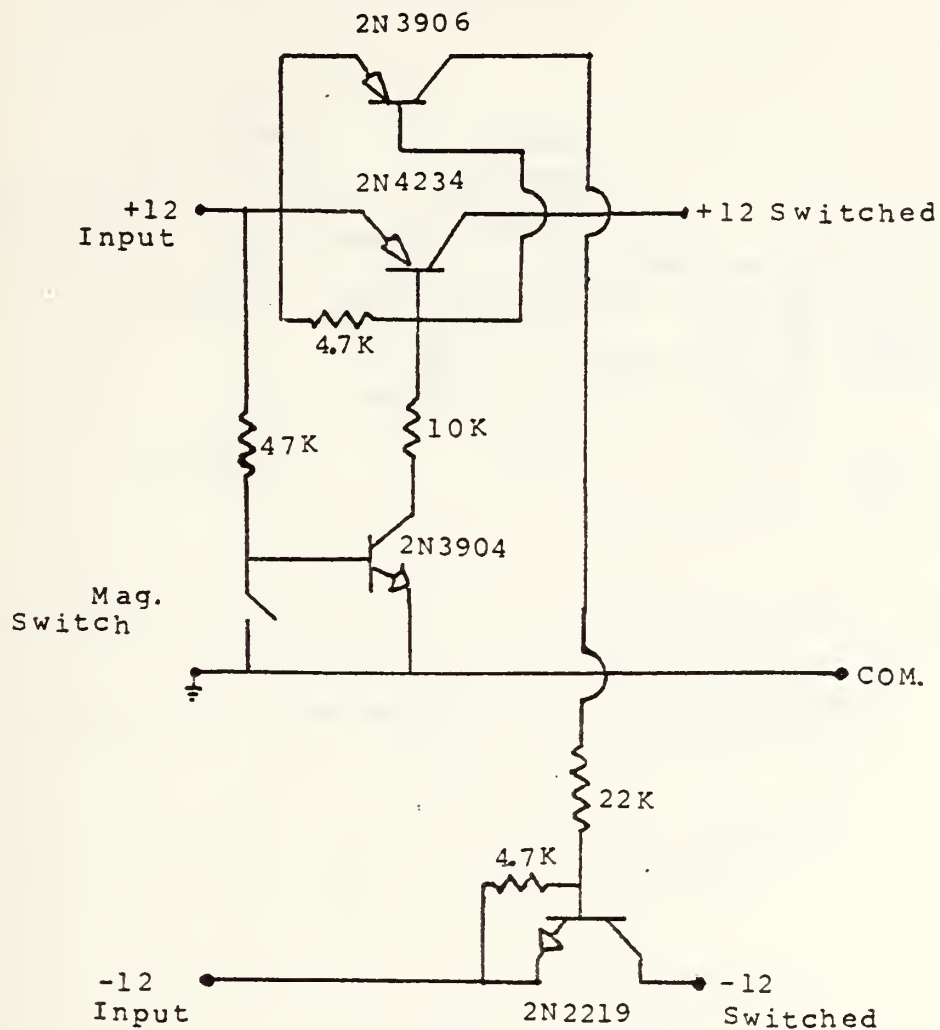
Figure A.2   Magnetic Activation Circuit

60
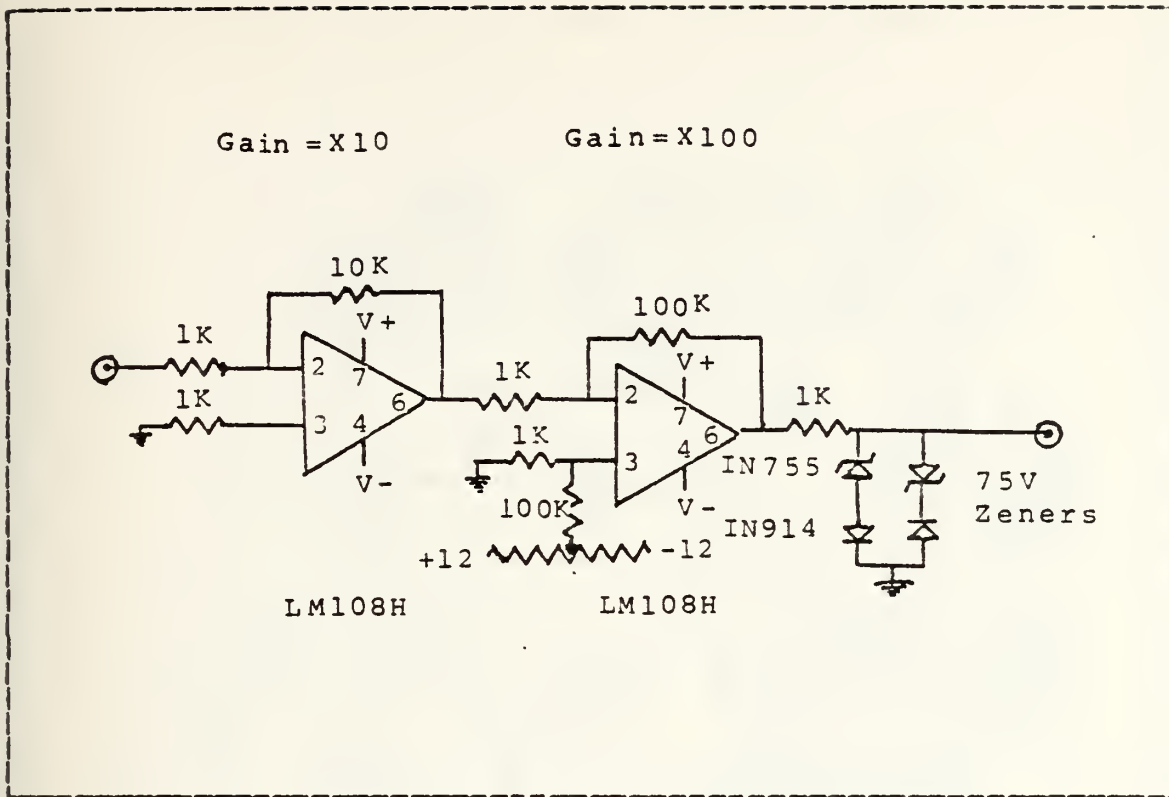
Figure A.3   Pre-amp. and PCM Preconditioner

Figure A.4   Pulse Code Modulation System

62
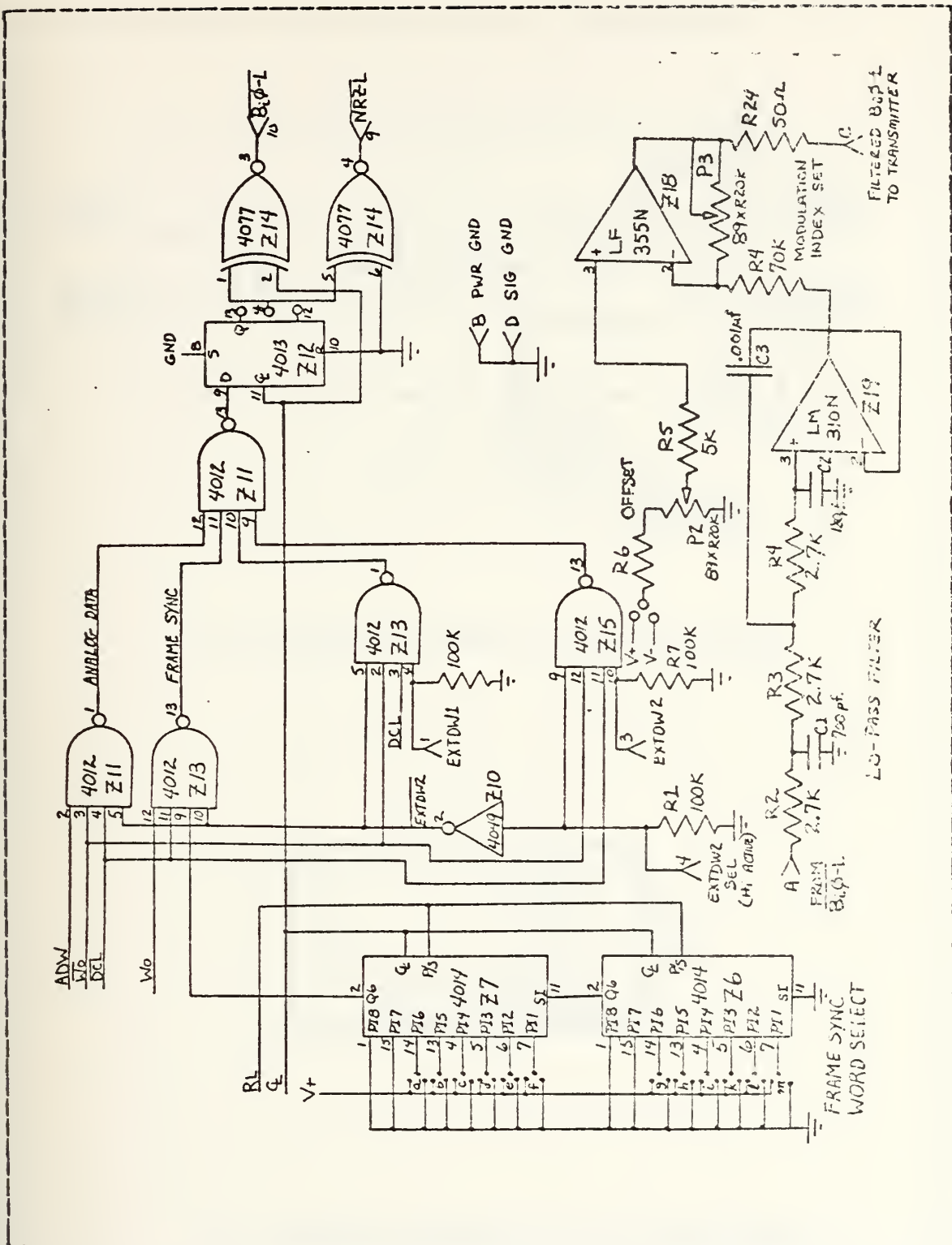
Figure A.5   Pulse Code Modulation System (continued)

63
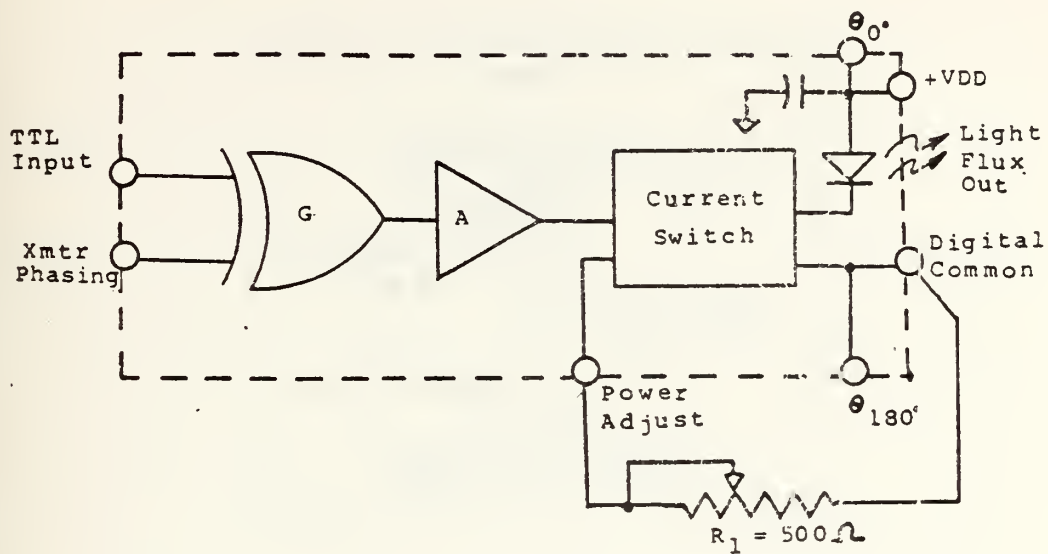
a) Optical Transmitter Block Diagram
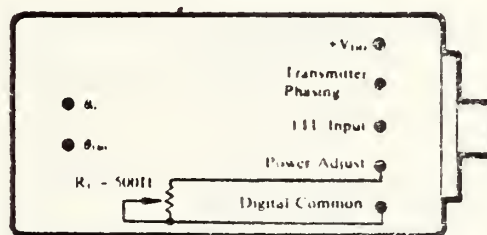
b) Optical Transmitter Pin Arrangement

Figure A.6   Optical Transmitter

64
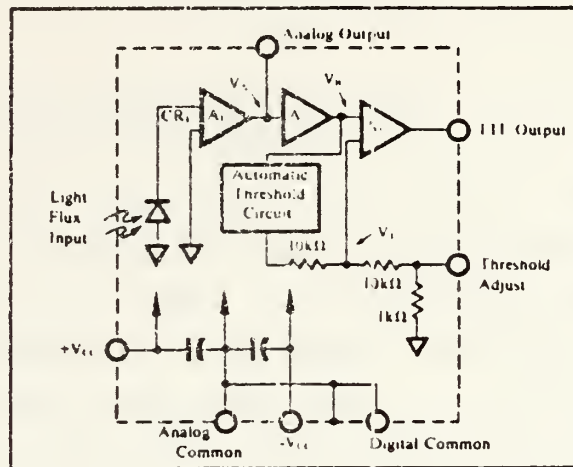
a) Optical Receiver Block Diagram
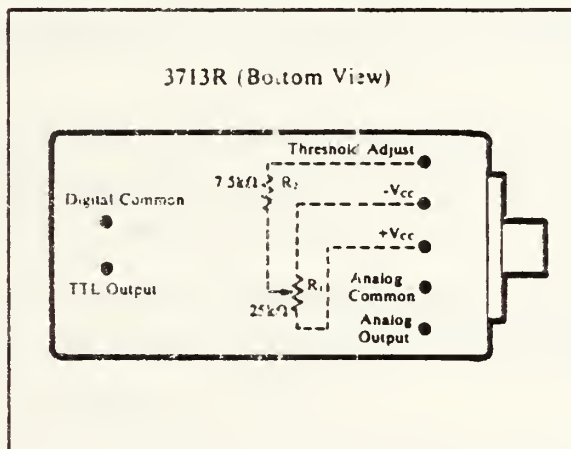
b) Optical Receiver Pin Arrangement

Figure A.7   Optical Receiver

65

APPENDIX B

A. SYSTEM AND EQUIPMENT PREPARATION

In order for equipment to perform and operate as designed, certain preventive maintenance measures and procedural steps should be taken. Such prudent steps, especially in undersea research, will most certainly allow maximum results and prolong equipment life.

The following list serves as a culmination of lessons-learned in previous and on going project work:

1. Spherical glass instrument spheres are composed of two Benthos glass hemispheres which have precision ground mating surfaces. As these surfaces are suseptable to chipping, care must be taken in handling. During assembly of the housing prior to deployment, certain procedures are necessary to maintain watertight integrity:

a. The glass sphere should be dry and warmed to room temperature using a heat gun to ensure adhesion of the sealing tape.

b. All mating surfaces must be cleaned with a solvent such as alcohol to remove any foreign matter, grease, or oil.

c. Prior to sealing the sphere, careful inspection of all equipment, electrical connections, and packing material should be made. The use of check off sheets and color coding was found to be particularly helpful in avoiding operator error.

2. Electronic equipment- A general concern is the proper application of power supply voltages. Assembly of a large number of electrical components within the confines of a small glass sphere, necessitates careful planning and utilization of limited power resources. Improperly applied voltages may result in damage to electronic circuitry and/or loss of data. Certain pieces of electronic equipment require particular consideration as follows.

a. Sensor system- After the sensor coils, preamplifiers, and their battery power supplies are sealed in their respective spheres, a voltage measurement should be taken to ensure operation and then the deactivation magnet positioned over the reed switch such that the voltage drops to zero.

b. PCM system- Extra care should be taken to ensure the x-coil is connected to the x-input channel of the preconditioner/amplifier and its x-output is connected to the x-input channel of the PCM system. The same holds for the y and z channels. An error in these connections will result in the wrong transfer function being applied to the data during the computer assisted data analysis. The procedures identified for the sensor system above, hold as well for the PCM system.

c. Tape recorder- The recorder heads and capstan drive should be cleaned and demagnetized before each acquisition run. This action will enhance the signal to noise ratio and maximize the decoding speed. High quality 1800 foot tapes are

recommended.

d. Fiber optic data link- Before packaging the fiber optic data link enclosure, a system check should be run to determine that the output is 200-240mv. Before connecting the power cables care should be taken to ensure the transmitter power lead has the ground on the pin marked with a dimple on the connector casing. The dimple should be aligned with the indent on the female power connector mounted in the end cap of the trans-mitter enclosure. Similar steps should be taken regarding the PCM data input. This concern isn't necessary with the receiver power input as it is a keyed connector. Once the connections are made remove the activating magnet from the PCM sphere and observe the idle PCM signal on an oscillosope. Adjust the transmitter power adjust potentiometer so that 200-240 mv is observed. Set the 0-degree/180-degree phase switch to the 0-degree position. Package the enclosures as follows:

1) Clean "O"-rings, "O"-ring grooves and mating surfaces with alcohol.

2) Lightly lubricate "O"-rings and pipe mating surface between "O"-ring and pipe end with vacuum grease.

3) Open vent plugs and gently slide end caps onto the enclosure ensuring the electrical wires are clear. CAUTION: care should be taken not to kink the fiber optic cable.

4) Both enclosures should be secured to the dispensing reel as shown in Figure B.2 and transported as a separate component.

68

3. Batteries- Gelyte batteries are used for most power requirements. These batteries should be checked prior to system usage and a systematic approach regarding service use and charging interval should be taken. The mercury batteries used in the sensor spheres provide a constant power source throughout their recommended life, but should be replaced at more frequent intervals to ensure successful system operation.

4. Connector/Cables - Before and after each use in a corrosive environment, all connectors should be thoroughly cleaned to extend service life. All rubber connectors should be lightly lubricated with silicon grease to ensure electrical continuity and prevent water intrusion. The use of color coding on cable and connectors lessen the possibility of error and is highly recommended.

B. SYSTEM DEPLOYMENT/RECOVERY

On the scheduled day of system deployment, the previously prepared system components are taken to the Monterey Bay Coast Guard Pier by pick up truck where they are on loaded to the R/V Acania. The on load is accomplished with assistance of the ship's crew and its on-board crane. Figure B.1 shows the shipboard layout of system components that has proven to be the most efficient starting point. Not shown in the figure is the fiber optic data link and storage reel. It is temporarily stored in the aft deck house with its interconnecting electrical cables.

The following steps are taken to facilitate final preparation and deployment. The numbers in parenthesis refer to the numbered items in Figure B.1.

Step 1: The crew passes the main support line (1) through the A-frame boom block to the winch on top of the aft deck house. The line is reeled on to the winch drum allowing enough slack so the line may easily be run down the port side of the ship out of the way of the follow on operations. The other end is secured to the sensor system (2) harness by means of a bowline.

Step 2: The spar buoy is assembled starting with the power supply section (6) and the free flooding section (7). The interconnecting cable (11) is connected to the receptacle in the power supply section's water tight plug and passed through the free flooding section. Remove six 1/4-20 screws from the freeflooding section. Align the mating index marks on each section and mate the sections. Additional alignment may be achieved by applying a long shafted screw driver as a lever in the free flooding ports. Secure the sections with the screws previously removed. Before connecting the power cable to the transmitter section (8), ensure the dummy load is in place on the section's antenna output coaxial cable. Make the power cable connection. Mate and fasten .the free flooding and transmitter sections as before. Do not assemble the antenna mast (9) on the spar buoy at this point.

Step 3: Take the fiber optic transmitter, receiver and storage reel, packaged as shown in Figure 5.2 from the aft deck house. In the vicinity of the can buoy (5) remove the electrical tape securing the transmitter to the storage reel. Using care not to break or kink the optic cable, reel off enough cable so that the transmitter may be positioned on the instrumentation section (4). Carefully align and thread the axle into the hole provided in the center of the electrical connection side of the can buoy. Tighten the fitting until it is snug. Secure the can buoy to the deck
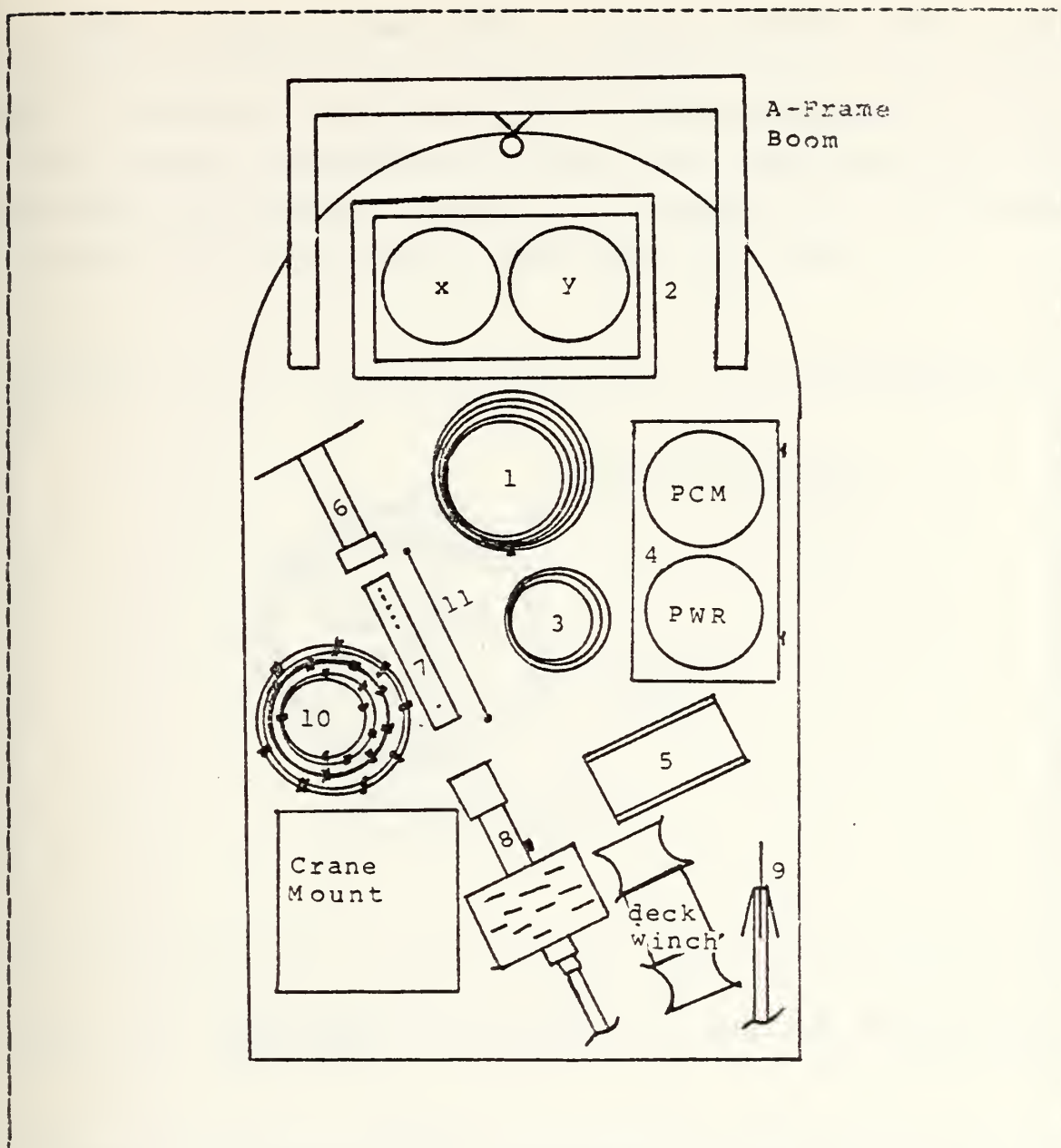
Figure B.1   Shipboard system component layout.

winch with line to prevent the buoy from rolling when the ship is under way. Do not fasten the electrical connections at this point.   Position the optic transmitter against the instrumentation subsection (4) frame between the two spheres

(on quick release clamp side) with the fiber optic cable protruding from the power supply sphere end of the transmitter enclosure. Ensure there is sufficient room for electrical cable connections at the PCM sphere end of the enclosure and securely fasten the transmitter to the frame with two inch Benthos glass sphere sealing tape.
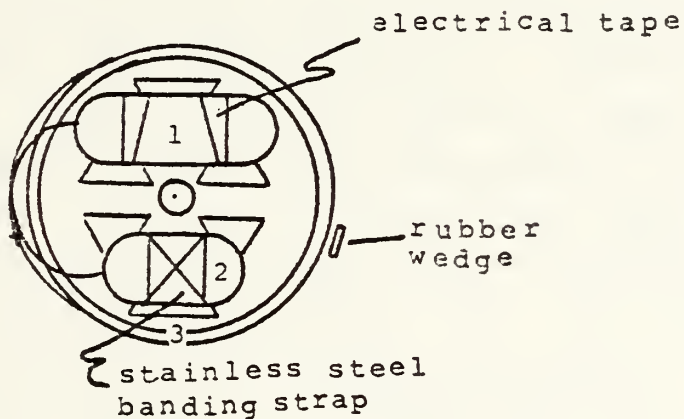
Figure B.2   Fiber Optic Enclosures (1) and (2), and storage reel (3).

Step 4:   Connect data transmission cable (3) to the sensor subsection (2) using color code for easy and error free connection. Prior to making connection apply a thin coat of vacuum grease to all connector shafts. Make connections and secure them with the locking sleeves. Do not screw locking sleeves too tightly or damage to the sleeves may occur. Fasten the other end of the cable to the cables protruding from the pulse code modulation (PCM) sphere.

72

Connect the PCM data cable to the optic transmitter data
input connector. Use care to match the dimple on the cable
connector with the indent on the connector housed in the
transmitter enclosure. This is essential with all the two
conductor Brantner connections in the system. Failure to
follow this procedure will result in damage to the
electrical components involved. Connect the power cable
between the power supply sphere and the optic transmitter
enclosure. Now connect the power cable between the can buoy
and the receiver enclosure.

Step 5: Test for idle PCM signal by connecting the test
cable between the optic receiver enclosure and an
oscilloscope. Remove the power actuating magnet on the top
of the PCM sphere. Adjust the oscilloscope to observe a 200
mv PCM signal. The signal should sync reasonably well.
Remove the actuating magnet from the sensor sphere (one at a
time) and observe the PCM pulses run. The system is now
checked out from sensors through the fiber optic link.
Remove the optic receiver data output test cable and install
the data cable between the can buoy and the optic receiver
enclosure. Install the spar buoy cable (10) to the can buoy
and test for the PCM signal by placing the oscilloscope
probes on pins 2 and 3. Replace the magnets on the sensor
sphere and the PCM sphere. Disconnect the spar buoy cable,
the optic receiver power cable and the optic receiver data
cable. The system is ready for deployment.

Step 1 through step 4 may be accomplished along side the
pier or en route to the deployment location.

Step 5: Fasten the line and cable to the spar buoy. When
on location (180 foot depth for this example) and the ship's
anchor is properly set, the ship's crew will fasten the spar
buoy to the on-board crane and hoist it over the starboard
side. When the fastener is at the rail, a timber hitch is

73

made about the spar buoy shaft and the spar buoy is made fast to the ship's rail. The crane then may be disconnected. Remove the four 1/4-20 hexhead bolts from the top of the spar buoy. Remove the dummy load from the end of the coaxial cable and connect the cable to the cable in the antenna mast section (9). Align the mating index marks and mate the sections. Secure the section in place with the bolts previously removed. The wrench utilized for this procedure should be fastened to the operator with a string to prevent loss over the side. When the sections are secure, the timber hitch may be removed and the spar buoy lowered into the water by the nylon tending line. When stable in the water, remove the tape on the spring loaded antenna ground plane. The antenna ground plane presents an eye hazzard. Use care in tending the spar buoy. The spar buoy cable should be faired along the starboard side outboard of any obstructions.

Step 6: secure the sensor cable connectors to one of the sensor sphere hardhats using electrical tape. Remove the actuating magnets. Allow some slack and tape the coaxial cable (3) to the main support line. The sensor subsection is hoisted up and the A-frame adjusted aft until the subsection is clear of the ship's stern. The sensor subsection is lowered in ten foot increments. A liberal amount of slack must be allowed between fixed points along the coaxial cables between the sensor subsection and the instrumentation subsection. Electrical tape is applied at ten foot intervals of the polypropylene main support line. A tab is placed on the tape to allow for easy removal during recovery.

Step 7: When approximately fifteen feet of the cable remain, the A-frame boom is adjusted in so that the main support line is very close to the stern of the ship. An ample amount of fiber optic cable is reeled off the storage

reel to allow the instrumentation subsection to be
positioned on the stern with PCM end down and quick release
clamps toward the line. The main support line is lowered to
where there is sufficient slack in the last section of the
coaxial cable. The cable connectors are fastened to the
Instrumentation subsection frame with electrical tape and
the actuating magnet is removed from the PCM sphere. The
quick release clamps are made fast to the main support line.
The main support line is hoisted off the deck and again the
A-frame boom is adjusted aft until the load is clear of the
stern. The load is lowered again in ten foot increments and
the optic cable is fastened to the main support line with
electrical tape as before. Care must be taken to prevent
breaks or kinks in the fiber optic cable. Coordination
between lowering the load and reeling off the fiber optic is
a must. When the 170 foot marker (two black stripes (150
ft.) followed by two successive single black stripes on the
main support line) is at the A-frame boom block, the winch
lowering the system is stopped. The remaining fiber optic
cable is secured to the storage reel with a rubber wedge
inserted in the storage groove and taped in place with
electrical tape. The storage reel is immobilized by
fastening a piece of parachute cord from the can buoy
strongback through the storage reel spokes. The power and
data cable connections are made between the can buoy and the
optic receiver enclosure. The spar buoy tending line is
fastened to the can buoy by means of a shackle and the spar
buoy cable is connected to the can buoy. The main support
line is lowered until the 170 foot mark is at deck level.
The excess fiber optic cable must be carefully tended at
this point. The can buoy quick release clamps are made fast
to the main support line. The load is hoisted and the
A-frame boom adjusted aft so the load is clear of the stern.

75

The can buoy is lowered into the water with the excess fiber optic cable. Simultaneously the spar buoy cable is released over the side. The end of the polypropylene main support line is unfastened from the winch cable and fastened to a marker buoy then released over the stern. The system is now deployed.

Step 8: Check with the receiving station personnel to ensure they are receiving a sea side PCM signal.

Step 9: The recovery operation is just the reverse of the deployment operation omitting the system checkout procedures.

APPENDIX C

A. SYSTEM TRANSFER FUNCTIONS

1. Introduction

The triaxial coil magnetometer system is diagramed in Figure C.1. Presently only the land based system employs three coils, the ocean system uses two coils. The data sensed by this magnetometer system is given by $Vx(t)$, $Vy(t)$ and $Vz(t)$, the output voltages generated by the input magnetic fields. The magnetic field components are the desired results therefore the system transfer function must be determined so that it can be removed from the output voltage. In the time domain the relationship between the output voltage and the magnetic field is a convolution integral:

$$V_0 i(t) = \int hi(t-t') bi(t') dt' \tag{1}$$

where $i=x,y,z$. It is more convenient to express equation 1 in the frequency domain by performing a Fourier transform:

$$V_0 i = Hi(\omega) Bi(\omega). \tag{2}$$

The transfer function $Hi(\omega)$ can easily be determined in terms of the ratio of output to input.

The next section discusses the components of the system and attempts to develop a system model. The last section describes the calibration measurements and the experimental determination of the transfer function.
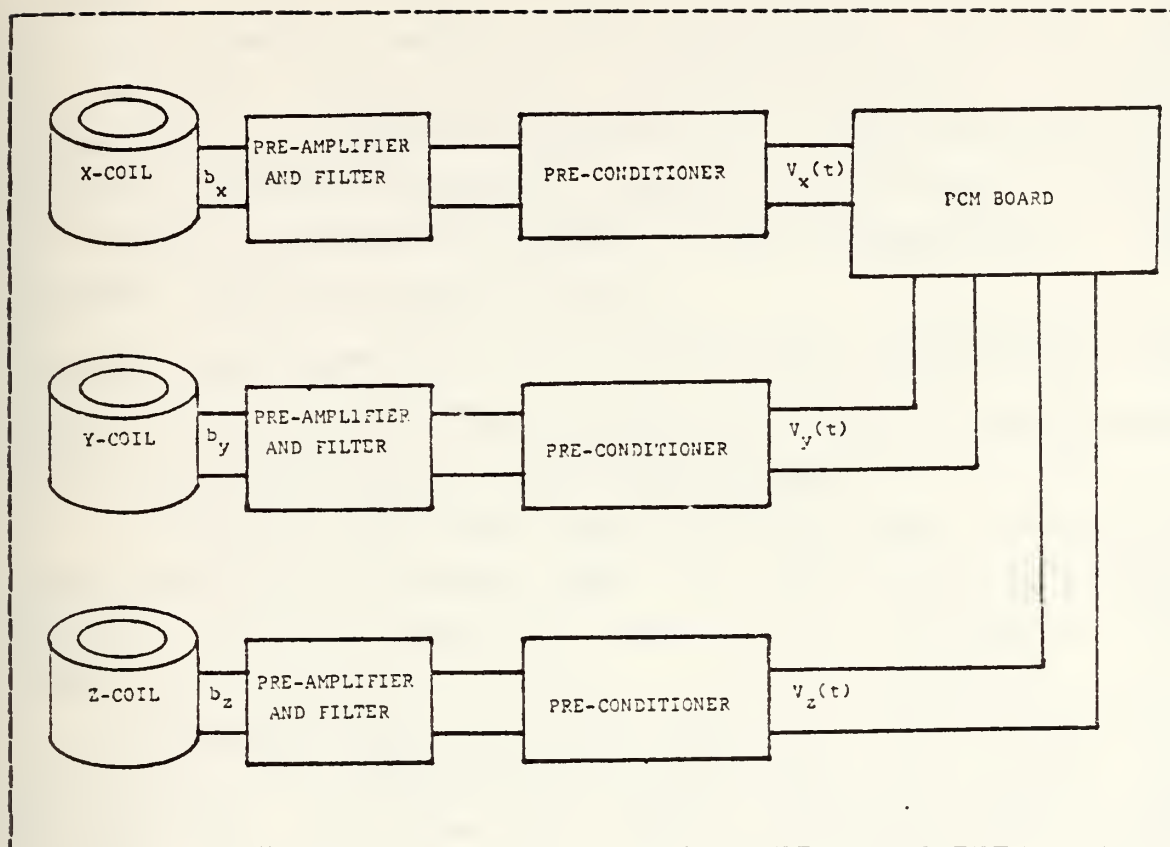
Figure C.1   System Component Configuration

2. System Description

The coil magnetometers are composed of 18 gauge
copper wire with approximately 5460 turns.   The individual
transfer function for the coil is:

$$Vc\,(\omega) = j\ KB\,(\omega) \tag{3}$$

where $Vc\,(\omega)$ is the spectrum of the voltage directly out of
the coil and K is a gain factor.

The next component in the system is the preamplifier
low pass filter.   The preamplifier essentially introduces a
gain of 1000 so the voltage signal can be sent to remote
instrumentation.   The low pass filter is a five pole

Chebyshev with a 3dB cutoff at 20 Hz. The filter is primarily used to remove 60 Hz signals from the system and to prefilter the data before it is digitalized. An additional pole is introduced because of a capacitive coupling between the second and third stages of the filter. Figure C.2 shows a pole-zero diagram of the preamplifier. The transfer function takes the form:

$$H(j\omega) = K/(j\omega+a)(j\omega+b)(j\omega+c-jd)(j\omega+c+jd)(j\omega+e-jf)(j\omega+e+jf) \quad (4)$$

where K is the gain of the preamplifier and the coeficients a - f are taken from the pole-zero diagram.

The preconditioner has additional gain of approximately 1000 and has zener diodes to limit the input voltage to the PCM board. Typically the cutoff is around 7 to 8 volts.

The magnitude and phase response of the preamplifier-filter and preconditioner are shown in Figures C.3 through C.8. The input test signal generating these curves had flat magnitude and phase character as shown in Figure C.9. The figures then represent the actual transfer functions of the preamplifier-filter preconditioner system for the x-y-z channels of land and ocean sensor systems. The figures show that the channels are well matched in magnitude and phase. The phase response is linear and virtually identical in every case. This is an important point since the phase part of the transfer function is not removed from the output voltage signal. However, since the data analysis is in terms of power spectral densities and coherences this fact has no bearing on the results.

The total transfer function of the system is the product of equations 3 and 4. Based on these formulas and the figures, the resulting transfer function should be fairly linear at the low frequency end.
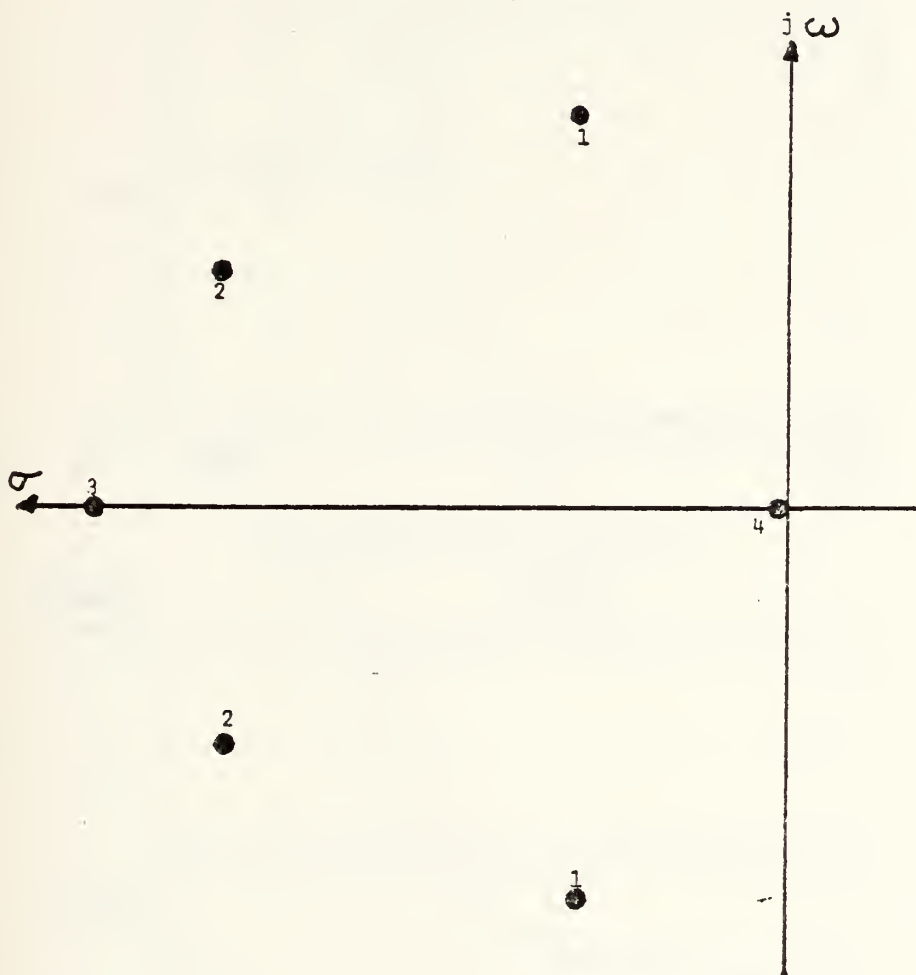
Figure C.2   Pole-Zero Diagram for Model 13-10A Amplifier

80
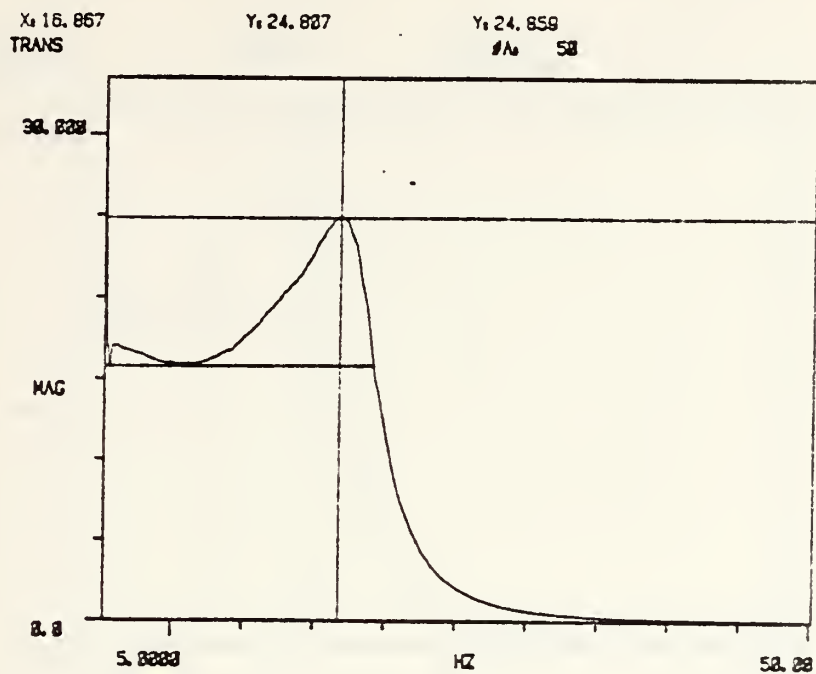
a) Magnitude Response
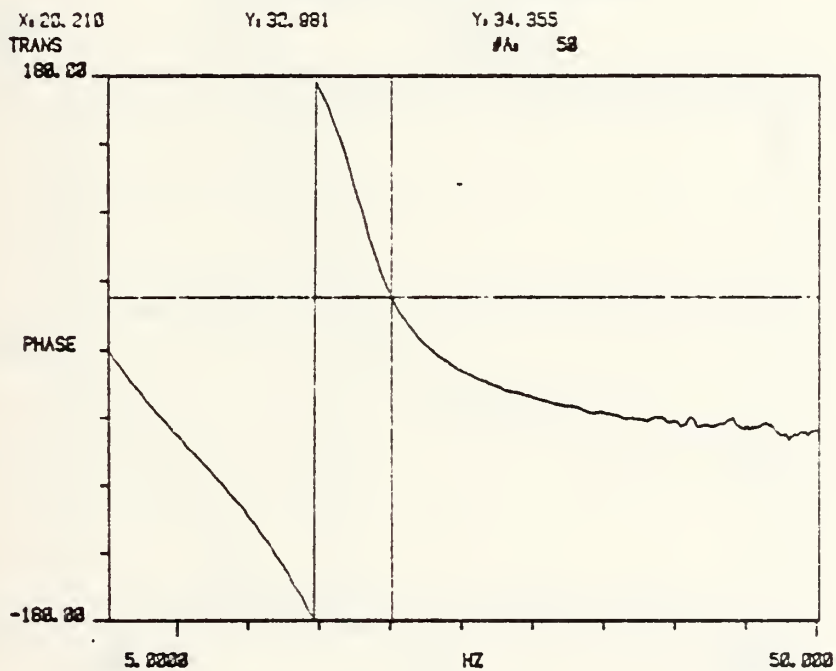
b) Phase Response

Figure C.3   Response of the Land X System

81
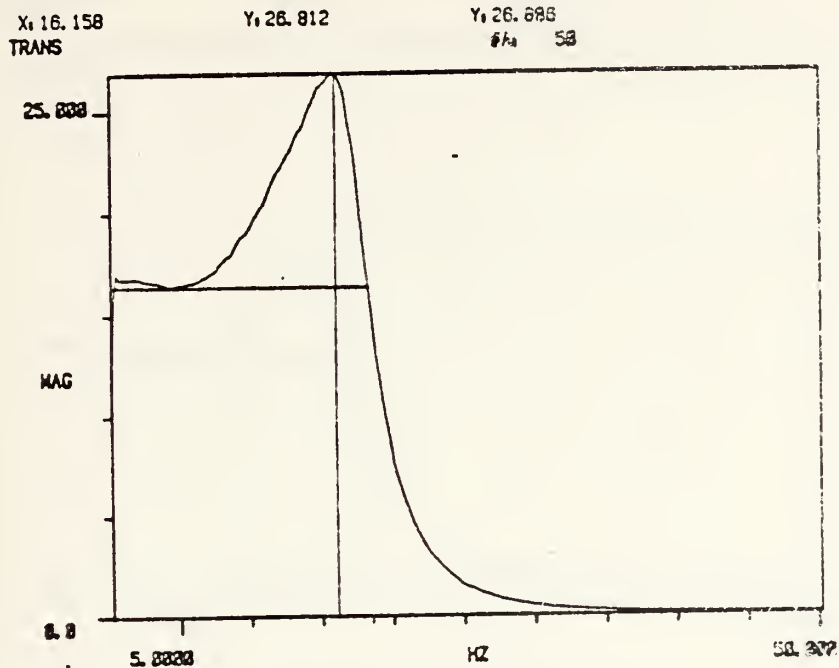
a) Magnitude Response
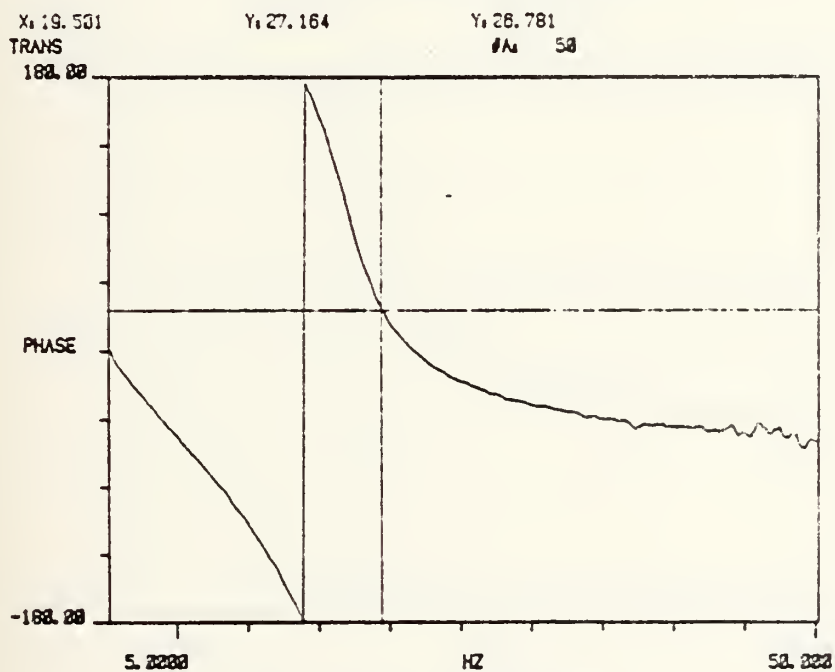
b) Phase Response

Figure C.4   Response of the Land Y System
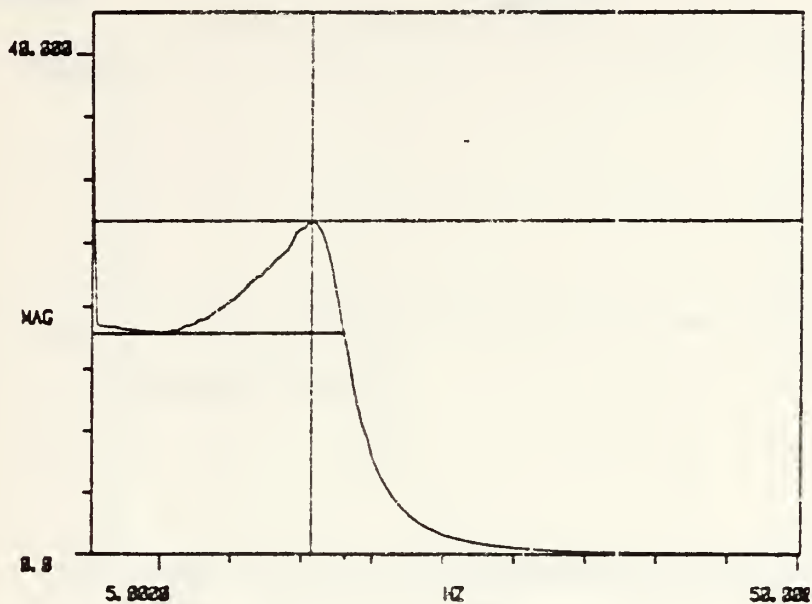
a) Magnitude Response
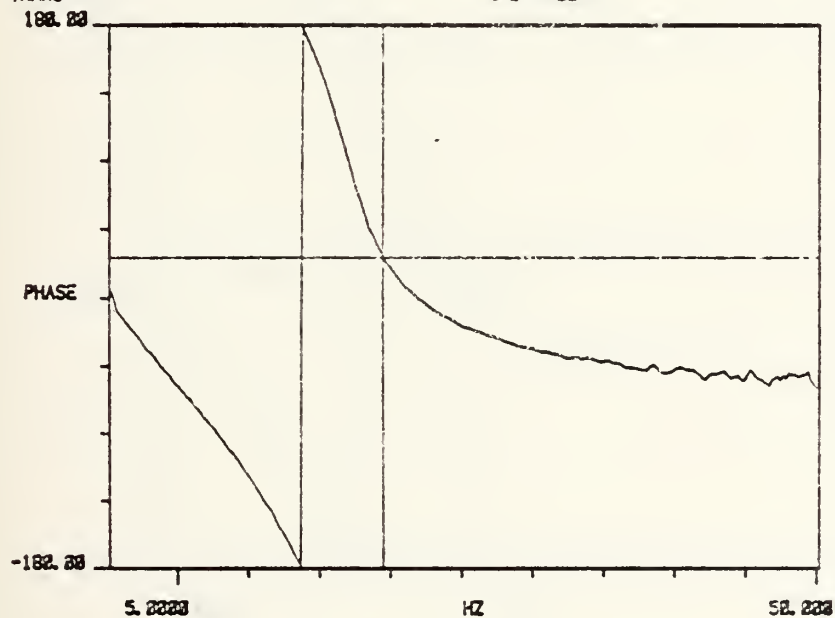
b) Phase Response

Figure C.5   Response of the Land Z System

83
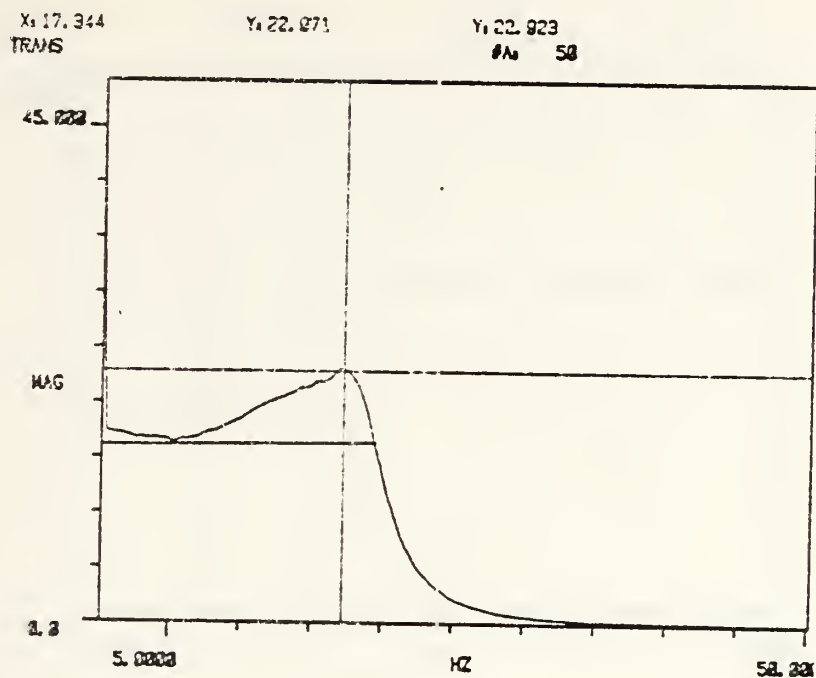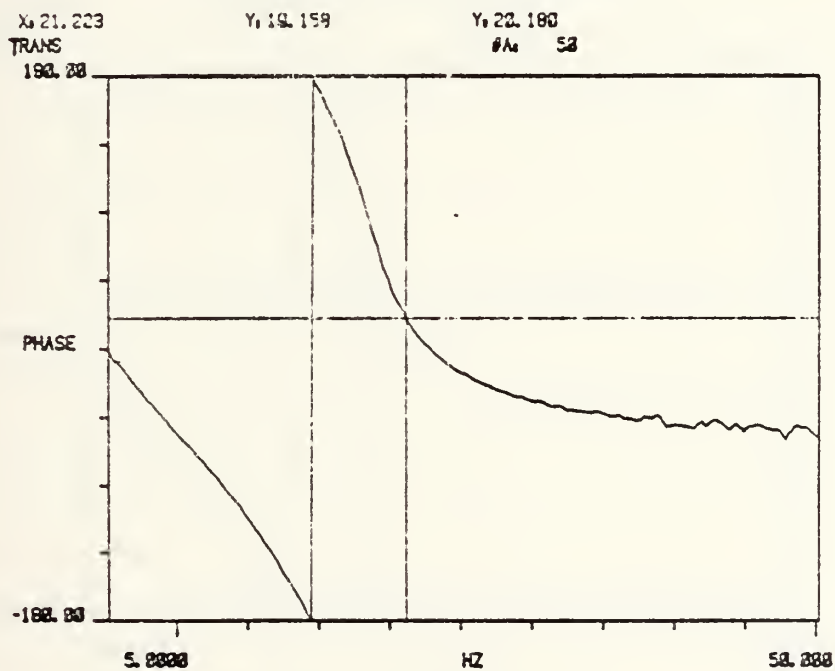
Figure C.6 Response of the Ocean X System

84
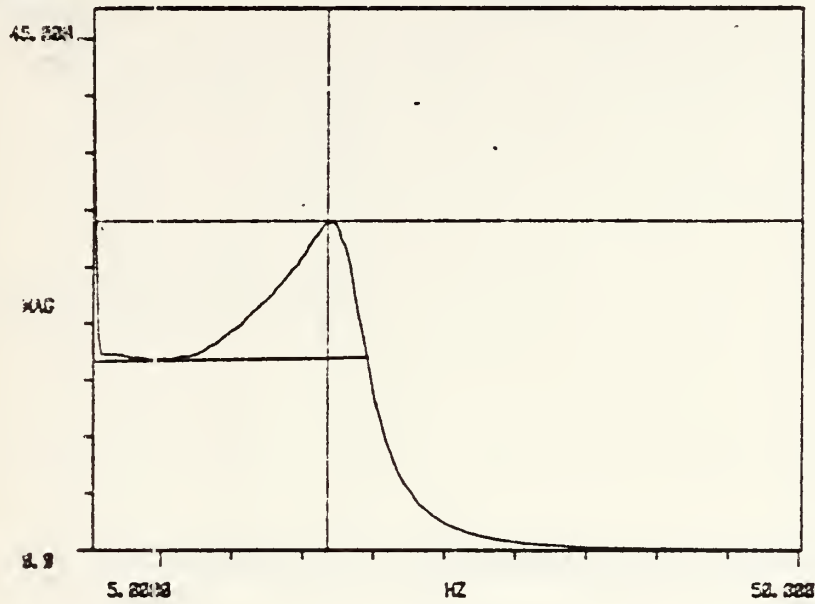
a) Magnitude Response
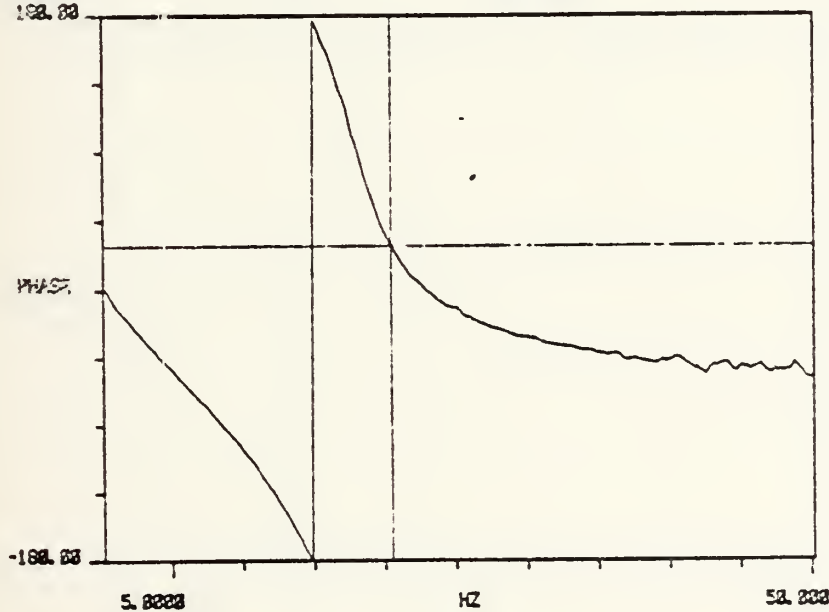
b) Phase Response

Figure C.7   Response of the Ocean Y System
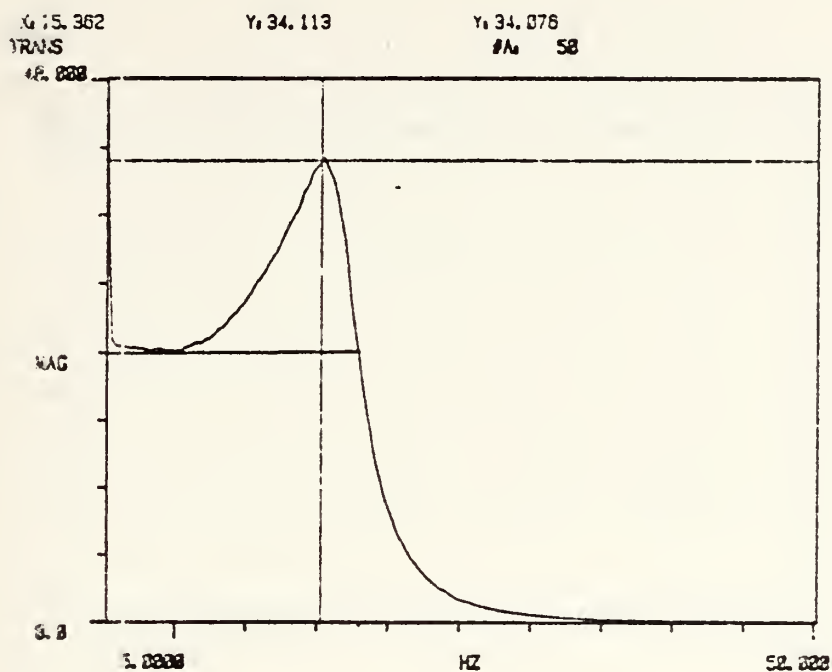
a) Magnitude Response
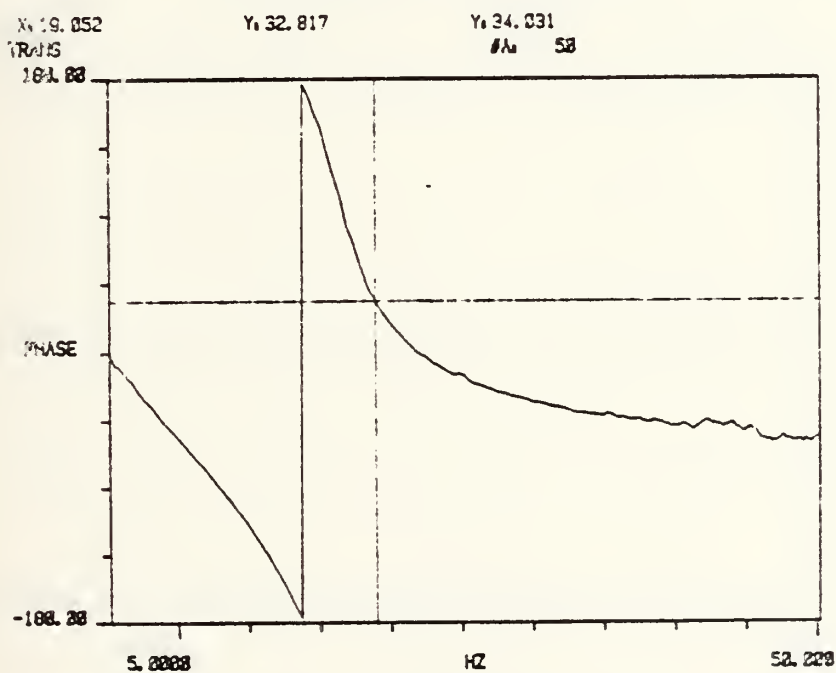
b) Phase Response

Figure C.8 Response of the Ocean Z System

86
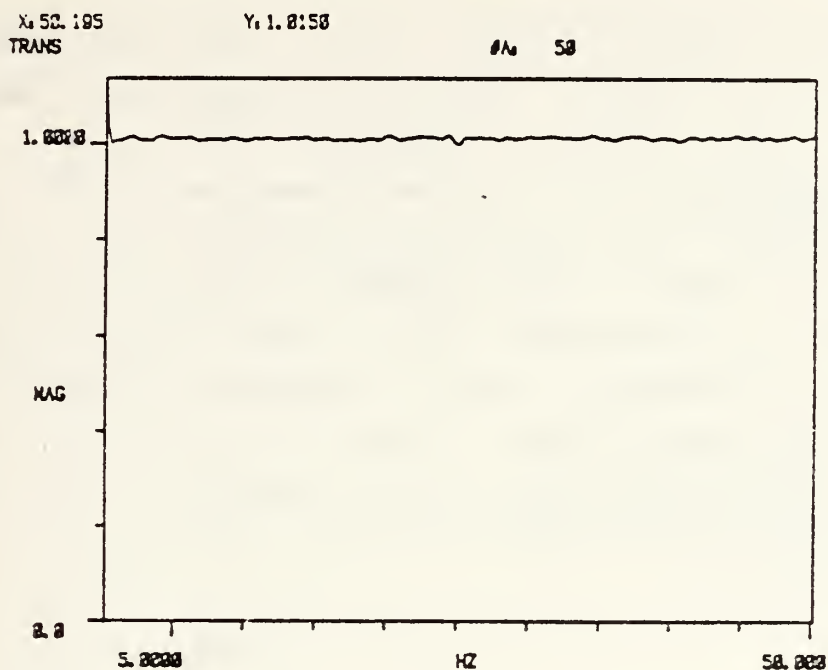
a) Magnitude Response
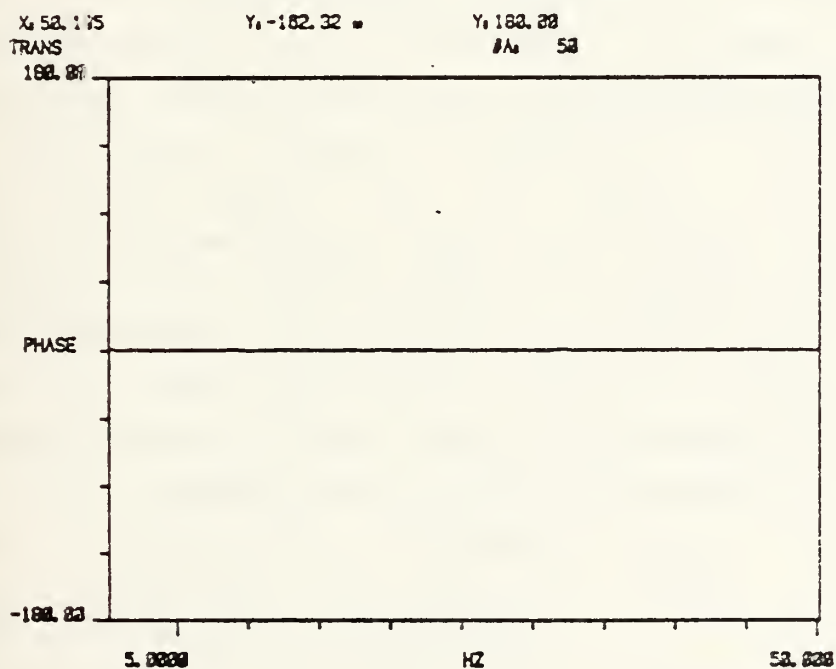
b) Phase Response

Figure C.9   Response of the Input Test Signal

3. Determination of the System Transfer Function

The magnitude of the system transfer function was determined experimentally through the use of a Helmholtz coil, a source of sinusoidal current and a spectrum analyzer. The experimental set up is illustrated in Figure C.10. A one turn Helmholtz coil with a 0.61 meter radius and a 0.61 meter separation between coils is used to provide a calibrated magnetic field to the sensing coil. The sensing coil is placed concentric to the Helmholtz coil and is centered vertically to ensure a uniform magnetic field is created about the sensing coil. The magnetic field in this region of the Helmholtz coil is directed along its axis and is given by [7]:

$$B_H = \mu_0 8 N I / 5 \sqrt{5} R \qquad (5)$$

to terms on the order of (L/R) where L is the linear dimension of the region, N is the number of turns, R is the Helmholtz coil radius and I is the driving current of the coil. The driving current is produced by a Wavetek signal generator model number 142. The current is measured by reading the voltage across a 995 ohm resistor in series with the Helmholtz coil. This voltage is measured by a spectrum analyzer (HP-3582A) to avoid any spurious signals generated by harmonics. Once the driving current is known, then the calibrating magnetic field can be determined. The voltage output of the sensor system is then measured by a spectrum analyzer. By repeating the measurements at a number of different frequencies and applied fields, the system transfer function can be measured.

The actual calibration was conducted at the La Mesa village site using the setup illustrated in Figure C.10. The Helmholtz coil, sensing coil and preamplifier are located approximately 40 meters from the shack which housed
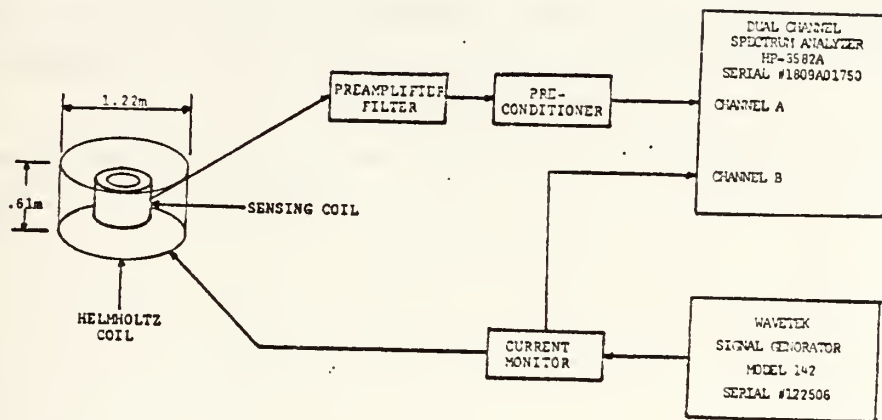
Figure C.10   System Calibration Experiment

the remainder of the experiment.   With the Helmholtz coil
disconnected, the background magnetic noise of this location
was repeatedly examined to ensure accurate readings. Figure
C.11 shows a typical background noise plot from the spectrum
analyzer directly (therefore the transfer function has not
been removed). The distinct features are Schumann reso-
nances, otherwise the background was low enough and stable
enough to adequately calibrate the system.   Only at the
Schumann frequencies was the background subtracted from the
measured output voltage. Calibration runs were conducted
from 0.05 Hz to 20.0 Hz with applied calibrated magnetic
field of 0.02, 0.2 and 1.0 nanoteslas (gamma). Figures C.12
through C.16 show the resulting calibration curves of the

89

land and ocean magnetometer systems. The true transfer function is represented by the 0.02 nT field of the Helmholtz coil. The larger applied field show saturation by the system caused by the protective zener diodes in the preconditioner. At the low frequency end, all the systems are closely matched. At 1 Hz an output voltage of 1 v indicates
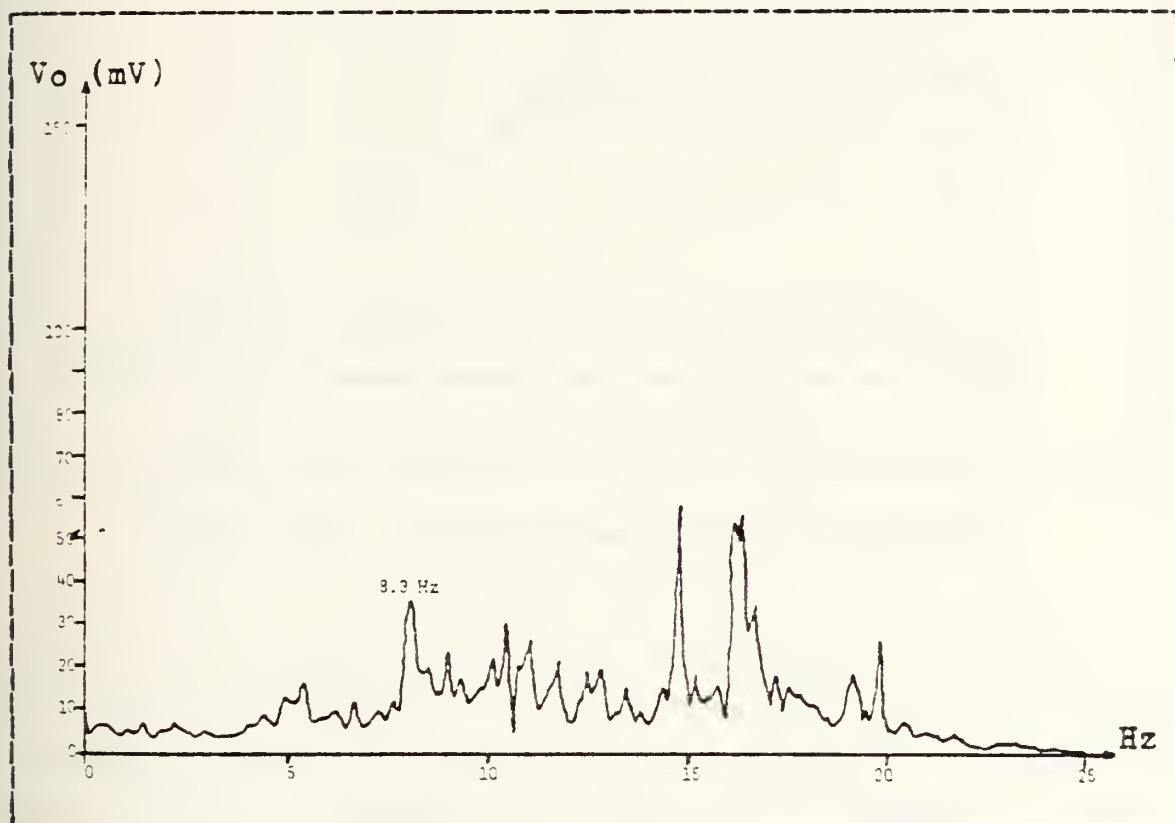
Figure C.11   Background Geomagnetic Noise f(Hz) 05/20/82
               1513 hrs.

a measured magnetic field of 0.4 nT. A 1 nT field is saturated above 2 Hz.

The computation of the actual equations representing the magnitude of the transfer functions presented a distinct problem because fitting the data to the theoretical transfer
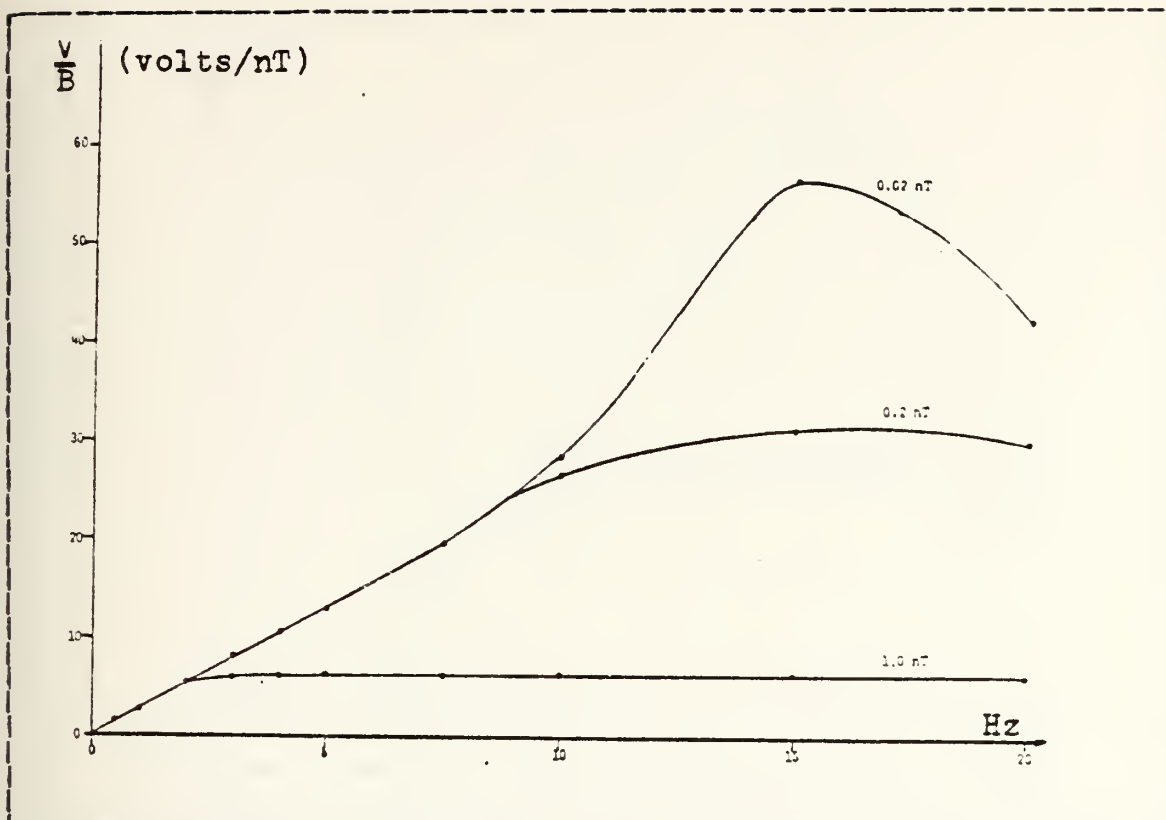
Figure C. 12   Land System X-Coil Calibration

function of the previous section is difficult. Ideally this
is desirable since the phase character of the system
transfer function can then be inferred. However, since the
primary area of interest is in the lower frequency region,
the transfer function was modeled in terms of linear
segments.   The equations derived in this manner have a
maximum error of 1% in the range of 0 to 10 Hz and 5% in the
10 to 20 Hz range.

In the actual computation each curve was broken into
convenient segments that could be represented by a straight
line. The range of the segments were 0 to 3 Hz, 3 to 5 Hz, 5
to 7.5 Hz, 7.5 to 10 Hz, 10 to 15 Hz and 15 to 20 Hz.   For
each segment the slope was first computed by:
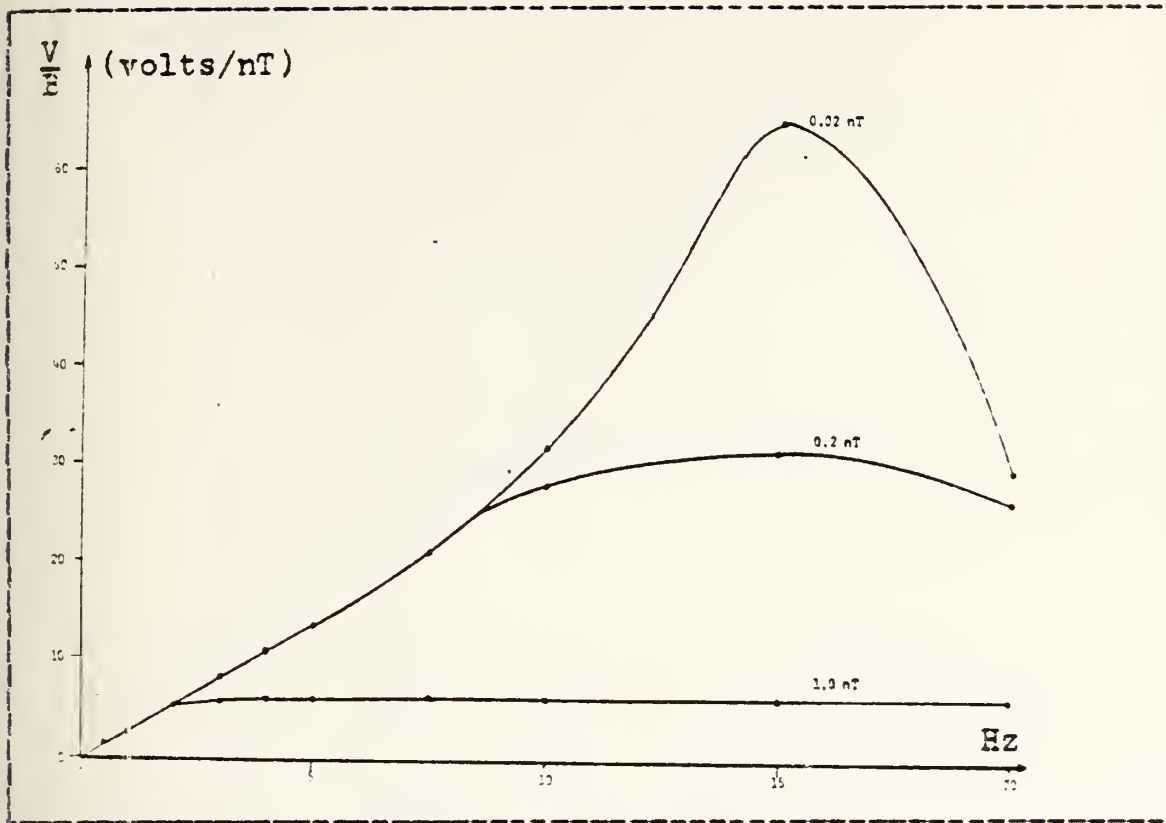
Figure C. 13   Land System Y-Coil Calibration

$$M = (Y2 - Y1) / (X2 - X1). \qquad (6)$$

Once the slope of the line was found the intersection with
the Y axis (b) was found from:

$$Y = M X + b. \qquad (7)$$

These computations were performed for each segment to yield
a series of five equations to model each sensing coil and
amplification system. The individual transfer functions can

be found in the computer program, see Table I.
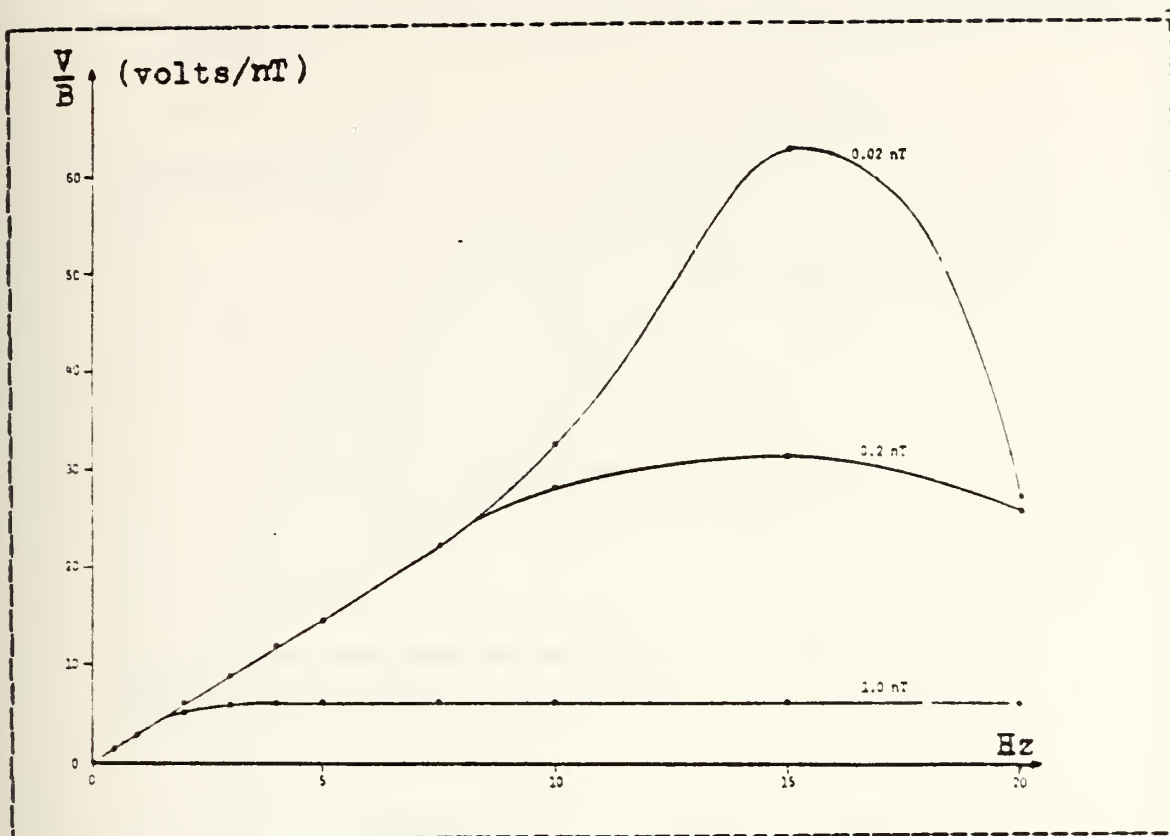
Figure C. 14   Land System Z-Coil Calibration
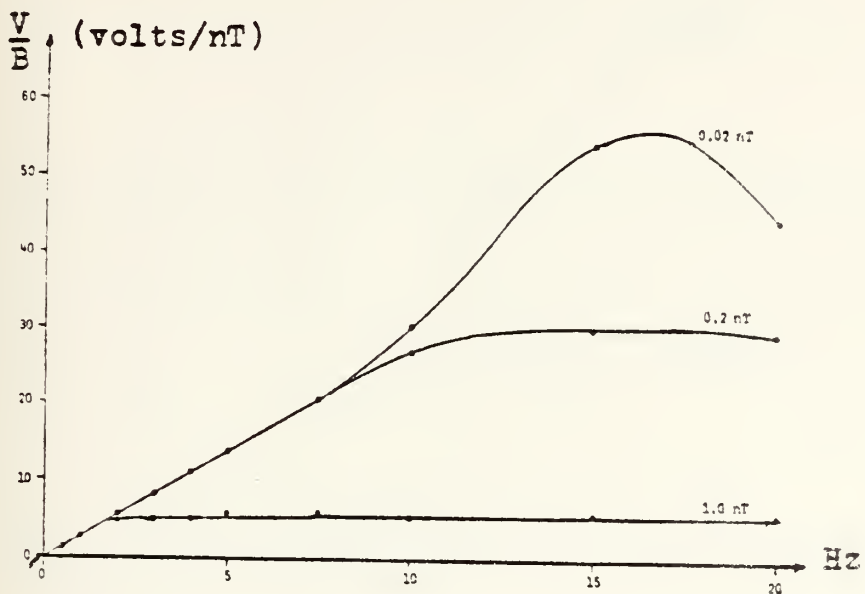
Figure C.15   Ocean System X-Coil Calibration
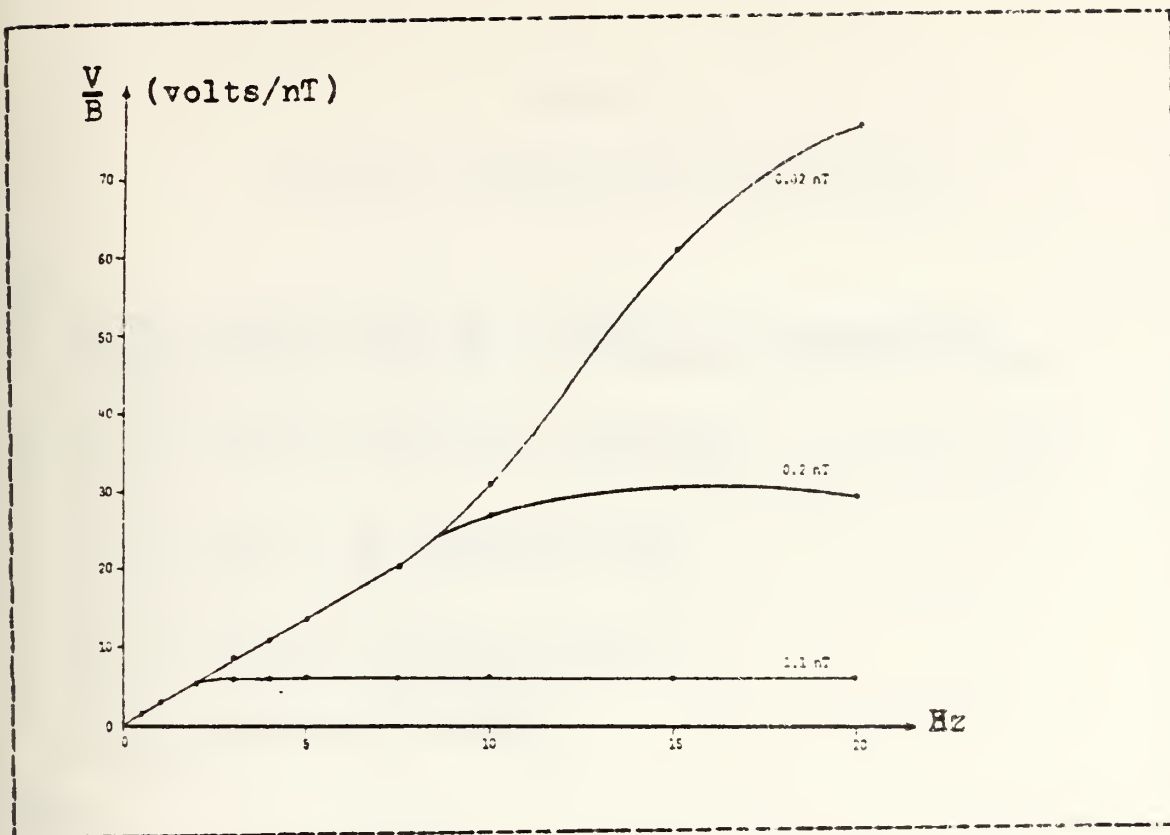
Figure C.16   Ocean System Y-Coil Calibration

95

TABLE I

Transfer Function Computer Program

```
SEA:
1   IF(FRQ.LE.15.) GO TO 2
    XXO(L)=XXO(L)/(-81.36+17.066*FRQ-0.5389*FRQ*FRQ)
    YYO(L)=YYO(L)/(-63.435+11.7106*FRQ-0.23279*FRQ*FRQ)
    GO TO 8
2   IF(FRQ.LE.10.) GO TO 3
    XXO(L)=XXO(L)/(-18.486+4.9029*FRQ)
    YYO(L)=YYO(L)/(-63.435+11.7106*FRQ-0.23279*FRQ*FRQ)
    GO TO 8
3   IF(FRQ.LE.7.5) GO TO 4
    XXO(L)=XXO(L)/(3.947*FRQ-9.358)
    YYO(L)=YYO(L)/(4.295*FRQ-11.837)
    GO TO 8
4   IF(FRQ.LE.5.) GO TO 5
    XXO(L)=XXO(L)/(2.8105*FRQ-0.5657)
    YYO(L)=YYO(L)/(2.800*FRQ-.50)
    GO TO 8
5   XXO(L)=XXO(L)/(2.723*FRQ)
    YYO(L)=YYO(L)/(2.717*FRQ)
    GO TO 8

LAND:
1   IF(FRQ.LE.15.) GO TO 2
    XXX(L)=XXX(L)/(105.5-3.14*FRQ)
    YYY(L)=YYY(L)/(181.32-7.588*FRQ)
    GO TO 8
2   IF(FRQ.LE.10.) GO TO 3
    XXX(L)=XXX(L)/(5.958*FRQ-30.97)
    YYY(L)=YYY(L)/(7.166*FRQ-39.99)
    GO TO 8
3   IF(FRQ.LE.7.5) GO TO 4
    XXX(L)=XXX(L)/(3.492*FRQ-6.31)
    YYY(L)=YYY(L)/(4.252*FRQ-10.35)
    GO TO 8
4   IF(FRQ.LE.5.) GO TO 5
    XXX(L)=XXX(L)/(2.6311*FRQ+0.14667)
    YYY(L)=YYY(L)/(3.012*FRQ-1.55)
    GO TO 8
5   IF(FRQ.LE.3.) GO TO 6
    XXX(L)=XXX(L)/(2.6311*FRQ+0.14667)
7   YYY(L)=YYY(L)/(2.702*FRQ)
    GO TO 8
6   XXX(L)=XXX(L)/(2.72*FRQ)
```

APPENDIX D

A. PULSE CODE MODULATION SYSTEM

The PCM circuit components are mounted on a 3 inch by 15 inch printed circuit board with a 15 pin double sided edge connector at each end. The pin assignments for the signal connector and the control connector are listed in tables D.1 and D.2, respectively. The circuit is diagramed in figures A.4 and A.5.

TABLE II

Signal Connector Pin Assignment

PIN	ASSIGNMENT
A	channel 1 input (analog)
B	channel 2 input (analog)
C	channel 3 input (analog)
D	channel 4 input (analog)
E	channel 8 input (analog)
F	channel 7 input (analog)
H	channel 6 input (analog)
J	channel 5 input (analog)
K	channel 15 input (analog)
L	channel 14 input (analog)
M	channel 13 input (analog)
N	channel 12 input (analog)
P	channel 11 input (analog)
R	channel 10 input (analog)
S	channel 9 input (analog)
1	-15V (max.)
3	common (signal)
15	+15v (max.)

The PCM system incorporates a crystal oscillator and associated CMOS integrated circuitry to develop the clocking pulses, a 16 channel CMOS analog multiplexer, a 12 bit CMOS analog-to-digital converter and associated circuitry to provide the pulse coding.

97

TABLE III

Control Connector Pin Assignment

PIN	ASSIGNMENT
1	EXTDW1 IN (CHNL 14)
2	Wo
3	EXTDW2 IN
4	EXTDW2 SEL
5	SAMP. RATE SEL IN
6	DCL
7	POWER GRD.
8	+15V
9	NRZ-L
10	Biø-L
11	EXT C̄
12	C1
13	C2
14	C4
15	C8
A	TX FILTER INPUT
B	SIG GND
C	TX FILTER OUTPUT
D	SIG GND
K	-15V
L	+12V INPUT
M	SAMPLE RATE 123
N	SAMPLE RATE 64
P	SAMPLE RATE 32
R	SAMPLE RATE 16
S	SAMPLE RATE 8

The crystal clock oscillator operates at a frequency of 24.576 KHz producing a square wave output with a loss bit rate of one bit in one million. This pulse train with pulse duration of 20.35 microseconds triggers the clock input of a binary up counter $Z17(1/2)$ and is also routed directly to pin M of the control connector. Pin 2 of Z17 is the counter enable input which is connected to V+ thereby constantly enabling the counter. Pin 7 is the reset input which is grounded. The counter is composed of four toggle flipflops that are incremented on the positive going edge of the clock pulses. The flip-flop outputs Q1 through Q4 are routed to control connector pins N, P, R, and S, respectively. The pulse repetition rate at pins M, N, P, R, and S represent sample rates of 128, 64, 32, 16, and 8. Selection of the sample

rate is dependent upon the Nyquist sampling criterion. If f is the highest frequency of interest in the analog data being sampled, then the sample rate should be equal to or greater than 2f for unbiased resolution. Currently a sample rate of 64 per second is employed to ensure the Nyquist sampling criterion is met over the frequency range of interest (0-20 Hz). A connection between the pin that represents the selected sampling rate and pin 5 of the control pin connector will establish that pulse repetition rate as the system clock.

The clock triggers Z8, a four stage binary up counter. Z8 inputs consist of a single clock, carry-in (clock enable), binary/decade, up/down, preset enable, and four individual jam signals. Four separate buffered Q signals and a carry out signal are provided as outputs. V+ input on pins 9 and 10 configure the circuit as an up binary counter. The jam signal is selected to develop the data word length. The counter starts at a count of 4 as configured and counts to 15 (12 counts). $\overline{CCO}$ goes high setting Z12. The preset enable signal on Z8 receives the high set output from Z12 (BTCR) and the Z12 counter is asynchronously preset to the jam signal count. The preset count is gated through Z9 and Z10 and the convert start signal to Z3, the 16 channel analog-to-digital converter. The carry out signal ($\overline{CCO}$) from the Z8 counter acts as the clock input to Z17(1/2) another four stage binary up counter. Its outputs, Q1 through Q4 represent the multiplex channel enable signals to Z2, the 16 channel analog multiplexer. Each channel is enabled for 12 clock pulses. The analog multiplexer, depending on the state of the multiplex enable signal, switches a common output to one of sixteen inputs. Its output is amplified, conditioned and passed to the 10 Volt input of Z3, the analog-to-digital converter. The parallel

digital output of Z3 is passed to Z4 and Z5 for parallel-to-serial conversion. The analog data word (ADW) is gated to NAND gate Z11 along with $\overline{Wo}$, $\overline{DCL}$, and $\overline{EXTWD2}$. Wo and $\overline{Wo}$ are developed in NOR gate Z9(1/2). Wo is high when C1 through C8 are zero and low otherwise. Then using Z17's counter zero count as intial sequencing point, the frame sync word is passed through Z13 pin 13 followed by channel 1 through channel 15 analog data words. Z12 and Z14 develop the signals to be biphase logic or non-return to zero (NRZ) logic. This system feeds the biphase logic $\overline{BI\emptyset-L}$ through a low pass filter and a signal conditioning circuit where the modulation index is set. In the sea system the offset and gain potentiometers are adjusted so the signal conforms to TTL levels. This final output is the data input to the optic transmitter.

APPENDIX E

A. OPTICAL FIBERS

1. Fiber types

Although many types of fibers have been tried in the recent past, present technology favors three classes of fibers for optical communications: single-mode step-index, multi-mode step-index, and multi-mode graded-index (see Figure E.1).

a. Single-Mode Step-Index

Single-mode fibers are typlified by a very thin core (1.5 to 8 micrometers) with uniform index of refraction surrounded by a cladding of considerably greater thickness whose index of refraction differs by a very small amount from that of the core. The "single mode" feature can be attributed to the abrupt interface between core and cladding as well as the small change in the refractive index. The cladding material is lossy so that any modes it accepts will quickly attenuate and not couple back into the core. Since the difference in refractive index from core to cladding is small, the numerical aperture is small also on the order of 0.14. The small aperture makes coupling to source/detector difficult [8, 9].

b. Multi-Mode Step-Index

The core diameter of multi-mode step-index fibers are larger (25-15) micrometers). The refractive index is uniform across the core diameter [9]. The cladding

refractive index is slightly lower than that of the core. The numerical aperture is small but the core size is larger than that of the single mode fiber, alleviating somewhat the coupling problem. The loss characteristics of these fibers can be extremely low and in general can be linked directly to the lower numerical apertures and manufacturing techniques employed.

c. Multi-Mode Graded-Index

Graded index fibers appear to be the optimum fiber (of those currently available) for long line applications [8]. The fibers have core diameter ranging from 20 to 150 micrometers with an index of refraction that varies as a function of the distance from the core center as shown in Figure E.2. The grade in the index removes the abrupt change that is typical of the step-index fiber. The net effect is that all modes cross the optical axis at about the same places and at about the same time [10].

2. Attenuation in Fiber Waveguides

a. Losses in General

The principal causes for attenuation losses are:
1) Material absorption: This loss can be mostly attributed to Hydroxyl and Transition metal ions in glass.
2) Scattering: This loss is primarily caused by geometric irregularities at the core-cladding interface.
3) Radiation losses: This loss is a result of bending the fiber cable at small radii of curvature [11].
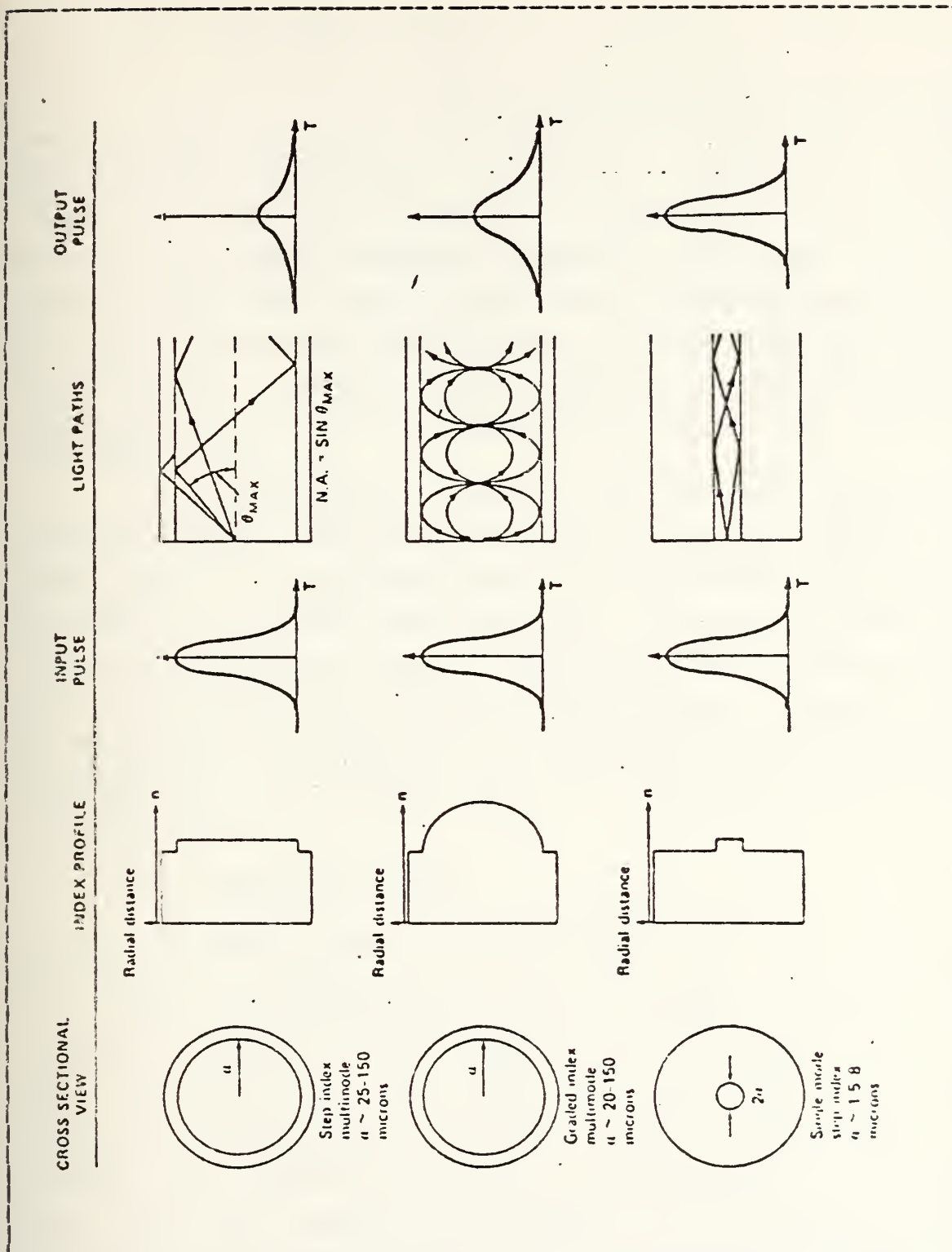
Figure E.1   Types of Optical Fibers

b.   Scattering Losses

All transparent materials scatter
due to frozen in thermal fluctuations of constituent atoms.
This intrinsic scattering represents the fundamental contri-
bution to attenuation in optical waveguides.   The glasses
utilized in fiber waveguides generally have more than one
oxide present that cause another form of scattering. This is
due to concentration fluctuations in the constituent oxides.
For high silica glasses, concentration fluctuations typi-
cally account for only approximately 25% of the observed
scattering loss.

In addition to these two intrinsic scattering
losses, induced scattering through non-linear effects can
exist such as stimulated Raman and Brillouin scattering.
Because of the small core size, the confined guidance and
the long interaction length, relatively low absolute power
levels are required to observe such effects. Actually 2000
watts has been injected into a 2 Km length of guide having a
75 micrometer core diameter with no non-linear attenuation
observed [11].

c.   Radiation Losses

These losses are associated with the waveguide
structure. The cladding has in practice been, a thickness of
a few tens of micrometers.   If the jacket is lossy (to
minimize crosstalk), some fraction of the mode field can
reach this region and be attenuated.   Additional radiation
losses are experienced when the optical wave guide is
curved. The presence of outside perturbations on a fiber
cause light loss through the cladding. In step-index fibers
this mechanism causes a change in the angle of incidence of
the light rays until a critical loss angle is reached. In
graded-index fibers loss occurs from mode mixing and loss of

the higher order modes in a simular fashion. These losses
can become appreciable in fiber cables for underwater appli-
cation. Losses as great as 1400 dB/Km have been reported
[12].

d. Loss Minimization

Fortunately it is known that fibers can be
protected from microbending and encased in constructions
capable of high pressure [13]. The size of these losses is
typically about 1 dB/km. Minimization of microbending losses
is achieved by encasing the fiber in alternately soft and
hard jackets. A transverse force applied to the stiff outer
jacket will be resisted and spread over a large area. The
soft inner jacket will comply with the force, attenuating it
and spreading it over a still larger area. The total force
will then be able to transmit to the fiber which is itself
stiff. For example ITT's T-1211 fiber is buffered with
RTV184, a silicon rubber, during the drawing process. This
has the advantage of protecting the fiber from contaminants
early on, particularily OH ions. A second buffer, Hytrel
7246, a hard polyester elastomer, is then applied. This
combination makes the fiber a good choice for underwater
cabling. Hytrel also gives the fibers hundreds of hours of
immunity from moisture [13].

e. Losses due to Hydrostatic Pressure

Hydrostatic pressures can also affect the atten-
uation in optical fibers. Silicon rubber clad silica (PCS)
is compressed in sea water. At 2000 psi, the numerical aper-
ture (NA) for this type fiber approaches zero and no light
is transmitted due to compression of the silicone and
increase of the silicone index of refraction [14].
Therefore, glass clad fibers must be used in underwater
cables.

3. Static Fatigue and Strength

    a.   Since the fiber optic utilized in a data link
for magnetic data collection need not be a supporting
element of the system the tensile strength is not a signifi-
cant factor.

    While the theoretical strength of optical fiber is
more than 600 kg/sq mm [15] the actual strength is related
to minimum strength points due to flaws and cracks on the
fiber surface.   For a breaking strain of 1 percent, the
minimum flaw size must be less than 1 micrometer, which is
difficult to assure in production runs [16].   Further more,
the growth of flaws is directly related to temperature,
applied strain, relative humidity and even pH. A pH of 7-8
causes the most severe flaw growth [17]. This value approxi-
mates the pH of the ocean.

4. Cable Configuration

    Cabling cf optical fibers has the objective of
providing useable strength at minimun weight while ensuring
environmental protection.   Extensive tests upon several
different configurations of mini-cables for underwater use
with and without conductors has been conducted by NOSC,
Hawaii [18].   The following presents some of these cables
whose characteristics may make them suitable for underwater
magnetic data collection operations.

    Figure E.2 represents three possible cable arrange-
ments, all similar, except for the composition of the load
bearing structure. This may be all Kevlar, a hybrid mix of
Kevlar and S-Glass, or all S-Glass in an epoxy matrix.

    a.   Lightweight Single Fiber Cable

        1)   Cable 5058 (all Kevlar):   This cable
survived 500,000 flexure cycles at 20 percent loading. The

106
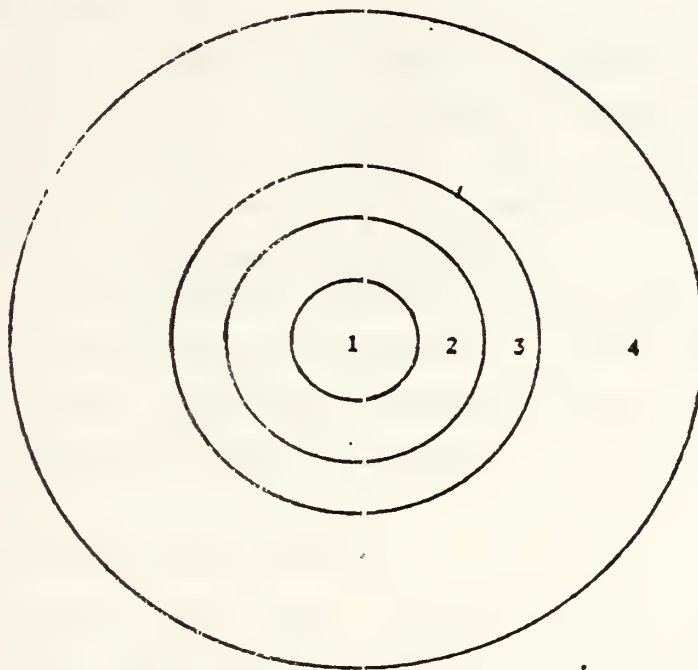
1. Low loss, graded index, optical fiber to 0.005" O.D.
2. Annulus of Dow Corning silicone (RTV 184) to
   nominal 0.014" O.D.
3. Annulus of polyester elastomer (Hytrel 7246) to
   nominal 0.020" O.D.
4. Loadbearing annulus to O.D. of 0.040"
   may be:
   a. 5058, twelve 380-Denier yarns of KEVLAR-49
   b. Ten 380-Denier yarns of KEVLAR-49 and
      5 ENDS HTS-901 S-Glass
   c. 32 ENDS S-Glass (nominally 6528 filaments)

Figure E.2   Lightweight Single Fiber Cable

breaking strength of this cable is 225 pounds with a tensile strength of 180,200 psi.

2) Cable 5083 (Hybrid):   This cable survived 2,370,000 flexure cycles without failure at 20 percent loading. Its breaking strength is 227 pounds and tensile strength is 180,000 psi.

3) Cable 5093 (all S-Glass):   This is the strongest combination with a breaking strength of 346 pounds and a tensile strength of 275,000 psi. This cable survived 750,000 flexure cycles at 20 percent loading without breaking before the test was stopped.

Those cables tested by NOSC Hawaii provide the extension of fiber optic technology to the underwater environment and those mentioned above allow for utilization in underwater magnetic data collection.

B. LIGHT SOURCES AND DETECTORS

Light sources for fiber optic systems require certain characteristics including long-life-time in use, high efficiency, reasonably low cost, sufficient optical power output, capability for various types of modulation and physical compatibility with fiber ends. There are three basic configurations: light emitting diode, solid state laser, and semiconductor injection laser.

1. Light Sources

a. Light Emitting Diode (LED)

LED's generate light when carriers injected across a p-n junction radiatively recombine, emmitting radiation over a solid angle of 2π steradians. The actual output power emitted into a unit solid angle per unit emission area is low for LED's even though the total power

108

output is reasonably high. There are two types of LED sources available, edge emitters and domed surface emitters. Domed emitters are rather complex to manufacture resulting in edge emitter LED's being more commonly utilized. Noise introduced by LED's into the optical fibers is relatively small in most cases and is proportional to the spectral width and the number of transmission nodes propagated in the fiber. Typical power verses drive response curves for LED's are usually linear (see Figure E.3). Most available LED sources have peak wavelengths of 800 to 850 nm and power outputs of approximately 1 nw. LED's are constructed to last in excess of 1 million hours [19, 8].
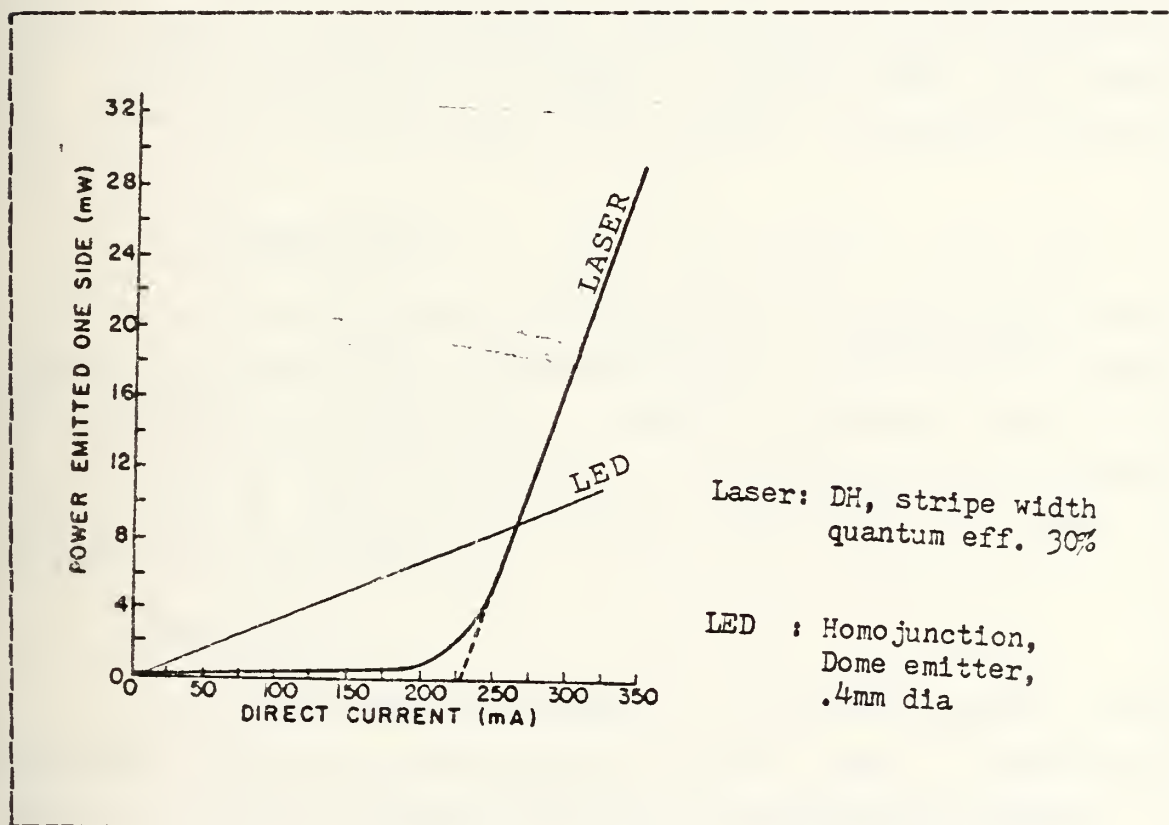
Figure E.3   Typical Power vs Drive Response Curves

b. Lasers

Double-heterojunction DH laser structures can be made with relatively long lifetimes when the lattice parameters of the electrical composition in the various layers and boundaries are carefully matched. In the DH laser with stripe geometry, the lasing region occurs only in the transverse direction under the width of the contact stripe.

The basic semiconductor material for both LED's and injection lasers is the GaAs combination. Doping elements like Al, As, In, Ge, and Sb, are used to shift the emission wavelength. The threshold current for typical DH lasers range from 0.7 to 14 kA/sq cm and the quantum efficiency from 10 to 50% compared with 3% for an LED resulting in a large incremental increase in output power for small increases in current beyond the current threshold (Figure E.4).

c. Comparison

Virtually all applications of fiber optic technology for local data communications to date have chosen LED's for use as the source. Bandwidth distance rates have been within the capabilities of this device and its cheaper cost, ease of use and operational expediency have made it competitive with lasers.

2. Detectors

In fiber optic systems, the most commonly used receivers utilize photodiodes (either PIN or avalanche types) to convert incident light into electrical energy.

a. PIN Photodiode (PIN)

        The PIN diode consists of a relatively large
(very lightly doped) region sandwiched between p and n doped
semiconducting regions. Photons absorbed in this region
create electron-hole pairs that are then separated by an
electric field, thus generating an electric current in the
load circuit. The quantum efficiency of the photodiode is a
function of wave length and temperature [8].

        b. Avalanche Photodiodes (APD)

        The APD is designed for applications requiring
greater sensitivity.   Because of a strong electric field
arising within it as a result of external biasing, the APD
exhibits an internal gain mechanism. They require a consid-
erably higher bias voltage than PIN diodes (bias voltages on
the order of 300 V are not uncommon) [8].

        c. Comparision of PIN and APD

        As a result of the high reverse bias require-
ments of the APD and the power constraints of the magnetic
data collection system the PIN diode is the obvious choice
for the system's detector.

C. TRANSMITTER/RECEIVER

There is a wide variety of commercially available trans-
mitter/receiver sets with the full range of source/detectors
previously mentioned. These preclude the necessity of
designing the associated circuitry. The Burr-Brown 3713T/R
is such a set.

111

D. SPLICING AND CONNECTING

A problem in many applications is in joining one length
of fiber or cable to another, either by splicing (relatively
permanent) or using connectors (intended for repeated
disconnection and reconnection).

1. Splicing

Improvements in manufacturing techniques that
continue to lower fiber attenuation have increased the need
for low-loss field splicing methods that will permit greater
spacing between repeaters. The coupling loss of a splice
depends on two types of factors: those that are intrinsic to
the fibers being spliced and extrinsic ones which depend on
the splicing technique. Intrinsic factors include core dia-
meter, numerical aperture, and refractive index profile.
These can be expected to vary randomly because they are
influenced by the manufacturing and quality control
processes. Their effect on splice loss can be treated
statistically. The factors introduced by the splicing method
include lateral misalignment, end separation, and end prepa-
ration quality. Of these, lateral misalignment is the most
critical.

The ideal splicing method is a field usable tech-
nique which minimizes these fiber extrinsic factors.
Splicing methods now available depend on either fusion or
adhesives [20].

a. Fusion Method

The fusion or "hot splice" method uses an elec-
tric arc or other heat source to fuse two fiber ends
together after they have been accurately aligned.

112

b. Adhesive Method

In the adhesive or mechanical approach, a mechanical device is used to align the fibers through reference to their outer diameters. The fibers then are bonded into this position permanently, usually with an epoxy adhesive.

2. Connecting

The same intrinsic and extrinsic factors apply to the design of fiber optic connectors with the added requirement that the connector system permit numerous disconnections and rematings without an appreciable increase in the coupling loss. There are two basic types of connectors: those which take the alignment reference from the outside diameters of the fibers themselves, and those which encapsulate the fibers then reference the outer diameters of the encapsulating members.

a. Capillary Type

The most obvious design based on alignment of the fibers themselves is the mating of two fibers inside a precision capillary with diameter only slightly greater than that of the fibers. A variation of the capillary approach is the quasi-capillary formed by three precision rods.

b. Other Types

The other commercial terminations fall into the second category. Some use a molded taper or cylindrical ferrule to align one fiber with another. Most of the available connectors which use mechanical alignment of machined members are "dry" (they do not use an index matching fluid), and many are based on the SMA-type connector developed for radio frequency transmission over copper coaxial cable [20].

113

E. OPTICAL DATA LINK ENGINEERING

The following paragraphs outline procedures for engineering a fiber optic data link utilizing the Burr-Brown 3713T transmitter and 3713R receiver [21].

1. Determining the Cable Type

Initially, the primary factor which determines subsequent design of a fiber optic system is the amount of attenuation expected. Fibers have been developed which exhibit attenuation of less than 1 dB/km. Commercial, fibers are available with attenuation of less than 6 dB/km at 0.85 micrometer [22]. The ruggedized graded-index optical cables that were tested by NOSC, Hawaii had attenuation of approximately 7 dB/km [23]. In most applications the cost of the fiber is inversely proportional to its attenuation. For this reason, selection of a fiber is more directly related to dollars than dB [22]. There are also environmental concerns. The mechanical stresses, environmental temperature extremes, and exposure to harsh chemicals must be considered when choosing a particular cable. Such things as jacketing material and the type of added strength members (see Figure E.2) determine a cable's mechanical and environmental

capabilities.

There are three basic types of optical fibers to choose from: step index, single-mode, and graded-index. Each type specifies the profile or variation of the fiber's index of refraction as a function of radial distance from the fiber's center as previously diagrammed in Figure E.1. While step-index fiber with a core diameter of 200 micrometers or larger is recommended for use with the 3713T and 3713R as it is the best compromise between core diameter, bandwidth, coupling loss, and cost, the graded index type

5088 (Hybrid) cable previously described is incorporated into the subject system design. The outside diameter disparity is reduced by application of several jackets of heat shrink tubing. For short lengths of fiber, the increased coupling loss associated with the smaller diameter core is tolerable.

2. Determining Launched Power

Once the mechanical characteristics and the cable type have been chosen, it becomes necessary to analyze link performance with various cables. The first analysis to undertake is the power launched into a particular cable from the optic transmitter.

Beginning with the LED source, four important optical parameters must be known in order to calculate accurately the device's interaction with the system. These are:

a. Total optical power

b. Peak wavelength of emission

c. Physical size of output port

d. Spatial profile of the emission pattern

Total output power (Po) is usually given in units of microwatts. For convenience the optical power, as well as the losses throughout the system and the detector sensitivity, can be expressed in dB. The total system loss is the sum of these individual components. To convert the LED total power output to dBm, refer it to a level of one milliwatt.

$$\text{LED output power (dBm)} = 10 \log(Po(uw)/1000) \qquad (1)$$

The peak wavelength of emission λ is necessary for determining the loss of the system fiber (which is a function of wavelength). It is not unusual for fiber attenuation to double or even triple over only a 100 nanometer range in wavelength.

A power loss can occur if there is a mismatch of areas of the emitting port and the fiber end. This loss expressed in dB, is:

LED-to-fiber area loss(dB) = $20\log(D2/D1)$ (2)

where D1 and D2 are the diameters of the system cores and the LED output port, respectively. If D1 is greater than D2, the area loss is zero.

The spatial emission pattern of the LED's output must be known, because a loss can occur if the high-order mode rays of the LED's output cannot be captured into the numerical aperture (NA) of the system fiber. This is called NA loss. Most data sheets give information on numerical aperture. If the NA of the LED is less than that of the fiber then no NA loss occurs at that interface. If the system cable has the smaller NA, then the loss is:

NA loss(dB) = $20\log(\text{NA source}/\text{NA system fiber})$ (3)

If there are no fiber splices or taps in the system the remaining losses will be at the fiber detector interface. These losses may be calculated as described above.

Typical gap and misalignment displacement in the various connector systems available for the fiber optic active component package are 0.15 mm and 0.05 mm respectively. Angular misalignment in these connectors is very small and can be ignored.

Beginning at the detector and working backwards, the required LED drive current can be calculated as follows.

Generally receiver sensitivity is a function of bandwidth and desired bit-error-rate (BER). The detector data sheet specifies the minimum power to be launched into the detector input port for a given BER. Therefore, it is necessary to calculate the coupling loss from the system

116

fiber to the detector. This will yield the optical power required at the detector end of the fiber. It is then a simple matter to subtract the loss of the cable to arrive at the required launched power. Detector minimum power can be converted to dBm by equation (1). Cable loss is calculated by multiplying cable length (km) by cable attenuation (dB/km).

$$PL = PDM - NALD - ALD - CL - FL - 3dB \qquad (4)$$

where,

PL = launched power
PDM = minimum detector power
NALD = detector NA loss
ALD = detector area loss
CL = cable loss
FL = Fresnel loss

For design ease the 3713T/R specification sheet includes the graph illustrated in Figure E.4. Power launched may be determined simply by entering the graph with the core

diameter.

   3.   Determining Maximum Cable Length

         Once the actual launched power into a specific cable (PL) and the attenuation of a fiber at a specific wavelength (L) are known, the maximum cable length may be obtained. First the loss margin (LM) is found by:

$$LM(dB) = 10 \log(PL/Pin,min) \qquad (5)$$

Pin,min is the minimum rated output power (with power adjusted set for maximum power) usually in microwatts. Pin,min is specified in the transmitter specification sheet. Then Xmax, the maximum cable length that will just present Pin,min to the transmitter is found by:

117
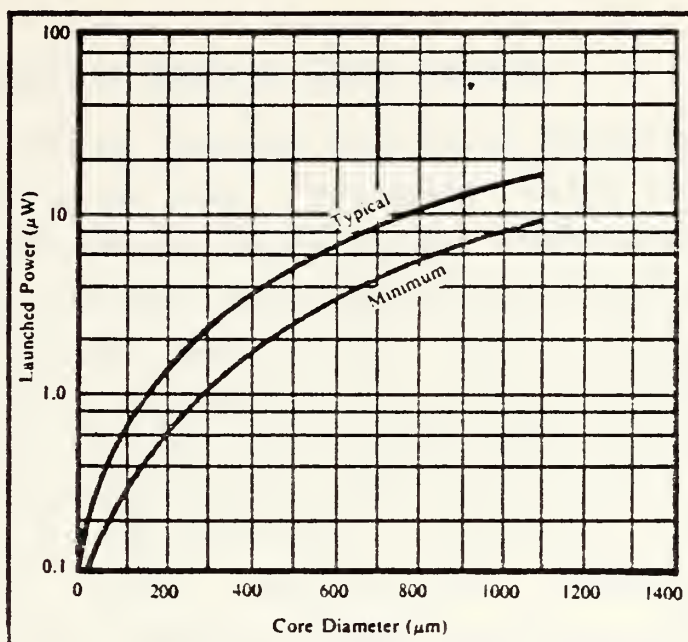
Figure E.4   Launched Power vs. Core Diameter

$$Xmax = LM (dB) /L_{\lambda}(dBm) \qquad (6)$$

If this length is too short, a cable with a larger diameter (larger PL) or less attenuation (smaller L_{λ}) or a transmitter with a higher Pin,min must be used.

The type 5088 cable, for example, has L_{λ} = 7dB/km at 660 nm and a core diameter 0.005 inch or 127 micrometers which corresponds to 0.9 microwatts. Pin,min = 30 nanowatts worst case for 10^{-9} BER. Thus:

$$LM = 10 \log(0.9 \text{ microwatts/3}) \text{ nanowatts}) \qquad (7)$$
$$LM = 10 \log 30 = 14.77 dB \qquad (8)$$
$$Xmax = 14.77 dB/7 \times 10^{-3} dBm \qquad (9)$$
$$Xmax = 2.11 \text{ km} \qquad (10)$$

This length is longer than required and is therefore sufficient.

4. Determining Minimum Cable Length

Short cable lengths with large diameter fibers may cause some receiver slew rate limit which will appear as duty cycle distortion. Limiting the power coupled into the receiver from the cable will prevent this from occuring.

The minimum cable length may be determined for a specific cable by calculating the power launched into it by using the typical curve from Figure E.4. The typical value of launched power should be used since this will give the most power into the receiver, resulting in the desired minimum cable length. Continuing the example of the type 5083 cable, the typical launched power is 0.9 microwatts. The minimum loss margin is found using the typical power launched into the cable and the maximum input to the receiver which is 1 microwatt for the 3713R as stated in the electrical specifications for the receiver.

$$LM\ min = 10\log\ (Pl/Pin,max) \qquad (11)$$
$$LM\ min = 10\log\ (0.9\ microwatt/1\ microwatt) = -0.46dB \qquad (12)$$

The minimum cable length for the specified cable in this example is:

$$Xmin = LM,min/L_\lambda \qquad (13)$$
$$Xmin = -0.46dB/7\times10^{-3}\ dBm = -65.7m \qquad (14)$$

If this minimum cable length is too long for a particular application, use a smaller core diameter cable, a cable with a higher loss, or the power launched into the cable may be reduced as described in section II.A.1.c by adjusting the transmitter power adjust. The negative sign in the minimum length indicates there is no minimum length limitation on

this fiber optic cable when used in conjunction with the 3713T/R set.

F. TYPICAL APPLICATIONS

The 3713T/R fiber optic link solves such data transmission problems as crosstalk, ringing, and echoes. Electromagnetic radiation interference is avoided when using a fiber optic data link in high noise environments. Lightning damage to cables and connected equipment can be eliminated where fiber optic cables replace metallic conductors. Fiber optic cables are not subject to shorting out when emersed in water.

APPENDIX F

TEST PROGRAM

```
//JOEM1MB JOB (1592,0129),'FISHER SMC.1399',CLASS=C
//*MAIN ORG=NPGVM1.1592P,LINES=(60)
//*FORMAT PR,DDNAME=PLOT.SYSVECTR,DEST=LOCAL
// EXEC FRTXCLGP,PARM.LKED='LIST,MAP,XREF',REGION.GO=2700K
//SYSUT1    DD  UNIT=SYSDA,SPACE=(CYL,(8,8))
//SYSUT2    DD  UNIT=SYSDA,SPACE=(CYL,(8,8))
//SYSLIN    DD  SPACE=(6080,(80,80)),UNIT=SYSDA
//FORT.SYSIN DD DSN=MSS.SYS3.NONIMSL.SOURCE(FOURT),DISP=SHR
//     DD  *
C          A LARGE NUMBER OF ARRAYS ARE UTILIZED
C          WITH THE INTENTION OF MAINTAINING EACH
C          BIT OF ORIGINAL DATA OR CALCULATION,
C          READY FOR RECALL AT ANY TIME FOR FURTHER
C          COMPUTAITON. EQUIVALENT ARRAYS ARE EMPLOYED
C          BECAUSE THE PLOTTING ROUTINE 'DRAWP' IS
C          NOT ABLE TO HANDLE COMPLEX ARRAYS.
C          ARRAYS 'ITB','RTB','ALAB' AND 'TITLE' ARE
C          USED TO GENERATE THE VERSATEC PLOTTER OUTPUT.
C          OCEAN ARRAYS ARE INDICATED VIA THE SUFFIX
C          'O', AND LAND ARRAYS ARE INDICATED WITH 'L'.
      COMPLEX*8  XXO(8192),YYO(8192),
     C CSO(8192),COO(8192),ZXO(8192),
     C CRO(8192),CTO(8192),CUO(8192),
     C CVO(8192),CWO(8192),CPO(8192),
     C ZYO(8192),COMOL(8192),COL(8192),
     C CUL(8192),CVL(8192),CWL(8192),
     C COPOL(8192),XXL(8192),YYL(8192),ZXL(8192),
     C ZYL(8192),CSL(8192),BPO(8192),
     C BMO(8192),BPL(8192),BML(8192),
```

121

```
C SPOL(8192) ,SMOL(8192) ,SPO(8192) ,
C SPL(8192) , SMO(8192) ,CTL(8192) ,
C CPL(8192) ,CRL(8192) ,SML(8192)
  DIMENSION TIME(8192) ,FREQ(8192) ,
C WORK(16384) ,FRQ2(8192)
  INTEGER*4  ITB(12) /12*0/
  REAL*4     RTB(28) /28*0.0/,
C CROO(16384) ,CPOO(16384) ,CUOO(16384) ,
C COOO(16384) ,CTOO(16384) ,CVOO(16384) ,
C CWOO(16384) ,CTLL(16384) ,
C CPLL(16384) ,CRLL(16384) ,COLL(16384) ,
C CULL(16384) ,CVLL(16384) ,
C CWLL(16384) ,COMOLL(16384) ,COPOLL(16384) ,
C SPOO(16384) ,SPLL(16384) ,
C SMOO(16384) ,SMLL(16384)
  REAL ALAB(22) /'PDXO','PDYO','ST1O',
C 'ST2O','ST3O','STOO','PHAO',
C 'GAMO','PDXL','PDYL','ST1L','ST2L',
C 'ST3L','STOL','PHAL','GAML',
C 'SPLO','SPIL','SMOO','SMLL','CPOL','CMOL'/
  REAL*8 TITLE(12)
  EQUIVALENCE(TITLE(1) ,RTB(5)) ,(CROO(1) ,
C CRO(1)) ,(CPOO(1) ,CPO(1)) ,
C (COOO(1) ,COO(1)) ,(CTOO(1) ,CTO(1)) ,(CUOO(1) ,CUO(1)) ,
C (CWOO(1) ,CWO(1)) ,(CVOO(1) ,CVO(1)) ,(CTLL(1) ,CTL(1)) ,
C (CPLL(1) ,CPL(1)) ,(CRLL(1) ,CRL(1)) ,(COLL(1) ,COL(1)) ,
C (CULL(1) ,CUL(1)) ,(CVLL(1) ,CVL(1)) ,(CWLL(1) ,CWL(1)) ,
C (COPOLL(1) ,COPOL(1)) ,(COMOLL(1) ,
C COMOL(1)) ,(SPOO(1) ,SPO(1)) ,
C (SPLL(1) ,SPL(1)) ,(SMOO(1) ,SMO(1)) ,(SMLL(1) ,SML(1))
  DATA XXO,YYO,CSO,COO,ZXO,ZYO,CRO,CTO,CUO,CVO,CWO,
C XXL,YYL,ZXL,ZYL,CSL,BPO,BMO,BPL,
C BML,SPOL,SMOL,SPO,SPL,SMO,
C SML,CTL,CRL,COL,CVL,COPOL,CWL,
```

122

```
C COPOL,COMOL/278528*(0.0,0.0)/
      DATA TIME,FREQ,FRQ2/24576*0.0/
      IFRAME=8192
      NR=30
      FNR=FLOAT(NR)
      P=0.0
      DO 70 L1=1,NR
C           THE DO LOOP ENDING WITH STATEMENT 70 ENABLES
C           THE PROGRAM TO PROCESS A LARGE AMOUNT OF DATA
C           BY REPEATING THE PROCESS IN BLOCKS.THE DATA
C           POINTS FROM EACH RUN THROUGH THE DO LOOP ARE
C           ADDED TOGETHER AND EVENTUALLY AVERAGED BY THE
C           NUMBER OF RUNS THROUGH THE DO LOOP. 'NR'
C           REPRESENTS THE NUMBER OF DATA SEQUENCES TO
C           BE AVERAGED. 1 SEQUENCE CURRENTLY EQUALS
C           8192 DATA POINTS FOR EACH CHANNEL OR 256
C           SECONDS OF DATA. FOR THIS TEST SINE AND
C           COSINE WAVES OF 4HZ WIL BE USED.
      DO 60 JJ=1,IFRAME
      XXO(JJ)=SIN(P*.785393163)
      YYO(JJ)=COS(P*.785393163)
      XXL(JJ)=SIN(P*.785393163)
      YYL(JJ)=COS(P*.785393163)
      P=P+1
   60 CONTINUE
C           THE FOLLOWING SECTION GENERATES THE TIME
C           AND FREQUENCY ARRAYS AND NORMALIZES
C           THE INPUT PCM DATA TO VOLTAGE FORM IN
C           PREPARATION FOR THE FAST FOURIER TRANSFORM
C           TO THE FREQUENCY DOMAIN.
      N=8192
      FN=FLOAT(N)
      DELTAT=1./32.
      T=FN*DELTAT
```

```fortran
      DELTAF=1./T
      DO 20 J=1,N
      TIME(J)=DELTAT*FLOAT(J)
      FREQ(J)=DELTAF*FLOAT(J)
      FRQ2(J)=ALOG10(FREQ(J))
   20 CONTINUE
C         THE NEXT FOUR STATEMENTS PERFORM
C         AN FFT ON THE INPUT TIME SERIES
C         DATA.
      CALL FOURT(XXO,N,1,-1,0,WORK)
      CALL FOURT(YYO,N,1,-1,0,WORK)
      CALL FOURT(XXL,N,1,-1,0,WORK)
      CALL FOURT(YYL,N,1,-1,0,WORK)
      DO 40 K4=1,N
      XXO(K4)=XXO(K4)/FN
      YYO(K4)=YYO(K4)/FN
      XXL(K4)=XXL(K4)/FN
      YYL(K4)=YYL(K4)/FN
   40 CONTINUE
C         THE NEXT LOOP CALCULATES THE
C         UNNORMALIZED SPECTRAL DENSITIES
C         FOR SINGLE SITE ORTHOGONAL
C         COMPONENTS OF THE GEOMAGNETIC FIELD,
C         THE INDIVIDUAL SITE CROS SPECTRA
C         BETWEEN COMPONENTS, THE INDIVIDUAL
C         ORTHOGONAL COMPONENTS OF RIGHT AND
C         LEFT CIRCULARLY POLARIZED SPECTRA,
C         AND TWO SITE CROSS SPECTRA FOR RIGHT
C         AND LEFT CIRCULAR POLARIZATION.
      DO 30 II=1,N
      ZXO(II)=ZXO(II)+(XXO(II)*CONJG(XXO(II)))
      ZYO(II)=ZYO(II)+(YYO(II)*CONJG(YYO(II)))
      CSO(II)=CSO(II)+(XXO(II)*CONJG(YYO(II)))
      ZXL(II)=ZXL(II)+(XXL(II)*CONJG(XXL(II)))
```

124

```
      ZYL(II)=ZYL(II)+(YYL(II)*CONJG(YYL(II)))
      CSL(II)=CSL(II)+(XXL(II)*CONJG(YYL(II)))
      BPO(II)=XXO(II)+((0.,1.)*YYO(II))
      BMO(II)=XXO(II)-((0.,1.)*YYO(II))
      BPL(II)=XXL(II)+((0.,1.)*YYL(II))
      BML(II)=XXL(II)-((0.,1.)*YYL(II))
      SPOL(II)=SPOL(II)+(BPO(II)*CONJG(BPL(II)))
      SMOL(II)=SMOL(II)+(BMO(II)*CONJG(BML(II)))
      SPO(II)=SPO(II)+(BPO(II)*CONJG(BPO(II)))
      SPL(II)=SPL(II)+(BPL(II)*CONJG(BPL(II)))
      SMO(II)=SMO(II)+(BMO(II)*CONJG(BMO(II)))
      SML(II)=SML(II)+(BML(II)*CONJG(BML(II)))
   30 CONTINUE
   70 CONTINUE
C         THE NEXT LOOP NORMALIZES THE  ABOVE
C         SPECTRA AND CALCULATES POWER SPECTRAL
C         DENSITIES.
      DO 33 I3=1,N
      ZXO(I3)=ZXO(I3)*T/FNR
      ZYO(I3)=ZYO(I3)*T/FNR
      CSO(I3)=CSO(I3)*T/FNR
      ZXL(I3)=ZXL(I3)*T/FNR
      ZYL(I3)=ZYL(I3)*T/FNR
      CSL(I3)=CSL(I3)*T/FNR
      SPOL(I3)=SPOL(I3)*T/FNR
      SPO(I3)=SPO(I3)*T/FNR
      SPL(I3)=SPL(I3)*T/FNR
      SMO(I3)=SMO(I3)*T/FNR
      SML(I3)=SML(I3)*T/FNR
      SMOL(I3)=SMOL(I3)*T/FNR
   33 CONTINUE
C         THE NEXT LOOP CALCULATES STOKES
C         PARAMETERS 0 THROUGH 3 OF THE
C         INDIVIDUAL SITE ORTHOGONAL
```

125

```
C              COMPONENTS AND THE COHERENCE OF
C              THE PLANAR CIRCULAR POLARIZATION
C              PARAMETERS BETWEEN SITES.
       DO 44 I4=1,N
       CTO(I4)=(ZXO(I4)+ZYO(I4))*2./T
       CPO(I4)=(ZXO(I4)-ZYO(I4))*2./(T*CTO(I4))
       CRO(I4)=(4*CSO(I4))/(CTO(I4)*T)
       COO(I4)=CSO(I4)/(CSQRT(ZXO(I4))*CSQRT(ZYO(I4)))
       CWO(I4)=ATAN2(AIMAG(COO(I4)),REAL(COO(I4)))
       COO(I4)=CSQRT(COO(I4)*CONJG(COO(I4)))
       CTO(I4)=4.3429448*CLOG(CTO(I4))
       CUO(I4)=4.3429448*CLOG(ZXO(I4))
       CVO(I4)=4.3429448*CLOG(ZYO(I4))
       CTL(I4)=(ZXL(I4)+ZYL(I4))*2./T
       CPL(I4)=(ZXL(I4)-ZYL(I4))*2./(T*CTL(I4))
       CRL(I4)=(4*CSL(I4))/(CTL(I4)*T)
       COL(I4)=CSL(I4)/(CSQRT(ZXL(I4))*CSQRT(ZYL(I4)))
       CTL(I4)=4.3429448*CLOG(CTL(I4))
       CUL(I4)=4.3429448*CLOG(ZXL(I4))
       CVL(I4)=4.3429448*CLOG(ZYL(I4))
       CWL(I4)=ATAN2(AIMAG(COL(I4)),REAL(COL(I4)))
       COL(I4)=CSQRT(COL(I4)*CONJG(COL(I4)))
       COPOL(I4)=SPOL(I4)/(CSQRT(SPO(I4))*CSQRT(SPL(I4)))
       COPOL(I4)=CSQRT(COPOL(I4)*CONJG(COPOL(I4)))
       COMOL(I4)=SMOL(I4)/(CSQRT(SMO(I4))*CSQRT(SML(I4)))
       COMOL(I4)=CSQRT(COMOL(I4)*CONJG(COMOL(I4)))
       SPO(I4)=4.3429448*CLOG(SPO(I4))
       SPL(I4)=4.3429448*CLOG(SPL(I4))
       SMO(I4)=4.3429448*CLOG(SMO(I4))
       SML(I4)=4.3429448*CLOG(SML(I4))
   44  CONTINUE
C              VERSATEC PLOT OF CALCULATED QUANTITIES
       NPTS=10./DELTAF+1.
C              'NPTS' DETERMINES NUMBER OF POINTS
```

126

```
C               NECESSARY TO PLOT THE 0 TO 10 HERTZ RANGE.
        ITB(2)=0
        ITB(3)=20
        ITB(4)=10
        ITB(6)=1
        ITB(7)=1
        ITB(12)=1
        RTB(1)=0
        RTB(2)=0
        RTB(3)=ALAB(1)
        READ(5,3000) TITLE
        CALL DRAWP(NPTS,FRQ2,CUOO,ITB,RTB)
        ITB(6)=1
        RTB(3)=ALAB(2)
        READ(5,3000) TITLE
        CALL DRAWP(NPTS,FRQ2,CVOO,ITB,RTB)
        ITB(6)=1
        RTB(3)=ALAB(3)
        READ(5,3000) TITLE
        CALL DRAWP(NPTS,FREQ,CPOO,ITB,RTB)
        ITB(6)=1
        RTB(3)=ALAB(4)
        READ(5,3000) TITLE
        CALL DRAWP(NPTS,FREQ,CROO,ITB,RTB)
        ITB(6)=1
        RTB(3)=ALAB(5)
        READ(5,3000) TITLE
        CALL DRAWP(NPTS,FREQ,CROO(2),ITB,RTB)
        ITB(6)=1
        RTB(3)=ALAB(6)
        READ(5,3000) TITLE
        CALL DRAWP(NPTS,FRQ2,CTOO,ITB,RTB)
        ITB(6)=1
        RTB(3)=ALAB(7)
```

127

```
READ(5,3000) TITLE
CALL DRAWP(NPTS,FREQ,CWOO,ITB,RTB)
ITB(6)=1
RTB(3)=ALAB(8)
READ(5,3000) TITLE
CALL DRAWP(NPTS,FREQ,COOO,ITB,RTB)
ITB(6)=1
RTB(3)=ALAB(9)
READ(5,3000) TITLE
CALL DRAWP(NPTS,FRQ2,CULL,ITB,RTB)
ITB(6)=1
RTB(3)=ALAB(10)
READ(5,3000) TITLE
CALL DRAWP(NPTS,FRQ2,CVLL,ITB,RTB)
ITB(6)=1
RTB(3)=ALAB(11)
READ(5,3000) TITLE
CALL DRAWP(NPTS,FREQ,CPLL,ITB,RTB)
ITB(6)=1
RTB(3)=ALAB(12)
READ(5,3000) TITLE
CALL DRAWP(NPTS,FREQ,CRLL,ITB,RTB)
ITB(6)=1
RTB(3)=ALAB(13)
READ(5,3000) TITLE
CALL DRAWP(NPTS,FREQ,CRLL(2),ITB,RTB)
ITB(6)=1
RTB(3)=ALAB(14)
READ(5,3000) TITLE
CALL DRAWP(NPTS,FRQ2,CTLL,ITB,RTB)
ITB(6)=1
RTB(3)=ALAB(15)
READ(5,3000) TITLE
CALL DRAWP(NPTS,FREQ,CWLL,ITB,RTB)
```

```
      ITB(6)=1
      RTB(3)=ALAB(16)
      READ(5,3000) TITLE
      CALL DRAWP(NPTS,FREQ,COLL,ITB,RTB)
      ITB(6)=1
      RTB(3)=ALAB(17)
      READ(5,3000) TITLE
      CALL DRAWP(NPTS,FRQ2,SPOO,ITB,RTB)
      ITB(6)=1
      RTB(3)=ALAB(18)
      READ(5,3000) TITLE
      CALL DRAWP(NPTS,FRQ2,SPLL,ITB,RTB)
      ITB(6)=1
      RTB(3)=ALAB(19)
      READ(5,3000) TITLE
      CALL DRAWP(NPTS,FRQ2,SMOO,ITB,RTB)
      ITB(6)=1
      RTB(3)=ALAB(20)
      READ(5,3000) TITLE
      CALL DRAWP(NPTS,FRQ2,SMLL,ITB,RTB)
      ITB(6)=1
      RTB(3)=ALAB(21)
      READ(5,3000) TITLE
      CALL DRAWP(NPTS,FREQ,COPOLL,ITB,RTB)
      ITB(6)=1
      RTB(3)=ALAB(22)
      READ(5,3000) TITLE
      CALL DRAWP(NPTS,FREQ,COMOLL,ITB,RTB)
 3000 FORMAT(6A8)
      STOP
      END
/*
//GO.SYSIN DD *
TEST POWER SPECTRAL DENSITY OF SIN 4HZ
```

129

IN XXO,30 AVGS,(REF DB VS LOG FREQ)
TEST POWER SPECTRAL DENSITY OF COS 4HZ
IN YYO,30 AVGS,(REF DB VS LOG FREQ)
TEST STOKES 1/STOKES 0 OF SIN 4HZ
IN XXO AND COS 4HZ IN YYO,30 AVGS
TEST STOKES 2/STOKES 0 OF SIN 4HZ
IN XXO AND COS 4HZ IN YYO,30 AVGS
TEST STOKES 3/STOKES 0 OF SIN 4HZ
IN XXO AND COS 4HZ IN YYO,30 AVGS
TEST STOKES 0 OF SIN 4HZ IN XXO AND
COS 4HZ IN YYO,30 AVGS,(REF DB VS LOG)
TEST PHASE OF SIN 4HZ IN XXO
AND COS 4HZ IN YYO,30 AVGS
TEST COHER OF SIN 4HZ IN XXO
AND COS 4HZ IN YYO,30 AVGS
TEST POWER SPECTRAL DENSITY OF SIN 4HZ
IN XXL,30 AVGS,(REF DB VS LOG FREQ)
TEST POWER SPECTRAL DENSITY OF COS 4HZ
IN YYL,30 AVGS.(REF DB VS LOG FREQ)
TEST STOKES 1/STOKES 0 OF SIN 4HZ
IN XXL AND COS 4HZ IN YYL,30 AVGS
TEST STOKES 2/STOKES 0 OF SIN 4HZ
IN XXL AND COS 4HZ IN YYL,30 AVGS
TEST STOKES 3/STOKES 0 OF SIN 4HZ
IN XXL AND COS 4HZ IN YYL,30 AVGS
TEST STOKES 0 OF SIN 4HZ IN XXL AND
COS 4HZ IN YYL,30 AVGS,(REF DB VS LOG)
TEST PHASE OF SIN 4HZ IN XXL
AND COS 4HZ IN YYL,30 AVGS
TEST COHER OF SIN 4HZ IN XXL
AND COS 4HZ IN YYL,30 AVGS
TEST RT CIRC POLARIZATION PSD OF SIN 4HZ IN
XXO AND COS 4HZ IN YYO, (DB VS LOG),30 AVGS
TEST RT CIRC POLARIZATION PSD OF SIN 4HZ IN

```
XXL AND COS 4HZ IN YYL, (DB VS LOG),30 AVGS
TEST LEFT CIRC POLARIZATION PSD OF SIN 4HZ
IN XXO AND COS 4HZ IN YYO (DB VS LOG),30 AVGS
TEST LEFT CIRC POLARIZATION PSD OF SIN 4HZ
IN XXL AND COS 4HZ IN YYL (DB VS LOG),30 AVGS
TEST COHER RT CIRC POLARIZATION OF SIN 4HZ
IN XXO,XXL AND COS 4HZ IN YYO,YYL, 30 AVGS
TEST COHER LEFT CIRC POLARIZATION OF SIN 4HZ
IN XXO,XXL AND COS 4HZ IN YYO,YYL, 30 AVGS
/*
//
```

APPENDIX G

MASS STORAGE PROGRAM

```
//JOEB1MB JOB (1592,0129),'FISHER SMC.1399',CLASS=F
//*MAIN ORG=NPGVM1.1592P
// EXEC FORTXCLG
//FORT.SYSIN DD DSN=MSS.SYS3.NONIMSL.SOURCE(FOURT),DISP=SHR
//      DD   *
C           THE ARRAY 'IN' WILL BE USED TO
C           RECEIVE THE DATA PASSED FROM
C           THE SUBROUTINE 'READ' AND THEN
C           TRANSFERRED TO THE APPROPRIATE
C           XXX OR YYY ARRAY.
      INTEGER*2 IN(16)
      COMPLEX*8 XXX(8192),YYY(8192)
      DIMENSION FREQ(8192),TIME(8192),WORK(16384)
      DATA XXX,YYY/16384*(0.0,0.0)/
      DATA TIME,FREQ/16384*0.0/
C           THE FOLLOWING SECTION READS THE
C           FIRST SIX SECONDS OF COMPUTER TAPE
C           AND DISCARDS THIS DATA.
      ITL=192
      DO 55 JJ=1,ITL
      CALL RD(20,IN,200,IREC,IRR)
   55 CONTINUE
      IFRAME=8192
      NR=20
      FNR=FLOAT(NR)
      DO 70 L1=1,NR
C           THE NEXT LOOP READS THE COMPUTER
C           TAPE USING THE PROGRAM PROVIDED
C           BY MR. TIM STANTON OF NAVAL POST-
```

132

```fortran
C          GRADUATE SCHOOL.
      DO 60 JJ=1,IFRAME
      CALL RD(20,IN,1000,IREC,IRR)
      XXX(JJ)=IN(2)
      YYY(JJ)=IN(3)
   60 CONTINUE
      N=8192
      FN=FLOAT(N)
      DELTAT=1./32.
      T=FN*DELTAT
      DELTAF=1./T
      DO 20 J=1,N
      TIME(J)=DELTAT*FLOAT(J)
      FREQ(J)=DELTAF*FLOAT(J)
C          THE NEXT 4 STEPS CONVERT THE
C          DATA TO VOLTAGE AND ENSURES THAT
C          NO ERRONEOUS DATA HAS BEEN INTRODUCED
C          INTO THE ARRAYS.
      XXX(J)=(XXX(J)-2045.5)*10./2045.5
      XXX(J)=REAL(XXX(J))
      YYY(J)=(YYY(J)-2045.5)*10./2045.5
      YYY(J)=REAL(YYY(J))
   20 CONTINUE
      CALL FOURT(XXX,N,1,-1,0,WORK)
      CALL FOURT(YYY,N,1,-1,0,WORK)
      DO 40 K4=1,N
      XXX(K4)=XXX(K4)/FN
      YYY(K4)=YYY(K4)/FN
   40 CONTINUE
C          THE NEXT LOOP APPLIES THE SYSTEM
C          TRANSFER FUNCTION TO THE TRANSFORMED
C          FREQUENCY DOMAIN DATA. THE TRANSFER
C          FUNCTION CONVERTS VOLTS TO NANOTESLAS.
      DO 9 L=1,N
```

133

```
      FRQ=FREQ(L)
    1 IF(FRQ.LE.15.)GO TO 2
      XXX(L)=XXX(L)/(105.5-3.14*FRQ)
      YYY(L)=YYY(L)/(181.32-7.588*FRQ)
      GO TO 8
    2 IF(FRQ.LE.10.)GO TO 3
      XXX(L)=XXX(L)/(5.958*FRQ-30.97)
      YYY(L)=YYY(L)/(7.166*FRQ-39.99)
      GO TO 8
    3 IF(FRQ.LE.7.5)GO TO 4
      XXX(L)=XXX(L)/(3.492*FRQ-5.31)
      YYY(L)=YYY(L)/(4.252*FRQ-10.85)
      GO TO 8
    4 IF(FRQ.LE.5.)GO TO 5
      XXX(L)=XXX(L)/(2.6311*FRQ+0.14657)
      YYY(L)=YYY(L)/(3.012*FRQ-1.55)
      GO TO 8
    5 IF (FRQ.LE.3.)GO TO 6
      XXX(L)=XXX(L)/(2.6311*FRQ+0.14657)
    7 YYY(L)=YYY(L)/(2.702*FRQ)
      GO TO 8
    6 XXX(L)=XXX(L)/(2.72*FRQ)
      GO TO 7
    8 CONTINUE
    9 CONTINUE
C           THE NEXT WRITE STATEMENTS SEND
C           THE CONVERTED DATA TO MSS
C           FOR FUTURE MANIPULATION AND RECALL.
C           THIS NEXT SET OF STATEMENTS ALSO
C           PROVIDES THE USER A DIAGNOSTIC.
      WRITE(21)XXX
      WRITE(6,*)XXX(1),XXX(3192)
      WRITE(21)YYY
      WRITE(6,*)YYY(1),YYY(3192)
```

```
   70 CONTINUE
      ENDFILE 21
      STOP
      END
       SUBROUTINE RD(IUN,IO,IRS,IREC,IRQ)
C
C        THIS PROCEDURE FURNISHED BY MR. TIM STANTON,
C        DEPARTMENT OF OCEANOGRAPHY.
C
C             READ DATA FROM IUN, ALLIGN , CHECK & RETURN
C
C      IUN=TAPE NUMBER, E3 20
C      IO=INTEGER*2 ARRAY, 16 LONG,
C      (VALUES 0-4095, SUBTRACT 2048, *5/2028. GIVES VOLTAGE
C      IRS= NUMBER OF RESINCS ALLOWED (ERRORS)
C      IREC= COUNTER OF RECORDS (FRAMES OF DATA)
C          BLOCK 512 BITS,   32 BITS = RECORD
C          800 BPI TAPE UNLABLED
C      IRQ= NUMBER OF ACTUAL RESINCS (ERRORS)
C
C
      INTEGER * 2 IO(16),IP(16)
      DATA IRR /0/
      IF (IREC.EQ.0) IS=0
      IER=0
   20    FORMAT (16A2)
      IF (IS.NE.0) GO TO 50
      READ (IUN,20,END=900) IP
      IREC=IREC+1
   40    IS=IS+1
      IF (IS.LT.17) GO TO 50
      READ (IUN,20,END=900) IP
      IS=1
      IREC=IREC+1
```

135

```
 50    ICH=IMASK(IP(IS),3,0)+1
C      WRITE (6,55) ICH,IS,IUN,IREC
 55    FORMAT (' RESYNCING ICH,IS,IUN,IREC ',4I8)
C
       IF (ICH.NE.1) GO TO 40
       DO 100 I=1,16
        IO(I)=ISHIFT(IP(IS),4)
       ICH=IMASK(IP(IS),3,0)+1
       IF (ICH.EQ.1) GO TO 80
       IER=IER+1
       WRITE (6,70) IUN,IREC,I,ICH,IER
 70    FORMAT ('UNIT',I3,'RECORD',I5,'CHAN & DATA CH ',2I4,
      $ 'ERRORS ',I7)
 80    IS=IS+1
       IF (IS.LT.17) GO TO 100
       READ (IUN,20,END=900) IP
       IS=1
       IREC=IREC+1
100    CONTINUE
C
       IF (IER.EQ.0) GO TO 150
       IRR=IRR+1
       IF (IRR.LT.IRS) GO TO 120
       WRITE (6,110)
110    FORMAT ('1 STOPPED IN SUB RD BECAUSE
      C OF IRR.GT.',I6,' AT L110')
       IRQ=IRR
       STOP
120    CONTINUE
       WRITE (6,130) IREC,IRR
130    FORMAT ('RESYNC AT FRAME',I6,'WITH TOTAL ERRORS',I7)
       IER=0
       IRQ=IRR
       GO TO 50
```

136

```
150      CONTINUE
         RETURN
 900     WRITE (6,910) IUN,IREC
 910     FORMAT ('1    END OF UNIT ',I3,' AT REC ',I7)
         STOP
         END
         FUNCTION ISHIFT (IN,NPLC)
C              RETURNS SHIFTED VALUE OF I*2 WORD IN
C              -VE LEFT,+VE RIGHT SHIFT
C
         INTEGER * 2 IN
         IP=IN
         IF (IP.LT.0) IP=IP+65536
         IF (NPLC.LT.0) GO TO 30
         ISHIFT=IP/(2**IABS(NPLC))
         RETURN
 30      ISHIFT=IP*(2**IABS(NPLC))
         IF (ISHIFT.GT.65535) ISHIFT=MOD(ISHIFT,65536)
         RETURN
         END
         FUNCTION IMASK (IN,IBL,IBR)
C              MASK I*2 WORD IN OUTSIDE BITS IBL & IBR
C
         INTEGER * 2 IN,IO
         IO=IN
         IF (IBR.EQ.0) GO TO 50
         IT=ISHIFT(IN,IBR)
         IO=IT
 50      IP=ISHIFT(IO,IBL-15-IBR)
         IO=IP
         IMASK=ISHIFT(IO,15-IBL)
         RETURN
         END
/*
```

137

```
//GO.FT21F001 DD  UNIT=3330V,MSVGP=PUB4A,DISP=(NEW,CATLG),
//            DSN=MSS.S1592.GMDT1A,
//            DCB=(RECFM=VBS,BLKSIZE=4096,LRECL=4092),
//            SPACE=(CYL,(8,8))
//GO.FT20F001 DD  UNIT=3400-4,VOL=SER=GMDT1A,DISP=(OLD,PASS),
//            LABEL=(1,NL,,IN),
//            DCB=(RECFM=FB,LRECL=32,BLKSIZE=512,DEN=2)
//
```

APPENDIX H

MAIN PROGRAM

```
//JOEK1MB JOB (1592,0129),'FISHER SMC.1399',CLASS=F
//*MAIN ORG=NPGVM1.1592P,LINES=(60)
//*FORMAT PR,DDNAME=PLOT.SYSVECTP,DEST=LOCAL
// EXEC FRTXCLGP,PARM.LKED='LIST,MAP,XREF',REGION.GO=2700K
//SYSUT1    DD  UNIT=SYSDA,SPACE=(CYL,(8,8))
//SYSUT2    DD  UNIT=SYSDA,SPACE=(CYL,(3,8))
//SYSLIN    DD  SPACE=(6080,(80,80)),UNIT=SYSDA
//FORT.SYSIN DD DSN=MSS.SYS3.NONIMSL.SOURCE(FOURT),DISP=SHR
//     DD  *
C          DETAILED DESCRIPTIONS OF THE
C          VARIOUS STEPS AND LOOPS ARE
C          CONTAINED IN APPENDICES B AND C.
      INTEGER*2 IN(16)
      COMPLEX*8 XXO(8192),YYO(8192),
     C CSO(8192),COO(8192),ZXO(8192),
     C CRO(8192),CTO(8192),CUO(8192),
     C CVO(8192),CWO(8192),CPO(8192),
     C ZYO(8192),COMOL(8192),COL(8192),
     C CUL(8192),CVL(8192),CWL(8192),
     C COPOL(8192),XXX(8192),YYY(8192),
     C XXL(8192),YYL(8192),ZXL(8192),
     C ZYL(8192),CSL(8192),BPO(8192),
     C BMO(8192),BPL(8192),BML(8192),
     C SPOL(8192),SMOL(8192),SPO(8192),
     C SPL(8192),SMO(8192),CTL(8192),
     C CPL(8192),CRL(8192),SML(8192)
      DIMENSION TIME(8192),FREQ(8192),
     C WORK(16384),FRQ2(8192)
      INTEGER*4 ITB(12)/12*0/
```

```
      REAL*4      RTB(28)/23*0.0/,CROO(16384),
C CPOO(16384),CUOO(16384),
C COOO(16384),CTOO(16384),CVOO(16384),
C CWOO(16384),CTLL(16384),
C CPLL(16384),CRLL(16384),COLL(16384),
C CULL(16384),CVLL(16384),
C CWLL(16384),COMOLL(16384),COPOLL(16384),
C SPOO(16384),SPLL(16384),
C SMOO(16384),SMLL(16384)
      REAL ALAB(22)/'PDXO','PDYO','ST1O',
C 'ST2O','ST3O','STOO','PHAO',
C 'GAMO','PDXL','PDYL','ST1L','ST2L',
C 'ST3L','STOL','PHAL','GAML',
C 'SPLO','SPLL','SMOO','SMLL','CPOL','CMOL'/
      REAL*8 TITLE(12)
      EQUIVALENCE(TITLE(1),RTB(5)),(CROO(1),
C CRO(1)),(CPOO(1),CPO(1)),
C (COOO(1),COO(1)),(CTOO(1),CTO(1)),(CUOO(1),CUO(1)),
C (CWOO(1),CWO(1)),(CVOO(1),CVO(1)),(CTLL(1),CTL(1)),
C (CPLL(1),CPL(1)),(CRLL(1),CRL(1)),(COLL(1),COL(1)),
C (CULL(1),CUL(1)),(CVLL(1),CVL(1)),(CWLL(1),CWL(1)),
C (COPOLL(1),COPOL(1)),(COMOLL(1),
C COMOL(1)),(SPOO(1),SPO(1)),
C (SPLL(1),SPL(1)),(SMOO(1),SMO(1)),(SMLL(1),SML(1))
      DATA XXO,YYO,CSO,COO,ZXO,ZYO,CRO,
C CTO,CUO,CVC,CWO,XXX,YYY,
C XXL,YYL,ZXL,ZYL,CSL,BPO,BMO,BPL,
C BML,SPOL,SMOL,SPO,SPL,SMO,
C SML,CTL,CRL,COL,CVL,COPOL,CWL,COPOL,
C COMOL/294912*(0.0,0.0)/
      DATA TIME,FREQ,FRQ2/24576*0.0/
      ITL=192
      DO 55 JJ=1,ITL
      CALL RD(20,IN,200,IREC,IRR)
```

```
    55   CONTINUE
         IFRAME=8192
         NR=20
         FNR=FLOAT(NR)
C               THE FIRST STATEMENTS OF LOOP 70
C               RECALLS DATA PREVIOUSLY STORED IN
C               THE IBM 3033 MASS STORAGE SYSTEM.
         DO 70 L1=1,NR
         READ(21)XXX
         READ(21)YYY
         DO 43 II=1,IFRAME
         XXL(II)=XXX(II)
         YYL(II)=YYY(II)
    43   CONTINUE
         DO 60 JJ=1,IFRAME
         CALL RD(20,IN,1000,IREC,IRR)
         XXO(JJ)=IN(2)
         YYO(JJ)=IN(3)
    60   CONTINUE
         N=8192
         FN=FLOAT(N)
         DELTAT=1./32.
         T=FN*DELTAT
         DELTAF=1./T
         DO 20 J=1,N
         TIME(J)=DELTAT*FLOAT(J)
         FREQ(J)=DELTAF*FLOAT(J)
         FRQ2(J)=ALOG10(FREQ(J))
         XXO(J)=(XXO(J)-2045.5)*5./2045.5
         XXO(J)=REAL(XXO(J))
         YYO(J)=(YYO(J)-2045.5)*5./2045.5
         YYO(J)=REAL(YYO(J))
    20   CONTINUE
         CALL FOURT(XXO,N,1,-1,0,WORK)
```

141

```fortran
      CALL FOURT (YYO,N,1,-1,0,WORK)
      DO 40 K4=1,N
      XXO(K4)=XXO(K4)/FN
      YYO(K4)=YYO(K4)/FN
40    CONTINUE
      DO 9 L=1,N
      FRQ=FREQ(L)
1     IF(FRQ.LE.15.)GO TO 2
      XXO(L)=XXO(L)/(-81.33 +17.066*FRQ - 0.5389*FRQ*FRQ)
      YYO(L)=YYO(L)/(-63.435 +11.7105*FRQ-0.23279*FRQ*FRQ)
      GO TO 8
2     IF(FRQ.LE.10.)GO TO 3
      XXO(L)=XXO(L)/(-18.436 + 4.9023*FRQ)
      YYO(L)=YYO(L)/(-63.435 +11.7105*FRQ -0.23279*FRQ*FRQ)
      GO TO 8
3     IF(FRQ.LE.7.5)GO TO 4
      XXO(L)=XXO(L)/(3.947*FRQ-9.368)
      YYO(L)=YYO(L)/(4.295*FRQ-11.837)
      GO TO 8
4     IF(FRQ.LE.5.)GO TO 5
      XXO(L)=XXO(L)/(2.8105*FRQ-0.5657)
      YYO(L)=YYO(L)/(2.800*FRQ-.50)
      GO TO 8
5     XXO(L)=XXO(L)/(2.723*FRQ)
      YYO(L)=YYO(L)/(2.717*FRQ)
      GO TO 8
8     CONTINUE
9     CONTINUE
      DO 30 II=1,N
      ZXO(II)=ZXO(II)+(XXO(II)*CONJG(XXO(II)))
      ZYO(II)=ZYO(II)+(YYO(II)*CONJG(YYO(II)))
      CSO(II)=CSO(II)+(XXO(II)*CONJG(YYO(II)))
      ZXL(II)=ZXL(II)+(XXL(II)*CONJG(XXL(II)))
      ZYL(II)=ZYL(II)+(YYL(II)*CONJG(YYL(II)))
```

```
      CSL(II)=CSL(II)+(XXL(II)*CONJG(YYL(II)))
      BPO(II)=XXO(II)+((0.,1.)*YYO(II))
      BMO(II)=XXO(II)-((0.,1.)*YYO(II))
      BPL(II)=XXL(II)+((0.,1.)*YYL(II))
      BML(II)=XXL(II)-((0.,1.)*YYL(II))
      SPOL(II)=SPOL(II)+(BPO(II)*CONJG(BPL(II)))
      SMOL(II)=SMOL(II)+(BMO(II)*CONJG(BML(II)))
      SPO(II)=SPO(II)+(BPO(II)*CONJG(BPO(II)))
      SPL(II)=SPL(II)+(BPL(II)*CONJG(BPL(II)))
      SMO(II)=SMO(II)+(BMO(II)*CONJG(BMO(II)))
      SML(II)=SML(II)+(BML(II)*CONJG(BML(II)))
   30 CONTINUE
   70 CONTINUE
      DO 33 I3=1,N
      ZXO(I3)=ZXO(I3)*T/FNR
      ZYO(I3)=ZYO(I3)*T/FNR
      CSO(I3)=CSO(I3)*T/FNR
      ZXL(I3)=ZXL(I3)*T/FNR
      ZYL(I3)=ZYL(I3)*T/FNR
      CSL(I3)=CSL(I3)*T/FNR
      SPOL(I3)=SPOL(I3)*T/FNR
      SPO(I3)=SPO(I3)*T/FNR
      SPL(I3)=SPL(I3)*T/FNR
      SMO(I3)=SMO(I3)*T/FNR
      SML(I3)=SML(I3)*T/FNR
      SMOL(I3)=SMOL(I3)*T/FNR
   33 CONTINUE
      DO 44 I4=1,N
      CTO(I4)=(ZXO(I4)+ZYO(I4))*2./T
      CPO(I4)=(ZXO(I4)-ZYO(I4))*2./(T*CTO(I4))
      CRO(I4)=(4*CSO(I4))/(CTO(I4)*T)
      COO(I4)=CSO(I4)/(CSQRT(ZXO(I4))*CSQRT(ZYO(I4)))
      CWO(I4)=ATAN2(AIMAG(COO(I4)),REAL(COO(I4)))
      COO(I4)=CSQRT(COO(I4)*CONJG(COO(I4)))
```

143

```fortran
      CTO(I4)=4.3429448*CLOG(CTO(I4))
      CUO(I4)=4.3429448*CLOG(ZXO(I4))
      CVO(I4)=4.3429448*CLOG(ZYO(I4))
      CTL(I4)=(ZXL(I4)+ZYL(I4))*2./T
      CPL(I4)=(ZXL(I4)-ZYL(I4))*2./(T*CTL(I4))
      CRL(I4)=(4*CSL(I4))/(CTL(I4)*T)
      COL(I4)=CSL(I4)/(CSQRT(ZXL(I4))*CSQRT(ZYL(I4)))
      CTL(I4)=4.3429448*CLOG(CTL(I4))
      CUL(I4)=4.3429448*CLOG(ZXL(I4))
      CVL(I4)=4.3429448*CLOG(ZYL(I4))
      CWL(I4)=ATAN2(AIMAG(COL(I4)),REAL(COL(I4)))
      COL(I4)=CSQRT(COL(I4)*CONJG(COL(I4)))
      COPOL(I4)=SPOL(I4)/(CSQRT(SPO(I4))*CSQRT(SPL(I4)))
      COPOL(I4)=CSQRT(COPOL(I4)*CONJG(COPOL(I4)))
      COMOL(I4)=SMOL(I4)/(CSQRT(SMO(I4))*CSQRT(SML(I4)))
      COMOL(I4)=CSQRT(COMOL(I4)*CONJG(COMOL(I4)))
      SPO(I4)=4.3429448*CLOG(SPO(I4))
      SPL(I4)=4.3429448*CLOG(SPL(I4))
      SMO(I4)=4.3429448*CLOG(SMO(I4))
      SML(I4)=4.3429448*CLOG(SML(I4))
   44 CONTINUE
      NPTS=10./DELTAF+1.
      ITB(2)=0
      ITB(3)=20
      ITB(4)=10
      ITB(6)=1
      ITB(7)=1
      ITB(12)=1
      RTB(1)=0
      RTB(2)=0
      RTB(3)=ALAB(1)
      READ(5,3000) TITLE
      CALL DRAWP(NPTS,FRQ2,CUO),ITB,RTB)
      ITB(6)=1
```

144

```
RTB(3)=ALAB(2)
READ(5,3000) TITLE
CALL DRAWP (NPTS,FRQ2,CVOO,ITB,RTB)
ITB(6)=1
RTB(3)=ALAB(3)
READ(5,3000) TITLE
CALL DRAWP (NPTS,FREQ,CPOO,ITB,RTB)
ITB(6)=1
RTB(3)=ALAB(4)
READ(5,3000) TITLE
CALL DRAWP (NPTS,FREQ,CROO,ITB,RTB)
ITB(6)=1
RTB(3)=ALAB(5)
READ(5,3000) TITLE
CALL DRAWP (NPTS,FREQ,CROO(2),ITB,RTB)
ITB(6)=1
RTB(3)=ALAB(6)
READ(5,3000) TITLE
CALL DRAWP (NPTS,FRQ2,CTOO,ITB,RTB)
ITB(6)=1
RTB(3)=ALAB(7)
READ(5,3000) TITLE
CALL DRAWP (NPTS,FREQ,CWOO,ITB,RTB)
ITB(6)=1
RTB(3)=ALAB(8)
READ(5,3000) TITLE
CALL DRAWP (NPTS,FREQ,COOO,ITB,RTB)
ITB(6)=1
RTB(3)=ALAB(9)
READ(5,3000) TITLE
CALL DRAWP (NPTS,FRQ2,CULL,ITB,RTB)
ITB(6)=1
RTB(3)=ALAB(10)
READ(5,3000) TITLE
```

145

```
CALL DRAWP (NPTS,FRQ2,CVLL,ITB,RTB)
ITB(6)=1
RTB(3)=ALAB(11)
READ(5,3000) TITLE
CALL DRAWP (NPTS,FREQ,CPLL,ITB,RTB)
ITB(6)=1
RTB(3)=ALAB(12)
READ(5,3000) TITLE
CALL DRAWP (NPTS,FREQ,CRLL,ITB,RTB)
ITB(6)=1
RTB(3)=ALAB(13)
READ(5,3000) TITLE
CALL DRAWP (NPTS,FREQ,CRLL(2),ITB,RTB)
ITB(6)=1
RTB(3)=ALAB(14)
READ(5,3000) TITLE
CALL DRAWP (NPTS,FRQ2,CTLL,ITB,RTB)
ITB(6)=1
RTB(3)=ALAB(15)
READ(5,3000) TITLE
CALL DRAWP (NPTS,FREQ,CWLL,ITB,RTB)
ITB(6)=1
RTB(3)=ALAB(16)
READ(5,3000) TITLE
CALL DRAWP (NPTS,FREQ,COLL,ITB,RTB)
ITB(6)=1
RTB(3)=ALAB(17)
READ(5,3000) TITLE
CALL DRAWP (NPTS,FRQ2,SPOO,ITB,RTB)
ITB(6)=1
RTB(3)=ALAB(18)
READ(5,3000) TITLE
CALL DRAWP (NPTS,FRQ2,SPLL,ITB,RTB)
ITB(6)=1
```

```
          RTB(3)=ALAB(19)
          READ(5,3000) TITLE
          CALL DRAWP(NPTS,FRQ2,SMOO,ITB,RTB)
          ITB(6)=1
          RTB(3)=ALAB(20)
          READ(5,3000) TITLE
          CALL DRAWP(NPTS,FRQ2,SMLL,ITB,RTB)
          ITB(6)=1
          RTB(3)=ALAB(21)
          READ(5,3000) TITLE
          CALL DRAWP(NPTS,FREQ,COPOLL,ITB,RTB)
          ITB(6)=1
          RTB(3)=ALAB(22)
          READ(5,3000) TITLE
          CALL DRAWP(NPTS,FREQ,COMOIL,ITB,RTB)
 3000     FORMAT(6A8)
          STOP
          END
          SUBROUTINE RD(IUN,IO,IRS,IREC,IRQ)
C
C             THIS PROCEDURE FURNISHED BY MR. TIM STANTON,
C             DEPARTMENT OF OCEANOGRAPHY.
C
C                    READ DATA FROM IUN, ALLIGN , CHECK & RETURN
C
C          IUN=TAPE NUMBER, EG 20
C          IO=INTEGER*2 ARRAY, 16 LONG,
C          (VALUES 0-4095, SUBTRACT 2043)*5/2028. GIVES VOLTAGE
C          IRS= NUMBER OF RESINCS ALLOWED (ERRORS)
C          IREC= COUNTER OF RECORDS (FRAMES OF DATA)
C               BLOCK 512 BITS,   32 BITS = RECORD
C               800 BPI TAPE UNLABLED
C          IRQ= NUMBER OF ACTUAL RESINCS (ERRORS)
C
```

147

```fortran
C
      INTEGER * 2 IO(16),IP(16)
      DATA IRR /0/
      IF (IREC.EQ.0) IS=0
      IER=0
 20   FORMAT (16 A2)
      IF (IS.NE.0) GO TO 50
      READ (IUN,20,END=900) IP
      IREC=IREC+1
 40   IS=IS+1
      IF (IS.LT.17) GO TO 50
      READ (IUN,20,END=900) IP
      IS=1
      IREC=IREC+1
 50   ICH=IMASK(IP(IS),3,0)+1
C     WRITE (6,55) ICH,IS,IUN,IREC
 55   FORMAT (' RESYNCING ICH,IS,IUN,IREC ',4I3)
C .
      IF (ICH.NE.1) GO TO 40
      DO 100 I=1,16
       IO(I)=ISHIFT(IP(IS),4)
      ICH=IMASK(IP(IS),3,0)+1
      IF (ICH.EQ.I) GO TO 30
      IER=IER+1
      WRITE (6,70) IUN,IREC,I,ICH,IER
 70   FORMAT ('UNIT',I3,'RECORD',I5,'CHAN & DATA CH ',2I4,
     $ 'ERRORS ',I7)
 80   IS=IS+1
      IF (IS.LT.17) GO TO 100
      READ (IUN,20,END=900) IP
      IS=1
      IREC=IREC+1
 100  CONTINUE
C
```

```fortran
       IF (IER.EQ.0) GO TO 150
       IRR=IRR+1
       IF (IRR.LT.IRS) GO TO 120
       WRITE (6,110)
110    FORMAT ('1 STOPPED IN SUB RD BECAUSE
     C OF IRR.GT.',I6,' AT L110')
       IRQ=IRR
       STOP
120    CONTINUE
       WRITE (6,130) IREC,IRR
130    FORMAT ('RESYNC AT FRAME',I6,'WITH TOTAL ERRORS',I7)
       IER=0
       IRQ=IRR
       GO TO 50
150    CONTINUE
       RETURN
900    WRITE (6,910) IUN,IREC
910    FORMAT ('1    END OF UNIT ',I3,' AT REC ',I7)
       STOP
       END
       FUNCTION ISHIFT (IN,NPLC)
C               RETURNS SHIFTED VALUE OF I*2 WORD IN
C               -VE LEFT,+VE RIGHT SHIFT
C
       INTEGER * 2 IN
       IP=IN
       IF (IP.LT.0) IP=IP+65536
       IF (NPLC.LT.0) GO TO 30
       ISHIFT=IP/(2**IABS(NPLC))
       RETURN
30     ISHIFT=IP*(2**IABS(NPLC))
       IF (ISHIFT.GT.65535) ISHIFT=MOD(ISHIFT,65536)
       RETURN
       END
```

149

```
      FUNCTION IMASK (IN,IBL,IBR)
C              MASK I*2 WORD IN OUTSIDE BITS IBL & IBR
C
      INTEGER * 2 IN,IO
      IO=IN
      IF (IBR.EQ.0) GO TO 50
      IT=ISHIFT(IN,IBR)
      IO=IT
 50   IP=ISHIFT(IO,IBL-15-IBR)
      IO=IP
      IMASK=ISHIFT(IO,15-IBL)
      RETURN
      END
/*
//GO.FT20F001 DD UNIT=3400-4,VOL=SER=GMDT1B,DISP=(OLD,PASS),
//             LABEL=(1,NL,,IN),
//             DCB=(RECFM=FB,LRECL=32,BLKSIZE=512,DEN=2)
//GO.FT21F001 DD UNIT=3330V,MSVGP=PUB4A,DISP=(OLD,KEEP),
//             DSN=MSS.S1592.GMDF1A,
//             DCB=(RECFM=VBS,BLKSIZE=4096,LRECL=4092)
//GO.SYSDUMP DD SYSOUT=A
//GO.SYSIN DD *
X COIL PSD, MTRY BAY,1122-1254 LOCAL,17AUG82,
20 AVGS, 32S/SEC,5VOLT, (DB NT**2 VS LOG FREQ)
Y COIL PSD, MTRY BAY,1122-1254 LOCAL,17AUG82,
20 AVGS, 32S/SEC,5VOLT, (DB NT**2 VS LOG FREQ)
STOKES NO. ONE, MTRY BAY, 1122-1254
LOCAL, 17AUG82, 20 AVGS, 32S/SEC, 5VOLT
STOKES NO. TWO, MTRY BAY, 1122-1254
LOCAL, 17AUG82, 20 AVGS, 32S/SEC, 5VOLT
STOKES NO. THREE, MTRY BAY, 1122-1254
LOCAL, 17AUG82, 20 AVGS, 32S/SEC, 5VOLT
STOKES NO. ZERO, MTRY BAY, 1122-1254 LOCAL,
17AUG82, 20 AVGS, 32S/SEC, 5VOLT, (LOG VS LOG)
```

```
PHASE OF X AND Y, MTRY BAY 1122-1254
LOCAL, 17AUG82, 20 AVGS, 32S/SEC, 5VOLT
COHER OF X AND Y COILS, MTRY BAY, 1122-1254
LOCAL, 17AUG82, 20 AVGS, 32S/SEC, 5VOLT
X COIL PSD, LA MESA,1122-12545LOCAL,17AUG82,
20 AVGS, 32S/SEC,10VOLT, (DB NT**2 VS LOG FREQ)
Y COIL PSD, LA MESA,1122-1254 LOCAL,17AUG82,
20 AVGS, 32S/SEC,10VOLT, (DB NT**2 VS LOG FREQ)
STOKES NO. ONE, LA MESA, 112201254
LOCAL, 17AUG82, 20 AVGS, 32S/SEC, 10VOLT
STOKES NO. TWO, LA MESA, 1122-1254
LOCAL, 17AUG82, 20 AVGS, 32S/SEC, 10VOLT
STOKES NO. THREE, LA MESA, 1122-1254
LOCAL, 17AUG82, 20 AVGS, 32S/SEC, 10VOLT
STOKES NO. ZERO, LA MESA, 1122-1254 LOCAL,
17AUG82, 20 AVGS, 32S/SEC, 10VOLT, (LOG VS LOG)
PHASE OF X AND Y, LA MESA, 1122-1254
LOCAL, 17AUG82, 20 AVGS, 32S/SEC, 10VOLT
COHER OF X AND Y COILS, LA MESA, 1122-1254
LOCAL, 17AUG82, 20 AVGS, 32S/SEC, 10VOLT
RT CIRC POLARIZATION PSD,MTRY BAY,1122-1254
LOCAL,17AUG82,20 AVGS,32S/SEC,5VOLT,(DB VS LOG)
RT CIRC POLARIZATION PSD, LA MESA, 1122-1254
LOCAL,17AUG82,20 AVGS,32S/SEC,10VOLT,(DB VS LOG)
LEFT CIRC POLARIZATION PSD, MTRY BAY,1122-1254
LOCAL,17AUG82, 20 AVGS,32S/SEC,5VOLT,(DB VS LOG)
LEFT CIRC POLARIZATION PSD, LA MESA, 1122-1254
LOCAL,17AUG82,20 AVGS,32S/SEC,10VOLT,(DB VS LOG)
COHER RT CIRC POLARIZATION MTRY BAY/LA MESA,
1122-1254 LOCAL, 17AUG82, 20 AVGS, 32S/SEC
COHER LEFT CIRC POLARIZATION MTRY BAY/LA MESA,
1122-1254 LOCAL, 17AUG82, 20 AVGS, 32S/SEC
/*
//
```
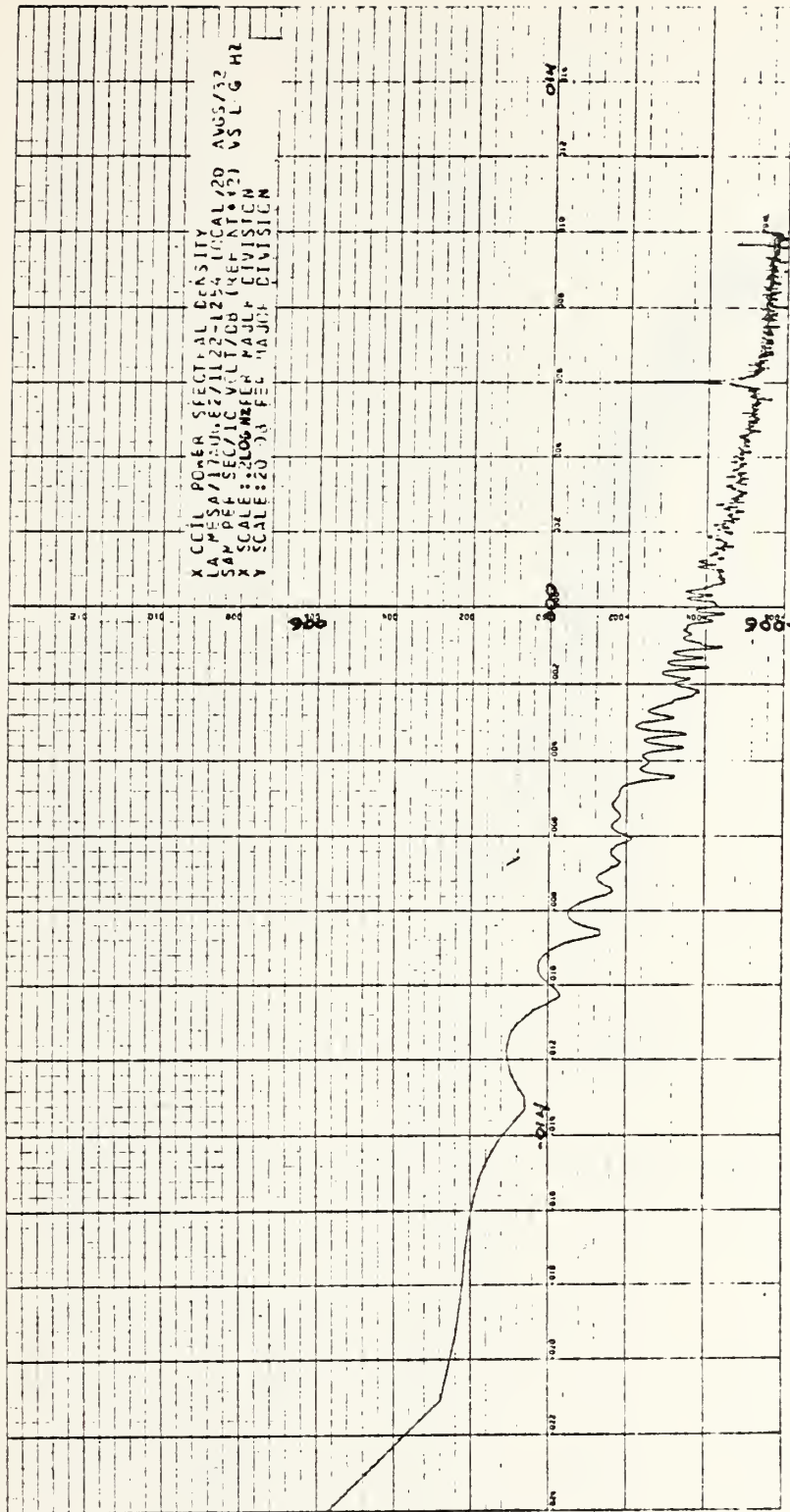
APPENDIX I

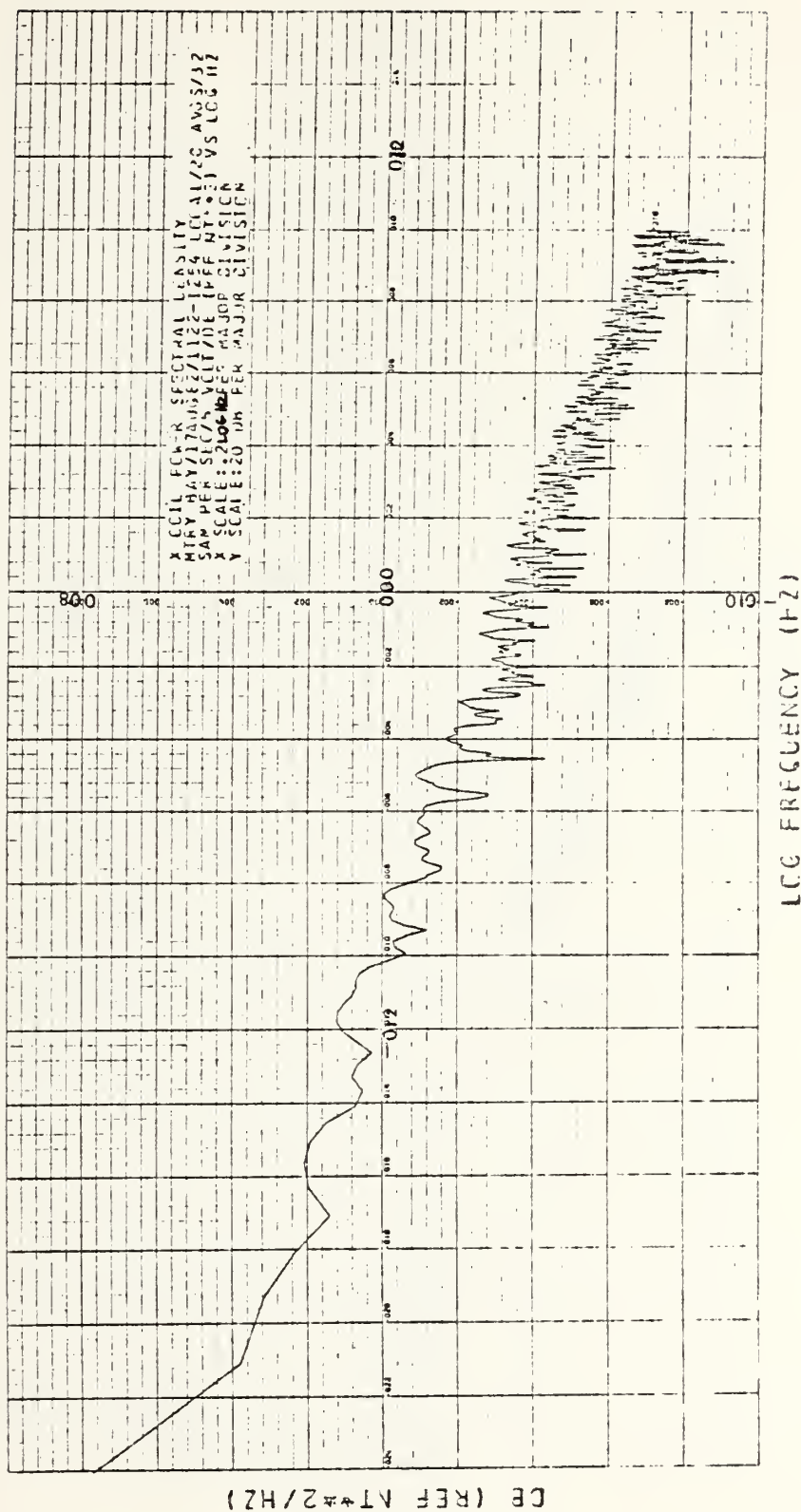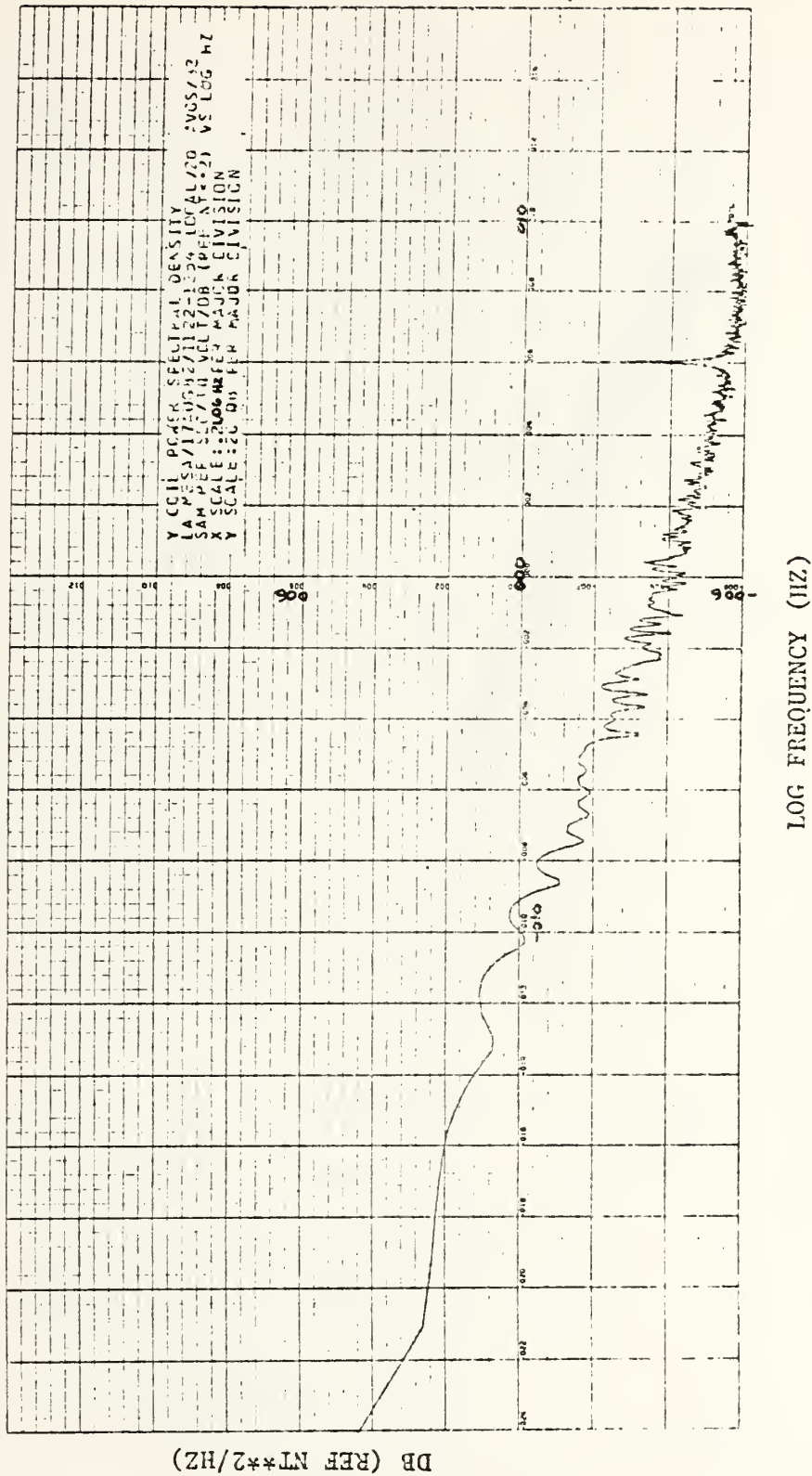## TYPICAL COMPUTER GENERATED PLOTS

Log Freqency [log Hz]
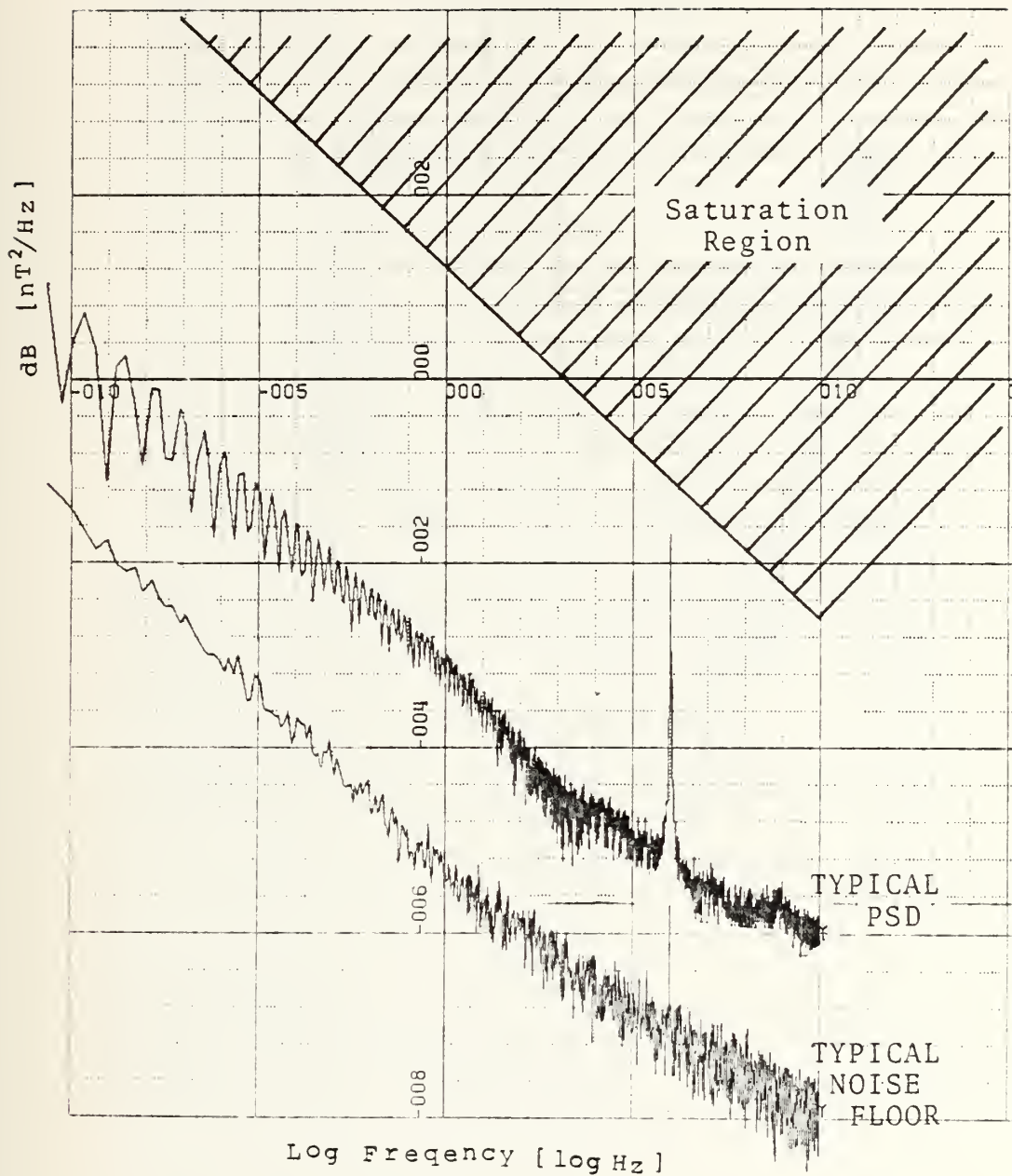
X-SCALE=5.00E-01 UNITS INCH.
Y-SCALE=2.00E+01 UNITS INCH.

153

LCG FREQUENCY (HZ)

CB (REF NT**2/HZ)

154

PCW FRECUENCY (HZ)

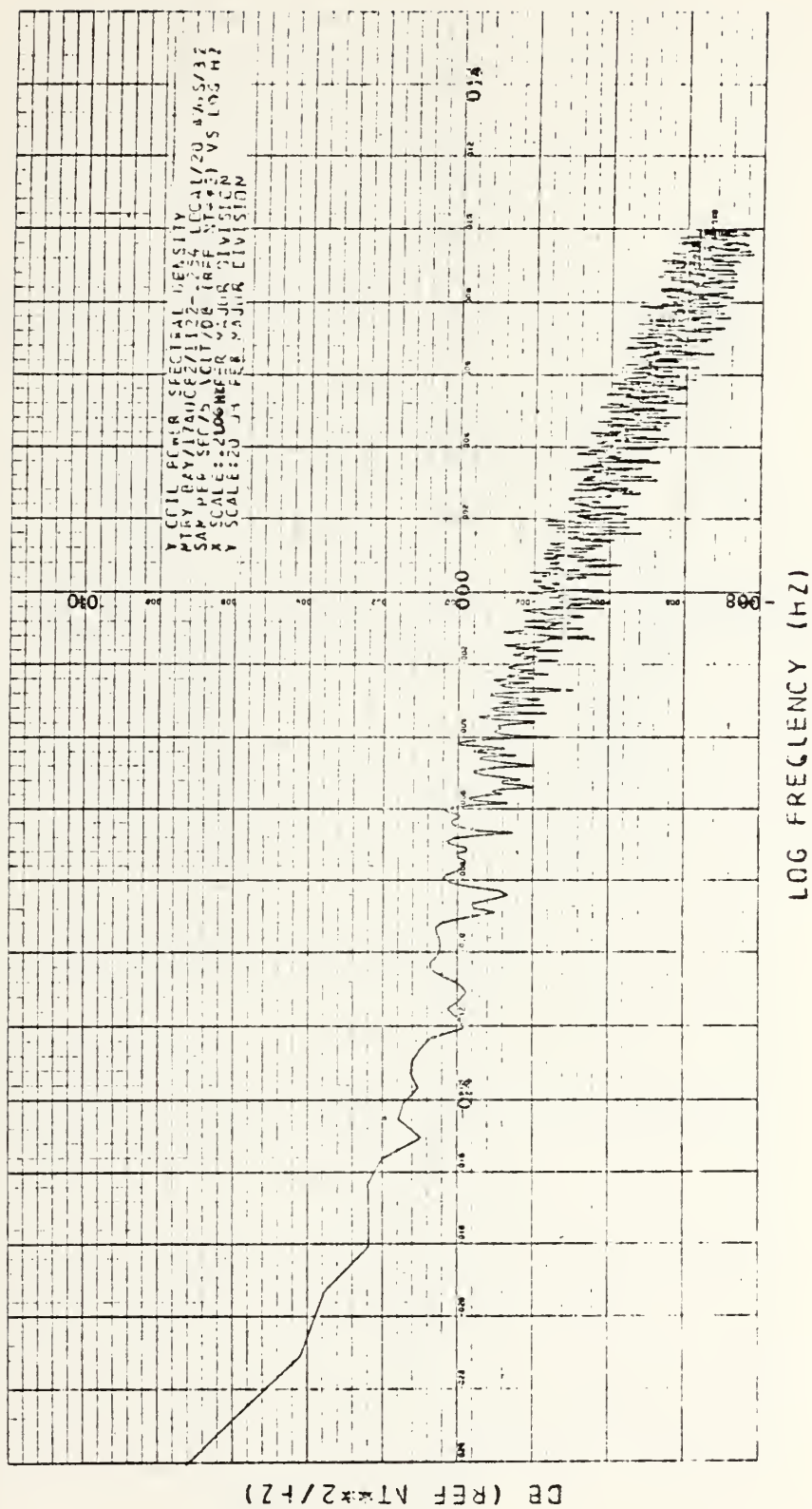CE (REF NT**2/HZ)
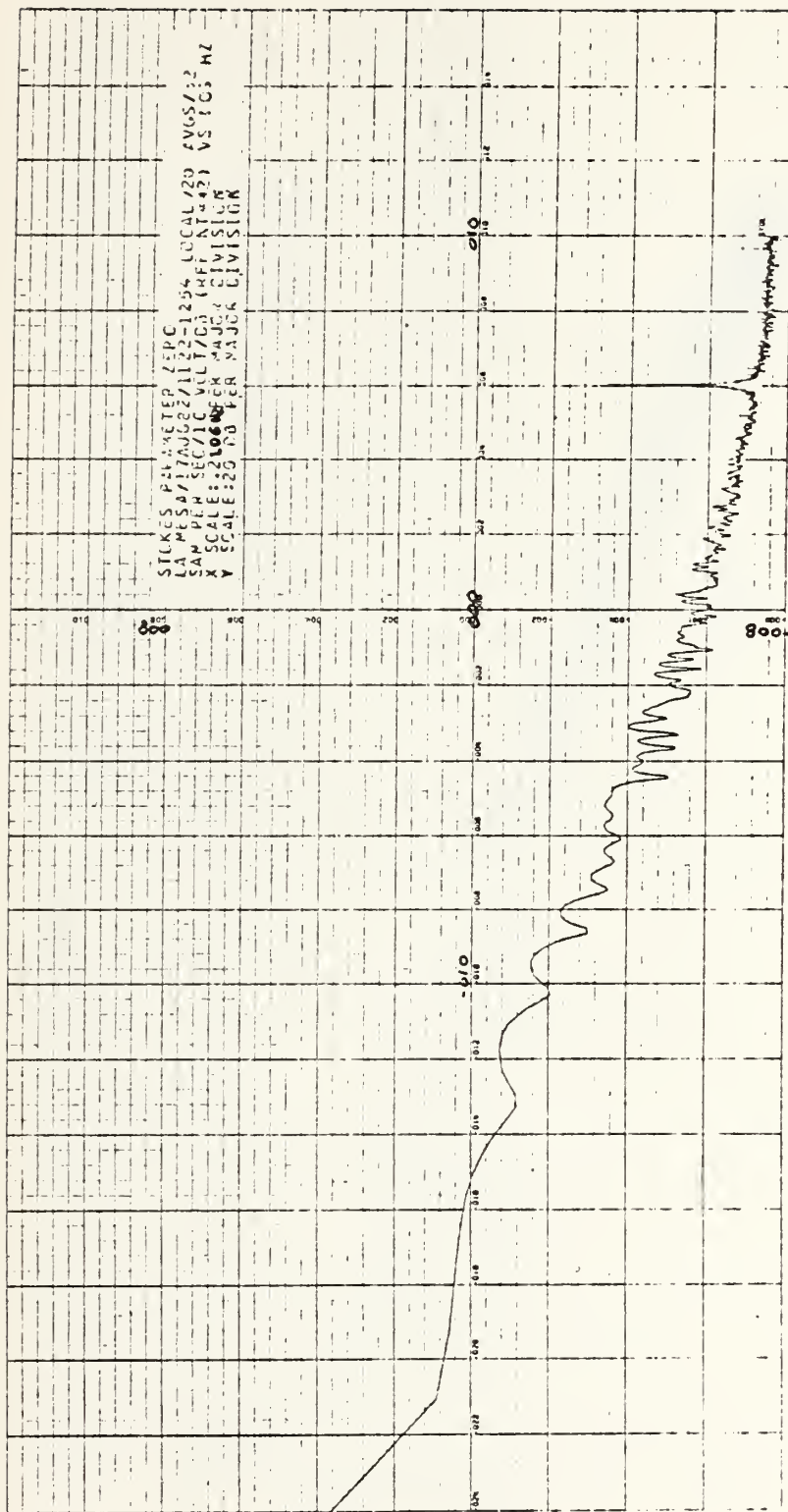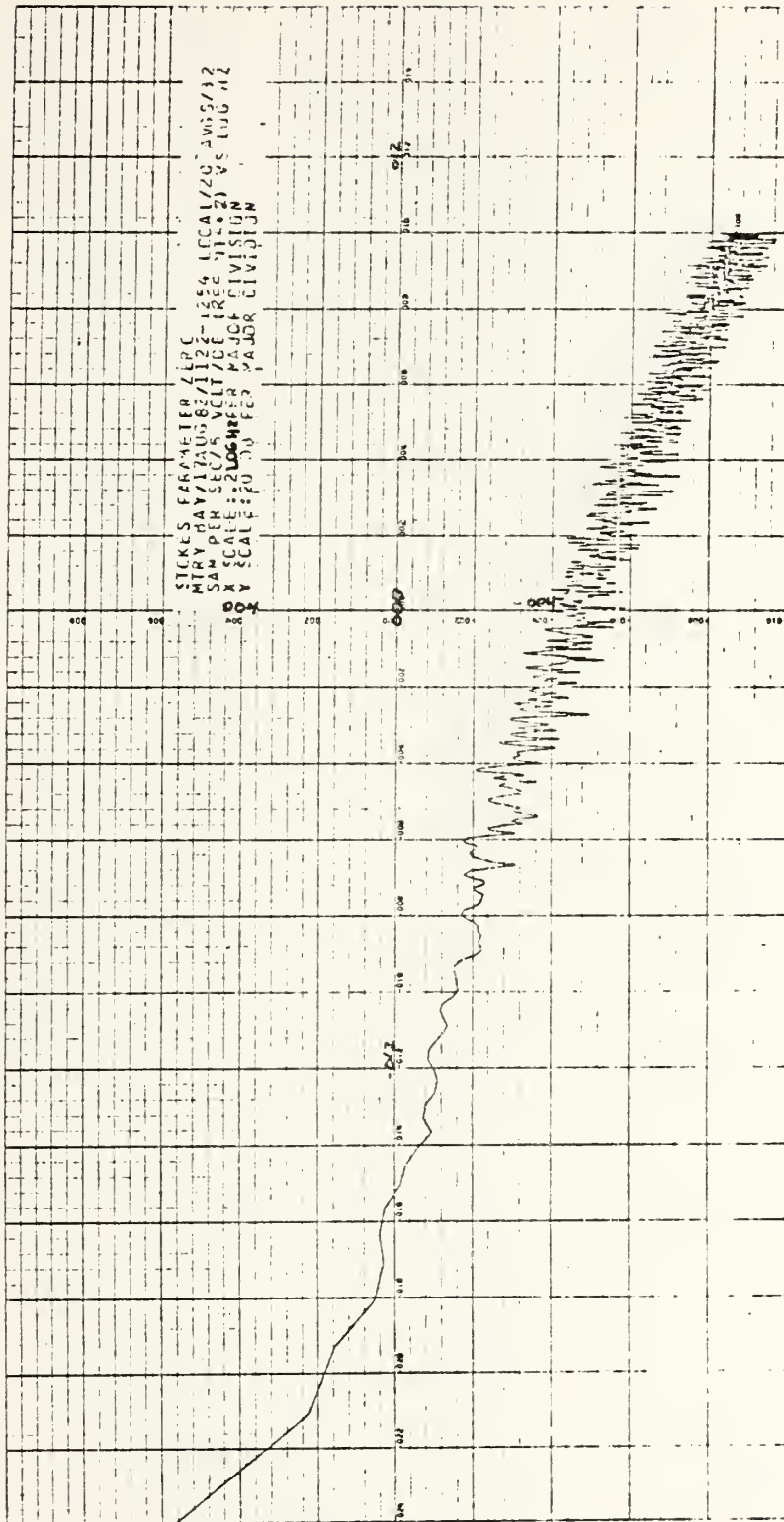
155

LOG FREQUENCY (HZ)

DB (REF NT**2/HZ)

LOG FRECUENCY (HZ)

LOG FREQUENCY (HZ)

DB (REF NT**2/HZ)

LOG FREQUENCY (HZ)

CB (REF NT**2/HZ)

159

RIGHT CIRCULAR POLARIZATION POWER SPECTRAL DENSITY

LOG FREQUENCY (HZ)

DB (REF NT**2/HZ)

160

RIGHT CIRCULAR POLARIZATION POWER SPECTRAL DENSITY
LA MESA/1/AUG82/11,22-11,54 LOCAL/20 AVGS/12
SAM PER SEC/10 VCLT/100 (REF AT=2) VS LGG HZ
X SCALE: 2LOG HPTZ PER MAJOR DIVISION
Y SCALE: 20 DB PER MAJOR DIVISION

LGG FREQUENCY (HZ)

DB (REF NT**2/HZ)

161

LOG FREQUENCY (HZ)

CB (REF AT**2/HZ)

162

LOG FREQUENCY (HZ)

DB (REF NT**2/HZ)

163

STOKES PARAMETER Q51 (NORMALIZED TO STOKES S)
BAY1 BAY1/AUGF11/2
2G AVGL
X SCALE:
X SCALE:

FREQUENCY (HZ)

S1/S0

STOKES PARAMETER THO (NORMALIZED TO STOKES 0)
LA MESA/1740GZ/1122-1124 LOCAL
20 AVGS/32.54 PER SEC/10 VOLT
X SCALE:.5 HZ PER MAJOR DIVISION
Y SCALE:.2 DB PER MAJOR DIVISION

FREQUENCY (HZ)

S2/SC

166

STOKES PARAMETER TWO (NORMALIZED TO STOKES 0)

FREQUENCY (HZ)

S2/S0

167

STOKES PARAMETER THREE (NORMALIZED TO STOKES 0)
LA MESA/TAUG42/112-136 LOCAL
20 AVG/1.2 SAM PER SECOND VOLT
X SCALE:.5 HZ PER MAJOR DIVISION
Y SCALE:.2 DU PER MAJOR DIVISION

FREQUENCY (HZ)

S3/S0

STOKES PARAMETER THREE (NORMALIZED TO STOKES 0)
PFRY SRY/17AUG22/112-1:56 LCET
20 AVGS/25 SEC FFT, SEC/DIV VOLT
X SCALE:.5 HZ PER MAJOR DIVISION
Y SCALE:.05 PER MAJOR DIVISION

FREQUENCY (HZ)

075

025

S3/S0

169

170

PHASE CF X AND Y CCILS
MTRY MAY/1740J(2/1154=1254 LCCAL
20 AVGS/.32 SA FER SEC/5 VCLT
X SCALE:.5 HZ FER MAJCR DIVISICN
Y SCALE:1 RADIAN PER MAJCR DIVISION

FREQUENCY (HZ)

RACIANS

171

COHERENCE OF X AND Y COILS
LAMBDA=/TAU=2.2/1122=1254 LOCAL
20 AVGS/12 SIN PER SEC/10 VLT
X SCALE::2 HZ PER MAJOR DIVISION
Y SCALE::1 UNIT PER MAJOR DIVISION

FREQUENCY (HZ)

COHERENCE

COHERENCE

FREQUENCY (HZ)

173

COHERENCE IF LEFT CIRCULAR POLARIZATION
MIKY DAY/LA MESA/17AUG82/1122-1254 LOCAL

2C AVGS/32 SAM PER SEC
X SCALE:.5 HZ PER MAJOR DIVISION
Y SCALE F:.1 UNIT PER DIVISION
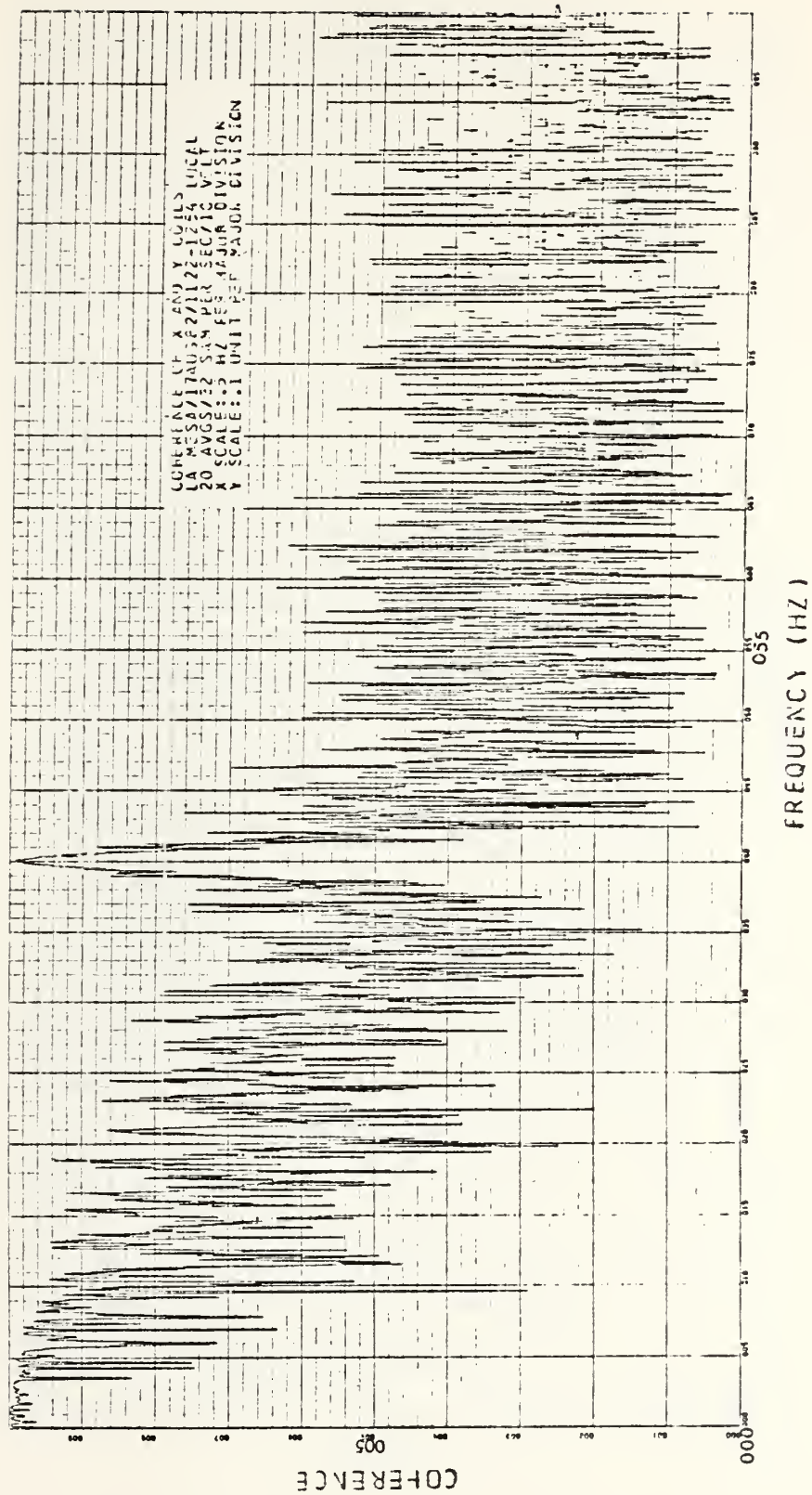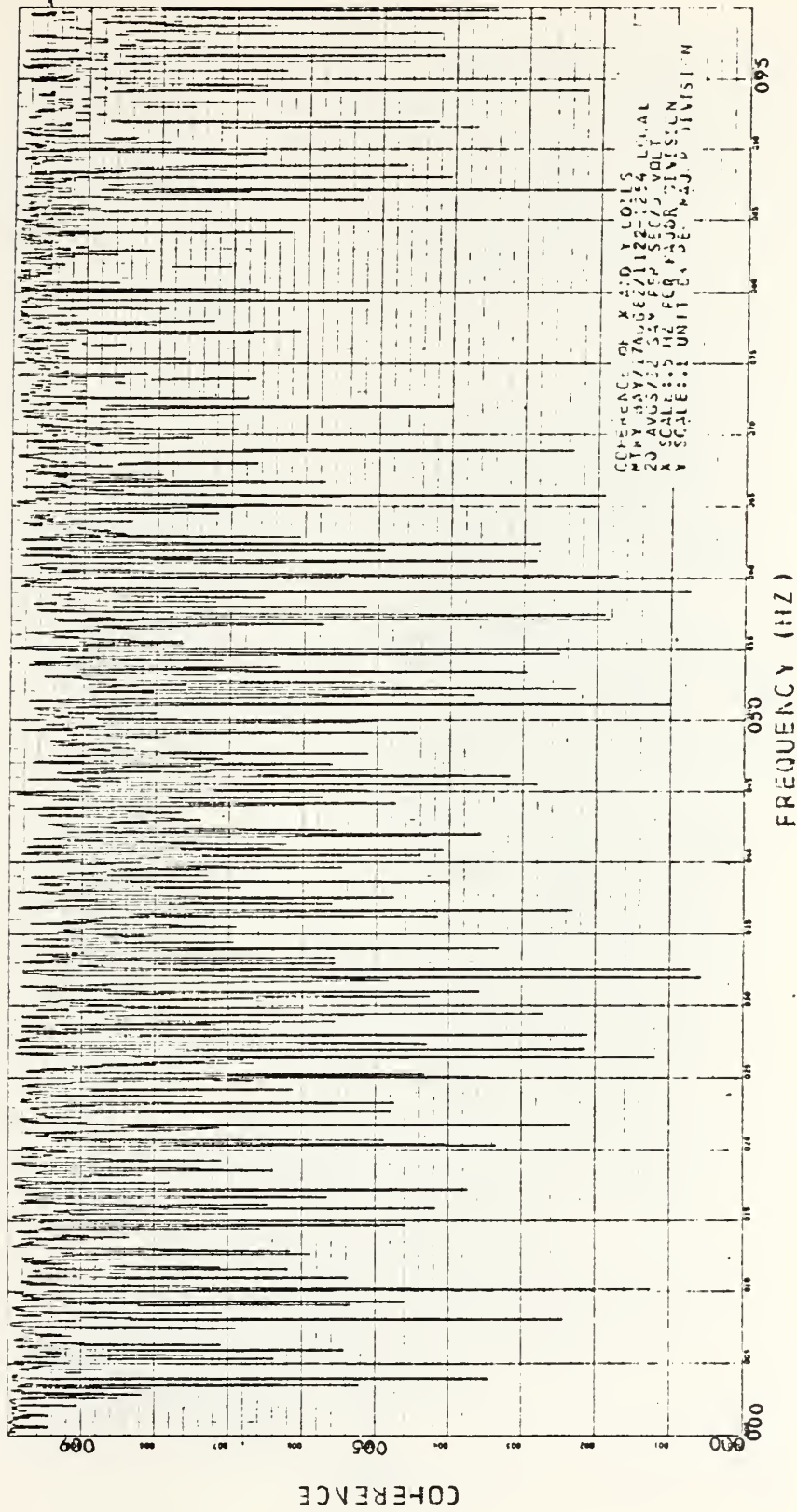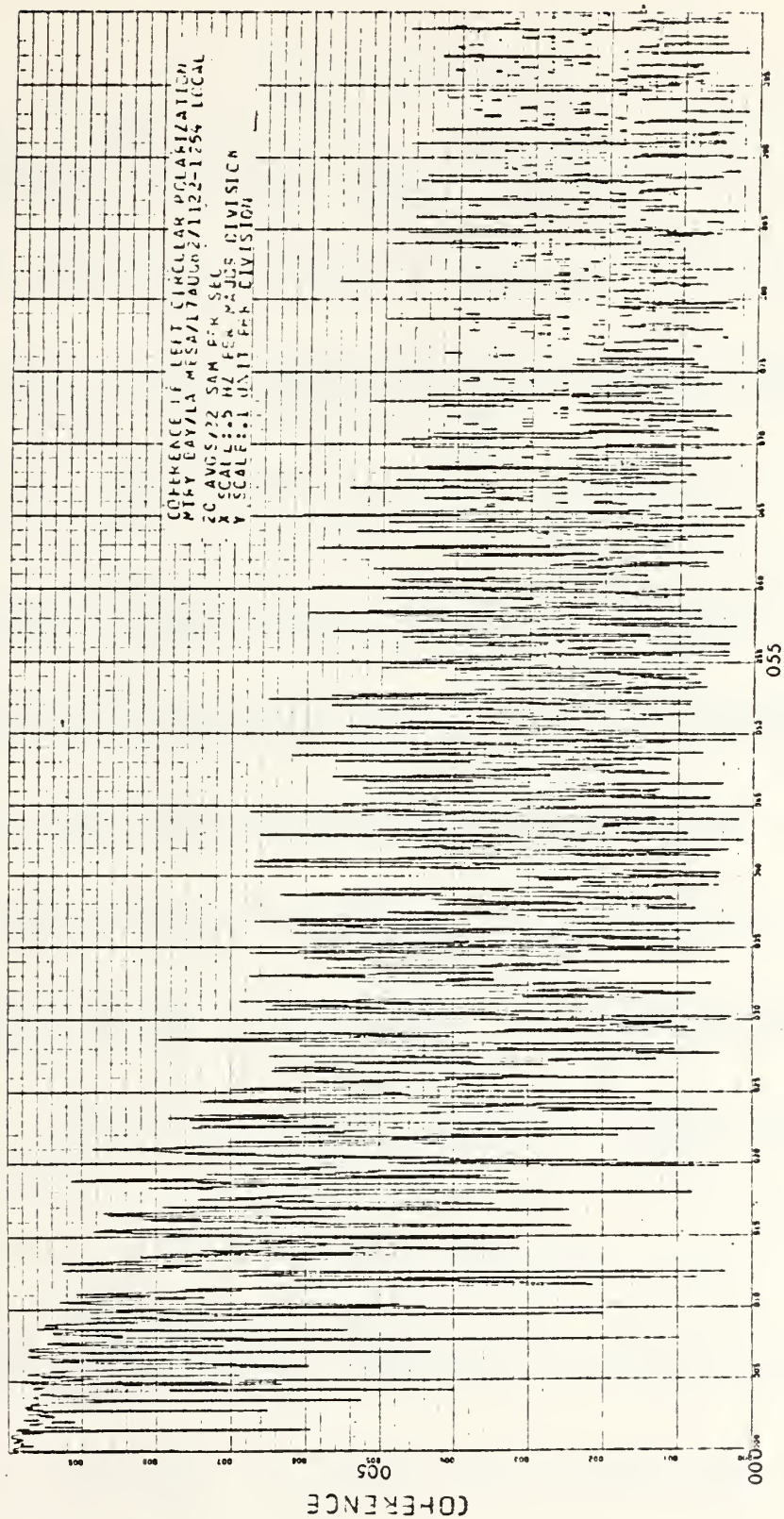
FREQUENCY (HZ)

COHERENCE

174

LIST OF REFERENCES

1. M.P. Ames and L.M. Vehslage, "Low Frequency Geomagnetic Fluctuations (0.025 to 20 Hz) on the Ocean Floor of Monterey Bay", Master's Thesis Naval Postgraduate School, Monterey, Ca, Dec. 1981.

2. J. Fagenbaum, "Optical Systems: A Review," IEEE SPECTRUM, vol. 16, no. 10, pp. 70-77, Oct.1979.

3. R. Cerny and T. Witkowitz, "Fiber-Optic Baseband Video Systems Can Provide Economic Advantages Now," Communication News, Sept. 1979.

4. F.F.E. Owen, "PCM and Digital Transmission Systems," McGraw Hill, Inc., 1982.

5. M.E. Thomas and P.M. Rutherford, "Oceanographic Data Telemetry Spar Buoy," Johns Hopkins University Applied Physics Laboratory memo SPM-82-104, July 20, 1982.

6. Joseph Fisher, "Study of Coherence in the Horizontal Plane of the Earth's Magnetic Field," Master's Thesis Naval Postgraduate School, Monterey, Ca, Dec. 1982.

7. O.D. Jefimenko, _Electricity and Magnetism_, Meredith Publishing Company, pp. 380, 1966.

8. C. Kleekamp and B. Metcalf, "Designer's Guide to Fiber Optics," Cahners Publishing Company, 1978.

9. C.M. Davis and R.E. Einzig, "Fiber Optic Sensor System (FOSS) Technology Assesment (Unclassified Version)," DSI-TR-80-001, Jan. 1, 1980.

10. R.M. Fuentez, "Optical Fibers," A descriptive paper for Naval Postgraduate School course EE 4900-5, Undated.

11. M.K. Barnoski, "Fundamentals of Optical Fiber Communications," Academic Press Inc., 1976.

12. C.D. Anderson, R.F. Gleason, P.T. Hutchison, and P.K. Runge, "An Undersea Communication System Using Fiber Guide Cables," Proc. IEEE, vol. 68, pp. 1299-1303, Oct. 1980.

13. G.A. Wilkens, "Fiber Optic Cables for Undersea Communications," Fiber and Integrated Optics, vol. 1, no. 1, pp. 39-61, 1977.

14. Optelecom Inc., "Report on Phase I-B to Bendix Field Engineering Corporation," Evaluation of Optical Fiber Cable for transmission of subsurface drill hole logging data.

15. T. Nakahara and N. Ushida, "Optical Cable Design and Characterization in Japan," Proc. IEEE, vol. 68, no. 10, pp. 1220-1226, Oct. 1980.

16. M.I. Schwartz, P.F. Gagen, and M.R. Santana, "Fiber Cable Design and Characterization," Proc. IEEE, vol. 68, no. 10, pp. 1214-1219, Oct. 1980.

17. H.C. Chandan and D. Kalish, "Strength and Dynamic Fatigue of Optical Fibers Aged in Various pH Solutions," paper presented at topical meeting on Optical Fiber Communication, Washington, D.C., Mar. 6, 1979.

18. G.A. Wilkens, "Recent Experience with Small Undersea, Optical Cables," paper presented at EASCON 79, Washington, D.C., Oct. 8, 1979.

19. An LF staff, "Tailoring Diodes to Match Fiber System Requirements," Laser Focus, Mar. 1978.

20. R.A. Wey, "Fiberoptic Communications," Laser Focus Buyers' Guide, 1982.

21. Burr-Brown Specification Sheet PDS-418, Apr. 1980, Burr-Brown Inc., 6730 South Tucson Blvd., Tucson, Arizona, 85706.

22. J.M. Davis, "An Underwater Fiber Optic Linked Video System," Master's Thesis Naval Postgraduate School, Monterey, Ca., Mar. 1981.

23. G. Wilkens, "Test Results for Three Ruggedized Optical Cable Units," NOSC, Hawaii Memo 5334/89, June 22, 1978.

INITIAL DISTRIBUTION LIST

No. Copies

1. Defense Technical Information Center 2
   Cameron Station
   Alexandria, Virginia 22314

2. Library, Code 0142 2
   Naval Postgraduate School
   Monterey, California 93940

3. Dr. Otto Heinz, Code 61Hz 2
   Department of Physics
   Naval Postgraduate School
   Monterey, California 93940

4. Dr. Andrew R. Ochadlick Jr., Code 610c 2
   Department of Physics
   Naval Postgraduate School
   Monterey, California 93940

5. Dr. Paul Moose, Code 62Me 1
   Department of Electrical Engineering
   Naval Postgraduate School
   Monterey, California 93940

6. Dr. Michael Thomas, Code 61 1
   Department of Physics
   Naval Postgraduate School
   Monterey, California 93940

7. Dr. John Powers, Code 62Po 2
   Department of Electrical Engineering
   Naval Postgraduate School
   Monterey, California 93940

8. LCDR Arnold R. Gritzke, USN 3
   114 Cleveland Avenue
   Lackawanna, New York 14218

9. LT Robert H. Johnson II, USN 3
   46 Grayson Circle
   Willingboro, New Jersey 08046

10. Captain Woodrow Reynolds, Code 68 1
    Department of Oceanography
    Naval Postgraduate School
    Monterey, California 93940

11. Robert C. Smith, Code 61 1
    Department of Physics
    Naval Postgraduate School
    Monterey, California 93940

12. LT Jeffrey M. Schweiger, USN 1
    44 Roundabout Road
    Smithtown, New York 11737

13. Dr. A. C. Fraser-Smith   1
    Radio Science Laboratory
    Stanford Electronics Laboritories
    Stanford University
    Palo Alto, California 94305

14. Dr. David M. Bubenik   1
    Assistant Director,
    Electromagnetic Sciences Laboratory
    SRI International
    333 Ravenswood Avenue
    Menlo Park, California 94025

15. Dr. Robert N. McDonough, 8-368   2
    The Johns Hopkins University
    Applied Physics Laboratory
    Johns Hopkins Road
    Laurel, MD 20801

16. Chief of Naval Research
    Department of the Navy
          Code 100C1   1
          Code 414   1
          Code 420   1
    800 North Quincy Street
    Arlington, VA 22217

17. Mr. William Andahazy   1
    Naval Ship Research and Development Center
    Annapolis Laboratory
    Annapolis, MD 21402

18. Department Chairman, Code 62   1
    Department of Electrical Engineering
    Naval Postgraduate School
    Monterey, California 93940

19. Professor O. B. Wilson, Code 70   1
    Department of Physics
    Naval Postgraduate School
    Monterey, California 93940

20. Mr. R. L. Marimon, Code 70   1
    Naval Undersea Warfare Engineering Station
    Keyport, Washington 98345

21. Commander B. Uber, Code 80   1
    Naval Undersea Warfare Engineering Station
    Keyport, Washington 98345

22. Mr. R. L. Mash, Code 50   1
    Naval Undersea Warfare Engineering Station
    Keyport, Washington 98345

23. Mr. Richard Peel, Code 7021   3
    Naval Undersea Warfare Engineering Station
    Keyport, Washington 98345

24. Administrative Department, Code 0115   5
    Naval Undersea Warfare Engineering Station
    Keyport, Washington 98345

25. Mr. George Wilkens   1
    Naval Ocean Systems Center (Hawaii)
    P.O. Box 997
    Kailua, Hawaii 96734